universität wien

DISSERTATION / DOCTORAL THESIS

Titel der Dissertation / Title of the Doctoral Thesis

“Air Templated Macroporous Polymers”

verfasst von / submitted by
Mohammad Jalalian

angestrebter akademischer Grad / in partial fulfilment of the requirements for the degree of
Doktor der Naturwissenschaften (Dr.rer.nat)

Wien, 2019/ Vienna 2019

Studienkennzahl lt. Studienblatt / degree programme code as it appears on the student record sheet:	A 796 605 419
Dissertationsgebiet lt. Studienblatt / field of study as it appears on the student record sheet:	Chemie
Betreut von / Supervisor:	Prof. Dr. Alexander Bismarck

ABSTRACT

Conventionally macroporous polymers are produced by blowing or templating methods, requiring the use of blowing agents or templating materials, which do increase the production cost of foams and could cause environmental issues. Here the procedure for producing dairy cream was mimicked: air was whipped into liquid resins or monomers to produce stable froths, which were subsequently cured or crosslinked to produce macroporous materials. Aqueous solution of phenolic resole, catalyst and surfactant was mechanically frothed and subsequently cured to produce macroporous phenolic panels with a size of 400 mm × 400 mm × 50 mm. The density of the open porous foams was controlled from 440 kg/m^3 to 180 kg/m^3 by controlling the whipping speed and time. The phenolic foams were pyrolysed to produce carbon foams panels with a carbon yield of 48%. Black liquor, an aqueous kraft mill by-product, was frothed; the crosslinking of the lignin resulted in stable biobased foams. Increasing the viscosity (by increasing the solute concentration) in the lignin solution led to an increased foam density and decreased pore sizes. The lignin foams were pyrolysed to produce carbon foams, retaining the shape and pore structure of the lignin foam precursor. To demonstrate the versatility of air templating method, non-aqueous epoxy resin, hardener, surfactant and silica particles were mechanically frothed and cured to produce epoxy composite foams. The silica particles had to be added into the resin mixture to increase the viscosity of the formulation and, thus, stabilize the liquid froths for curing at elevated temperature. Increasing the silica loading in the formulation led to an increase of the foam density and decrease of the average pore size of the epoxy foams.

ZUSAMMENFASSUNG

Konventionell makroporöse Polymere wurden durch Blas- oder Templatverfahren hergestellt, was die Verwendung von Treibmitteln oder Templatmaterialien erfordert, die die Kosten für die Herstellung der Schäume erhöhen und Umweltprobleme verursachen können. Hier wurde das Verfahren zur Herstellung von Milchcreme nachgeahmt: Luft wurde in flüssigen Harzen oder Monomeren geschlagen, um stabile Schaumstoffe zu erzeugen, die anschließend gehärtet oder vernetzt wurden, um makroporöse Materialien herzustellen. Eine wässrige Lösung von Phenolresol, Katalysator und Tensid wurde mechanisch aufgeschäumt und anschließend gehärtet, um makroporöse Phenolplatten mit einer Größe von 400 mm × 400 mm × 50 mm herzustellen. Die Dichte der offenen porösen Schaumstoffe wurde durch Variation der Aufschlaggeschwindigkeit und -zeit auf 440 kg/m³ bis 180 kg/m³ eingestellt. Die Phenolschäume wurden pyrolysiert, um Kohlenstoffschaumplatten mit einer Kohlenstoffausbeute von 48% herzustellen. Schwarzlauge, ein wässriges Kraftmühlen-Nebenprodukt, wurde aufgeschäumt; Die Vernetzung des Lignins führte zu einem biobasierten Schaum. Eine Erhöhung der Viskosität (nämlich der Konzentration des gelösten Stoffes) in der Ligninlösung führte zu einer Erhöhung der Dichte und einer Verringerung der Porengrößen der Schäume. Die Ligninschäume wurden pyrolysiert, um Kohlenstoffschäume herzustellen, wobei die Form und die poröse Struktur des Ligninschaumvorläufers beibehalten wurde. Um die Vielseitigkeit des Luft-Templatverfahrens zu demonstrieren, wurden nichtwässriges Epoxidharz, Härter, Tensid und Silicapartikel mechanisch aufgeschäumt und gehärtet, mit dem Ziel Epoxidverbundschäume herzustellen. Die Siliciumdioxidpartikel müssen der Harzmischung zugesetzt werden, um die Viskosität der Formulierung zu erhöhen und somit die flüssigen Schaumstoffe für das Aushärten bei erhöhter Temperatur zu stabilisieren. Die Erhöhung des Siliciumdioxidpartikelanteils in der Formulierung führte zu einer Erhöhung der Schaumdichte und einer Abnahme der durchschnittlichen Porengröße der Epoxidschäume.

ACKNOWLEDGMENTS

Firstly, I would like to express my sincere gratitude to my supervisor Prof. Dr. Alexander Bismarck for the continuous support during my doctoral research, for his patience, motivation, and immense knowledge. His guidance helped me all the time during research and writing of this thesis.

I would like to offer my special thanks to Dr. Qixiang “John” Jiang for his endless support throughout the project work. He has been a thoughtful supervisor who always pioneered in enthusiastic encouragement and useful critique of this research work.

I would like to thank Dr. Robert Woodward and PaCE group, which remained at Imperial College London for the amazing cooperation.

I would also like to thank Victor Burre for his invaluable contribution in part of my thesis while he was working with me in the lab. I would like to thank Dr. Andreas Mautner and Dr. Marta Fortea Verdejo for kindly answering my many questions and giving me advice. I would also like to thank all the other members of my research group, who made me feel at home and supported me over the years. I would especially like to thank Dr. Sara Fathinejad, for always being willing to help and encourage me during my PhD.

I am deeply grateful for the support of my family: my mother, my sisters and brothers who have always encouraged my scientific interest and helped me during my life.

Finally, I acknowledge JSP and FWF for their financial support.

LIST OF PUBLICATIONS

1. Publication I

Mohammad Jalalian, Qixiang Jiang, Arnaud Coulon, Martin Storb, Robert Woodward and Alexander Bismarck. Mechanically whipped phenolic froths as versatile templates for manufacturing phenolic and carbon foams. *Materials & Design* **168** (2019) 107658. DOI: org/10.1016/j.matdes.2019.107658

Mohammad Jalalian: Formal analysis, Investigation, Methodology, Resources, Writing - original draft. Qixiang Jiang: Conceptualization, Supervision, Writing - review & editing. Arnaud Coulon: Project administration, Resources, Visualization. Martin Storb: Project administration, Resources, Visualization. Robert Woodward: Formal analysis, Investigation, Methodology. Alexander Bismarck: Conceptualization, Supervision, Writing - review & editing, Funding acquisition

2. Publication II

Mohammad Jalalian, Qixiang Jiang, Marc Birot, Hervé Deleuze, Robert T. Woodward, Alexander Bismarck. Frothed black liquor as a renewable cost effective precursor to low-density lignin and carbon foams. *Reactive and Functional Polymers*, **132** (2018) 145-151. DOI: org/10.1016/j.reactfunctpolym.2018.07.027

Mohammad Jalalian: Formal analysis, Investigation, Methodology, Resources, Writing - original draft. Qixiang Jiang: Conceptualization, Supervision, Writing - review & editing. Marc Birot: Formal analysis, Investigation, Methodology. Hervé Deleuze: Conceptualization, Writing - review & editing, Funding acquisition (ANR – part of joined project and for visiting Professorship for AB). Robert Woodward: Formal analysis, Investigation, Methodology. Alexander Bismarck: Conceptualization, Supervision, Writing - review & editing, Funding acquisition (JSP and FWF part of project)

3. Publication III

Mohammad Jalalian, Qixiang Jiang, and Alexander Bismarck. Air Templated Macroporous epoxy foams with silica particles as property-defining additive. *ACS Applied Polymer Materials*, **1** (2019) 335-343. DOI: 10.1021/acsapm.8b00084

Mohammad Jalalian: Formal analysis, Investigation, Methodology, Resources, Writing - original draft. Qixiang Jiang: Conceptualization, Supervision, Writing - review & editing. Alexander Bismarck: Conceptualization, Supervision, Writing - review & editing, Funding acquisition

TABLE OF CONTENTS

1. INTRODUCTION AND OUTLINE

Porous polymers with pore diameters greater than 50 nm are macroporous polymers[1]. Macroporous polymers are lightweight materials and can be tailored to possess excellent mechanical property / density ratios; they are ideal for applications where weight is a penalty with other requirements on the properties of the materials. Macroporous polymers can be classified into open-cell and closed-cell structures (Figure 1). Open-cell foams have interconnected cells, which allow the passage of a gas or fluid through the cellular structure from one cell to the next: polymer foams have been used as supports for tissue engineering [2-4] and catalyst [5] as well as separation media [6, 7]. Whereas in closed-cell foams, the cell walls are not interconnected and gas or fluid cannot move through the cells but is immobilised in each compartment cell. Therefore, closed-cell foams are good thermal insulators [8] and acoustic barriers [9].

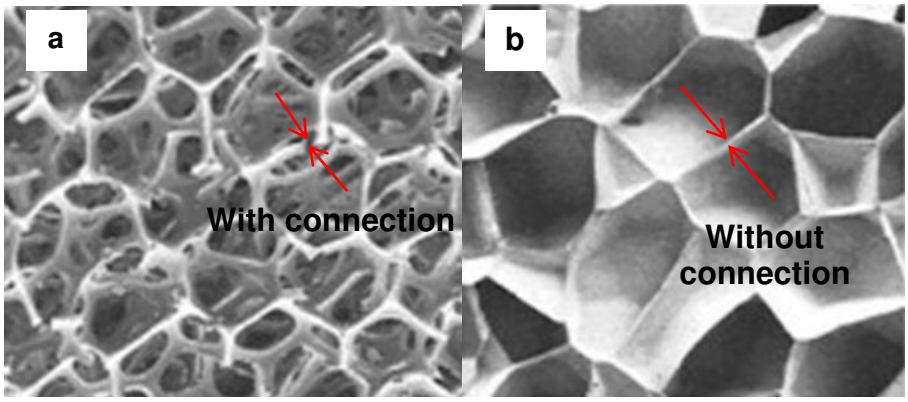

Figure 1. SEM images, represent the foam structures; a) open cell, b) closed cell[10]

Nowadays, majority of polymer foams, such as polyurethane (PU) and extruded polystyrene (XPS), are prepared by using chemical or physical blowing agents [11]. Usually liquid formulations (e.g. resins or polymer melts) are mixed with the blowing agents; during the solidification of the liquid formulations by curing or cooling the blowing agents create gas by physical gasification or chemical reactions, producing the macroporous structure of the solid polymer foams [12]. However, some physical blowing agents could cause environmental issues. For instance, chlorofluorocarbons (CFC) can diffuse into stratosphere and catalytically destroy the ozone layer and, therefore, their use was banned in the 1980s. Other blowing agents, such as pentane, are very flammable, leading to associated risks during production[13]. On the other hand, using solid or liquid templates to produce macroporous polymers (e.g. salt leaching, surfactant templating, emulsion templating, etc.) is very versatile, because the template structure predefines the pore structure of the resulting polymer foams. Taking emulsion

templating as an example, emulsions with external monomer phase and internal (droplet) templating phase are prepared and subsequently polymerised. After the purification and removal of the internal templating phase, tailor-made macroporous polymers are produced, where the pores are replica of the dispersed droplets and the porosity is determined by the internal phase ratio of the emulsion templates. However, such templating methods always require the removal or recycling of the templates. One can image that if 1 m^3 emulsion templated macroporous polymers with 90% porosity is produced, 900 L internal phase needs to be removed by solvent exchange and drying. This costs enormous energy and materials, making templated polymer foams very expensive and difficult to scale.

Air templating can be used as an alternative method to produce polymer foams from liquid precursors. Air templating refers to whipping air into a mixture of liquid resins or monomers to create stable liquid froths, which are subsequently cured or crosslinked to produce macroporous polymers. Importantly, it does not require any extra porogens (e.g. blowing agents or templates) but air to produce the polymer foams, therefore providing potentially a low-cost, environmentally friendly and scalable manufacturing method.

Although some work on air templated macroporous polymers or material has been conducted, quite some open questions on this topic remain, which include the scalability and versatility of air templating method as well as potential applications of air templated macroporous polymers. To address these questions three types of resins were mechanically whipped to produce liquid froths, which were cured to produce air templated macroporous polymers. For decades phenolic foams have been industrially produced via physical blowing processes using aqueous phenolic resoles as starting materials: the resulting closed-cell phenolic foams possessed outstanding thermal insulating and fire resistance and are used for buildings and industrial facilities, such as pipelines or tanks. Furthermore, aqueous system can be easily foamed and the resulting foams stabilised. Therefore, this research work started with manufacturing air templated phenolic foams, aiming at investigating their scalability and applicability. Lignin is the second abundant natural biobased polymer, which is commonly extracted during the pulping process. Black liquor, an aqueous solution of lignin, is a by-product from kraft pulping mills; however, most of the black liquor is burnt to recover energy to provide power for the paper mills. In this work air templated lignin foams were produced by whipping air in to black liquor and subsequently curing the froths. The work aimed to demonstrate the possibility of using low-cost biobased by-products as raw material for the production of air templated macroporous materials for value added applications.

Contrary to aqueous systems, non-aqueous froths are much more difficult to prepare and stabilise and were therefore rarely investigated. In order to expand the applicability of the air templating method from aqueous resin to non-aqueous resin systems, a liquid epoxy resin was frothed; an efficient stabilising method for such air-in-oil systems has to be identified. Furthermore, when using these three resin systems, the morphology, physical and mechanical properties of the air templated macroporous polymers were investigated and correlated to the formulations and whipping conditions of the liquid froths, in order to demonstrate that air templating allows for the production of tailor-made macroporous polymers.

2 LITERATURE REVIEW

2.1. MACROPOROUS POLYMER FOAMS

Polymer foams have attracted a large amount of attention due to their desired properties, such as low density, high porosity, high surface area and attractive mechanical properties. They are used as substrates for tissue engineering, column packing in (gas and gel permeation) chromatography[14], and some polymer foams are used as sandwich cores or as thermal insulators[15]. Moreover, they have been widely used in our daily life as packaging materials, insulators in fridges and fridge-freezers, comfort seating materials, in mattresses, shoes and sports materials and so on[16].

Generally, porous polymers are classified into open and closed cell structures, which consist of spherical pores interconnected or comparted via pore throats, respectively[17, 18] (Figure 2). Based on the pore size polymer foams can be classified into microporous materials when containing pores with average pore diameters smaller than 2 nm, mesoporous with average pore sizes ranging from 2 to 50 nm and macroporous with average pore sizes exceeding 50 nm[1]. The pore size is defined as the diameter in the case of cylindrical and spherical pores, while in case of slit-shaped pores, the pore size is determined as the distance between opposite walls of the pores[19]. Microporous polymers can be used as membranes for instance in fuel cells, sensors and as drug delivery systems because of their high surface area[20]. Mesoporous polymers are used for a wide range of applications, such as electrical and optic applications,[21] ion-exchange materials and catalysis supports[22]. They are usually modified with particles to increase surface area and thermal stability to be utilized in a variety of fields from environmental remediation and as separation media[23]. Macroporous polymers are used in ion-exchange resins, catalyst supports, adsorbents, carriers, chromatographic media, thermal insulations etc.[24].

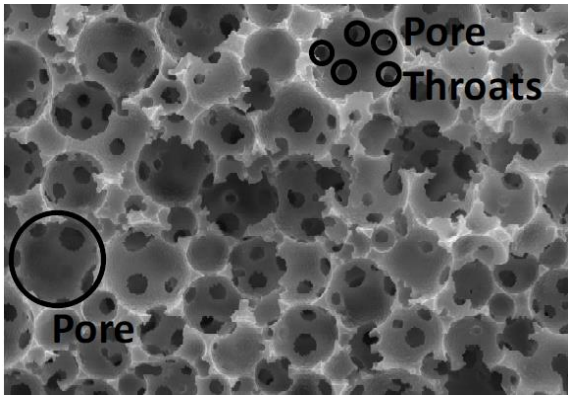

Figure 2. Typical SEM image of a porous polymer showing pore and pore throats[18].

2.2. PROCESSES TO PREPARE MACROPOROUS POLYMERS

2.2.1. FOAMING WITH BLOWING AGENTS

Chemical and physical blowing is a conventional way to prepare macroporous polymer foams, including the most commonly seen polyurethane (PU) and polystyrene (PS) foams[25]. Blowing processes are classified as either physical and chemical blowing[26]. In physical blowing processes, a solvent or inert gas dissolves in thermoplastic melt under high pressures. After the melt is shaped by extrusion or injection moulding, the blowing agents gasify under reduced pressure or elevated temperature and expands the melt. The solidification of the liquid (melt), frothed formulation results in foams with low densities. Chlorofluorocarbons (CFCs), hydrochlorofluorocarbons (HCFCs), argon, n-pentane, CO_2 and N_2 are the general types of physical foaming agents which were and are used with several polymers, such as PU, PS, polyethylene (PE) etc.[27-29]. However, with the ever-growing environmental issues, the harmful effects of these chemicals for instance on the ozone layer had to be addressed[30, 31]. CFCs and HCFCs were widely used to foam PU due to their low cost and high solubility[32]. However, the production and large scale use of CFCs was banned already in the 1990s, also use of the alternative HCFCs will be phased out until the middle of the 2020s.

Chemical blowing agents decompose at elevated temperature and release a gaseous reaction product, usually CO_2 or N_2, which act as blowing agent[33]. This process is usually exothermic and irreversible, while certain compounds, such as bicarbonates, decompose through a thermal dissociation and evolve gas in reversible endothermic reactions[34, 35]. Chemical blowing agents are used to produce high density foams. Moreover, they are often used for foaming thermoplastics[36]. Chemical blowing agents include azo compounds, hydrides, carbonates and bicarbonates, nitrites, peroxides, N-nitroso compounds, oxygen-containing acid derivatives, urea derivatives, hydrazines, semicarbazides, azides, and triazoles[37].

2.2.2. PHASE SEPARATION

Phase separation process utilize a polymer solution: by changing the solubility of the polymer in the solution for instance by controlling the temperature or by addition of a non-solvent, the polymer phase separates from the solvent, creating polymer rich and polymer poor regions[38], which after solvent removal and purification forms the polymer phase and pores. This technique is used, depending on the process condition, to

produce polymer foams with pore sizes ranging from 0.1 nm to 100 μm[39]. This technique can be employed for the preparation of nanoscale structures and is frequently used to prepare three-dimensional high porosity scaffolds used as cell support for tissue engineering[40]. The phase separation of the polymers from the solvents can be driven via different methods[41]. Thermally induced phase separation (TIPS) refers to the process where the solubility of the polymers in the solvent is decreased with decreasing temperature[42] which drives the phase separation of a homogeneous polymer solution to create a multi-phase system. After the removal of the solvent by extraction, evaporation or freeze drying porous structure is formed[43]. One advantage of TIPS is the possibility to produce a porous polymer with an interconnected pore structure using an easy-to-tune, fast and adaptable process[44]. However, this method is limited to thermoplastic polymers, since it does require mobile polymer backbones to enable the distribution and phase separation of the polymer molecules below its glass transition temperature (T_g).

Air casting process utilises a polymer solution with a mixture of a volatile solvent and a less volatile non-solvent. Along with the evaporation of the solvent, the polymer undergoes phase separation in the non-solvent. Also, before the phase separation, the polymer / solvent / non-solvent can be formed into a bicontinuous phases by chemical or thermal cooling in order to enhance the phase separation during the air casting[45]. Furthermore, instead of using air, using a non-solvent vapour as the casting tool was also possible to lead the phase separation of the polymer solution[46].

In immersion precipitation, a polymer solution is cast or extruded as a thin film. Upon the immersion of the film in a non-solvent polymer precipitation occurs due to solvent exchange of the good solvent for a non-solvent[47]. Phase diagrams are used to predict, whether a polymer solution (polymer – solvent pair) is suitable for the production of porous polymers using phase separation methods[48]. Such phase transitions can be predicted using Ternary isothermal phase diagrams[49].

Contrary to aforementioned physical induced phase separation process, chemically induced phase separation (CIPS) utilises polymerisation in homogeneous monomer solution to induce phase separation[50]. The initial system consists of polymeric precursors and a low-molecular weight liquid with a low boiling point[51]. The low molecular weight liquid has to be a good solvent for the reactive precursors but poor for the polymer. During the polymerisation of the precursors, the liquid forms a second phase. The removal of the liquid phase by drying results in a porous polymer[52]. This method has been used to produce thermoset porous polymers, such as epoxy,[51] cyanurate[53] and dicyclopentadiene based polymer networks[54].

2.2.3. PARTICLE LEACHING

The term leaching commonly describes the process in which soluble constituents (e.g. salts) are washed, extracted and carried away by a permeating fluid[55]. This method involves mixing of (water-soluble) porogen into a polymer solution followed by casting the mixture into the desired shape. The solvent is removed by evaporation or lyophilisation and the porogens are removed by solvent leaching[56]. This process does involve the selective leaching of water-soluble inorganic salt particles, such as NaCl or KCl, or of organic compounds, such as gelatin or wax microspheres, which are usually used as porogens to template the pores. The porosity of the resulting porous scaffold is defined by the ratio of the particulate porogen and polymer, while its pore size is defined by the particle size of the porogen. One of the problems of leaching is contaminations in the porous polymeric structures, including residual solvents and porogens which may affect cell cultures when the porous polymer is to be used as scaffold[57]. Leaching process has been used to prepare porous scaffolds (e.g. for tissue engineering applications)[58, 59].

2.2.4. POROUS POLYMERS MADE BY SINTERING

Sintering is a processing technique in which a solid mass of material is formed by the fusion of many small pieces, usually powder[60]. This process involves the heat treatment of powder compacts at elevated temperatures at which the diffusional mass transport is appreciable[61]. For instance, a powder of a thermoplastic polymer is cast into a desired shape; it is heated to near-melting-temperature in order to fuse the particles together. Sintering occurs results in a reduction of the total surface energy[62].

Sintering process can be used to prepare porous polymers[63] with average pore sizes in the range from 0.1 to 10 µm. This method has been used for thermoplastics and non-melt processable polymers[64]. Moreover, it can be used to prepare porous hydroxyapatite scaffolds[65] and porous polymer composites[66]. For example, porous polymer composites consisting of PE and polypropylene (PP) powder prepared by the continuous extrusion sintering method can be used as filter elements for air purification[67]. In this method, the mixed powder of two polymers is extruded through a head die, which forms porous composite materials. During the continuous extrusion process, polymer particles undergo severe plastic deformation and take the complex shape of porous structures. Due to the continuous manufacturing process, control of the

porosity and mean pore size is possible by varying the die temperature of the extruder. However, the technique is limited to manufacturing flat-sheet or tubular membranes but control over pore structure is limited[68].

2.2.5. EMULSION TEMPLATING

An emulsion is a heterogeneous system of two or more immiscible liquid phases where one liquid (called the continuous phase) contains a dispersion of the other liquid (internal phase). In other words, an emulsion is a special type of mixture made by combining of two liquids, which are thermodynamically unstable and eventually, will separate into two immiscible phases[69]. Hence, emulsifiers have to be used to hinder destabilization of the emulsions[70]. Emulsions are usually used in our daily lives, such as food (milk, mayonnaise) as well as cosmetic products (body lotions, creams) and several paints[71]. Emulsions formed by dispersing water droplets in an oil phase are called water-in-oil (W/O) emulsions, or when dispersing oil droplets in water they are called oil-in-water (O/W) emulsions[72].

Emulsion templating has been used to prepare porous polymers since the 1960's[73] and was further developed by Unilever in the 1980's[74]. Porous polymers, called polyM/HIPEs, can be synthesised by polymerisation of high or medium internal phase (ratio) emulsions[75], when the continuous phase consists of monomers or suitable prepolymers. After polymerisation of monomers in the continuous phase and subsequent removal of the droplet phase macroporous polymers are formed[76].

In majority of cases high internal phase emulsions (HIPEs) with an internal droplet phase volume ratio of exceeding 74.05 V/V% are used to produce macroporous polymers, known as polyHIPEs[77]. Emulsions with an internal phase volume ratio between 30-74% and less than 30% are termed medium internal phase emulsions and low internal phase emulsions, respectively[78]. Porous polymers produced by polymerisation of such emulsions are named polyMIPEs and polyLIPEs, respectively. Most of polyHIPEs are synthesised by free radical polymerisation (FRP), however other polymerisation methods, including step-growth, atom transfer radical polymerisation (ATRP), ring opening metathesis polymerisation (ROMP) were also carried out in emulsion templates[79]. In order to prevent the template to undergo coalescence prior to polymerisation, emulsion templates need to be stabilised by suitable emulsifiers, which can be either molecular surfactants[80] or particulates[81]. Most of the macroporous polymers produced by polymerisation of surfactant-stabilised emulsion templates possess an open-porous structure[82], while macroporous polymers with closed-cell

porous structures have been produced by polymerisation of particle-stabilised M/HIPEs[81]. Because of the liquid nature of emulsion templates, they can be moulded or printed to assume any desired shapes. polyHIPEs with a wide range of shapes and sizes from 50 ml to 3 L have been reported[83]. The attractiveness of emulsion templating is that the porosity, pore size and pore interconnectivity can be easily controlled and thus polyHIPEs have been explored for various applications such as tissue engineering scaffolds[84], separation media[85], supports for heterogeneous catalysts and reagents[86]. Moreover, the open cellular pore morphology makes them good candidates as damping materials for acoustic insulation within engine compartments and other enclosures[87]. Unfortunately, some of the undesired properties of polyHIPEs, brittleness and friability for poly(styrene-co-divinylbenzene) based polyHIPEs as an example[88], have hindered the industrial applications. Furthermore, the need for the removal of the templating phase after the polymerisation of the emulsion templates is quite energy intensive.

2.2.6. AIR OR FOAM TEMPLATING

Alternatively, macroporous polymers have been prepared by mechanically beating air into liquid monomers or resins to prepare liquid foams, which can subsequently be polymerised (Figure 3).

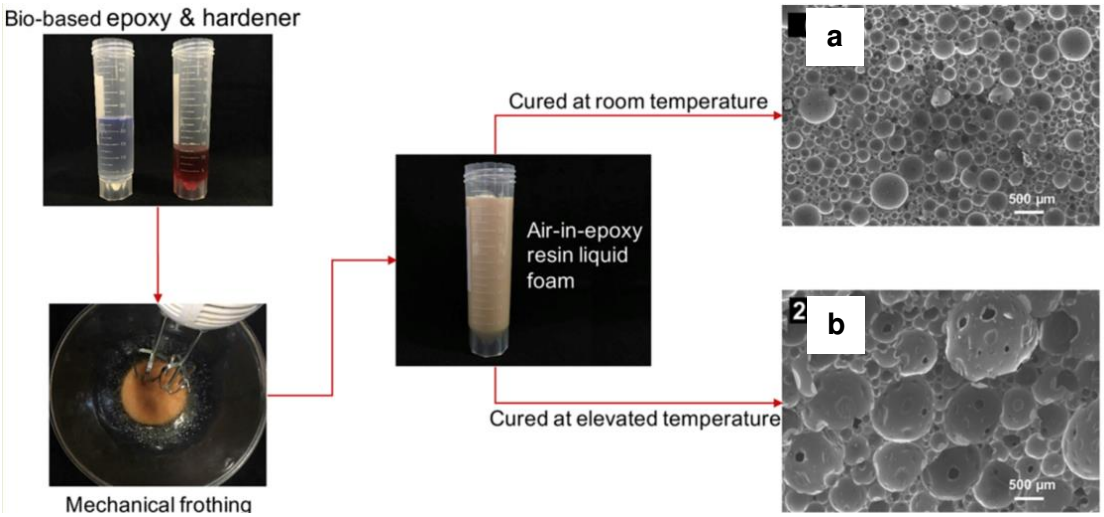

Figure 3. Schematic illustration of the air templating technology for the preparation of macroporous polymers involving mechanically whipping air into a monomer mixture producing a stable froth which was subsequently polymerised at room temperature (a) and at elevated temperature (b) (based on W. Song et al.[89])

The mechanical whipping technique was developed long time ago (in 1941), when John H. Kelly. Jr.[90] reported the preparation of cellular rubber. This foam was made by whipping or beating air into an aqueous latex suspension or some other aqueous liquids containing a water-soluble foaming agent, such an alkali or ammonia soap or saponins. Wong et al.[91] reported the preparation of frothed foams with ethanol / water as the liquid phase containing polytetrafluoroethylene (PTFE), polyvinylidene difluoride (PVDF), polyetherimide (PEI) or polyether ether ketone (PEEK) powder, which also acted as particulate stabiliser. Closed-cell macroporous polymers were produced by drying the liquid, particle-stabilised foam followed by sintering the remaining scaffold formed by polymer particles. However, this method was disadvantageous at the shrinkage of the foam template during drying and the sintering. Marlin et al.[92] prepared a macroporous polyurethane foam by mechanically frothing air into a mixture of isocyanate, polyol, surfactant and catalyst. The liquid foam was subsequently cured by thermal polymerisation. Murakami and Bismarck[93] reported the synthesis of monolithic air templated macroporous polymers. Oligomeric tetrafluoroethylene (OTFE) particles were employed to stabilise air bubbles in fluorinated monomers creating a stable oil (non-aqueous) foam that could be UV-polymerised resulting in closed-cell macroporous polymers. Lee et al.[94] manufactured porous polymerised acrylated epoxidised soybean oil (polyAESO) foams by air templating. The highly viscous AESO with the addition of the bacterial cellulose provided kinetic stability to the liquid foam by hindering liquid film drainage. However, after polymerisation, the macroporous polymers presented irregular shape pores and a porosity of only 59%. In a following work, Lau et al.[95] reported air templated macroporous epoxy resins. In their work a viscous bio-based epoxy was frothed without using any surfactant or particle stabilisers. The froths were subsequently polymerised resulting in epoxy foams with porosities ranging from 75% to 80% and elastic compression moduli of 88 MPa to 160 MPa.

In analogy to emulsion templating, the pore structure of the polymer foams prepared by the air templating method is also defined by the air bubbles dispersed in the monomer phase by mechanically whipping. This technique is advantageous not only because that it can be applied to produce macroporous polymers with open- or closed cell structures from different monomers, but also because that it uses the simply air as a porogen. Furthermore, after the polymerisation of the whipped froths, no further purification or washing is required. Therefore, air templating could be superior to other templating methods, such as emulsion templating or particle leaching and is anticipated to be scalable.

To be able to use air templating to produce macroporous polymers, a suitable liquid resin or monomer system is needed. The resins were firstly screened so that the resulting polymers have desired properties for practical applications. Furthermore, both aqueous and non-aqueous resins will be selected to investigate the versatility of the air templating method.

2.3. POTENTIAL RESIN SYSTEMS: PHENOLIC RESOLES

Phenolic resins were among the first synthetic polymers reported by L.H. Baekeland in 1907, and since then they are known under their trade name Bakelite[96]. Phenolic resins were used as bonding agents for joining of wood, glasses, metals, paper and rubber to other substrates with a favourable cost performance[97]. The manufacturing of new lightweight materials which simultaneously possess high mechanical properties at low cost make phenolic resins attractive for the applications such in aircrafts, electronic devices, automotive, kitchen parts, buildings and so on[98]. Phenolic resins have a low density, low toxicity, low spread flammability and smoke development but high char formation when they burn[99]. However, their main disadvantage as matrix for composites is their low toughness. Furthermore, polycondensation reaction of phenolic resin results in the generation of water, which remains as residue in the composite. In case meeting a heat or fire, steam can be generated in the composites and, therefore, damage the structure of the material[100].

Phenolic resins are synthesised by reaction between phenol and formaldehyde; the products depend on the stoichiometry of phenol to formaldehyde and the pH during the exothermic reaction[101]. With excess formaldehyde and an alkaline catalyst, phenol alcohol with methylol side or end groups are produced; this products are often called phenolic resole[102]. The resoles are usually liquid and can be further cured with heat in the presence of catalyst through the condensation of the methylol groups[103] (Figure 4).

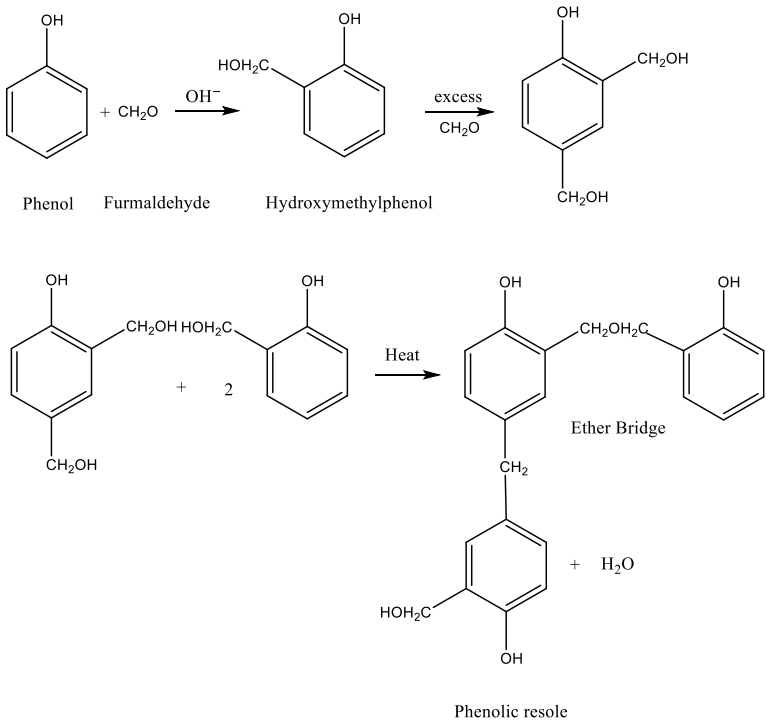

Figure 4. The synthesis mechanism of phenolic resole in alkaline media

Phenolic novolacs are produced when the molar ratio of formaldehyde to phenol is less than one using acidic catalyst[104]. In the final structure, phenol units are mainly linked with methylene groups[105] (Figure 5). Novolac resins can be used as moulding compounds, wood adhesives, and friction materials because of their good mechanical strengths, excellent bonding performance, water and heat resistance and durability[106].

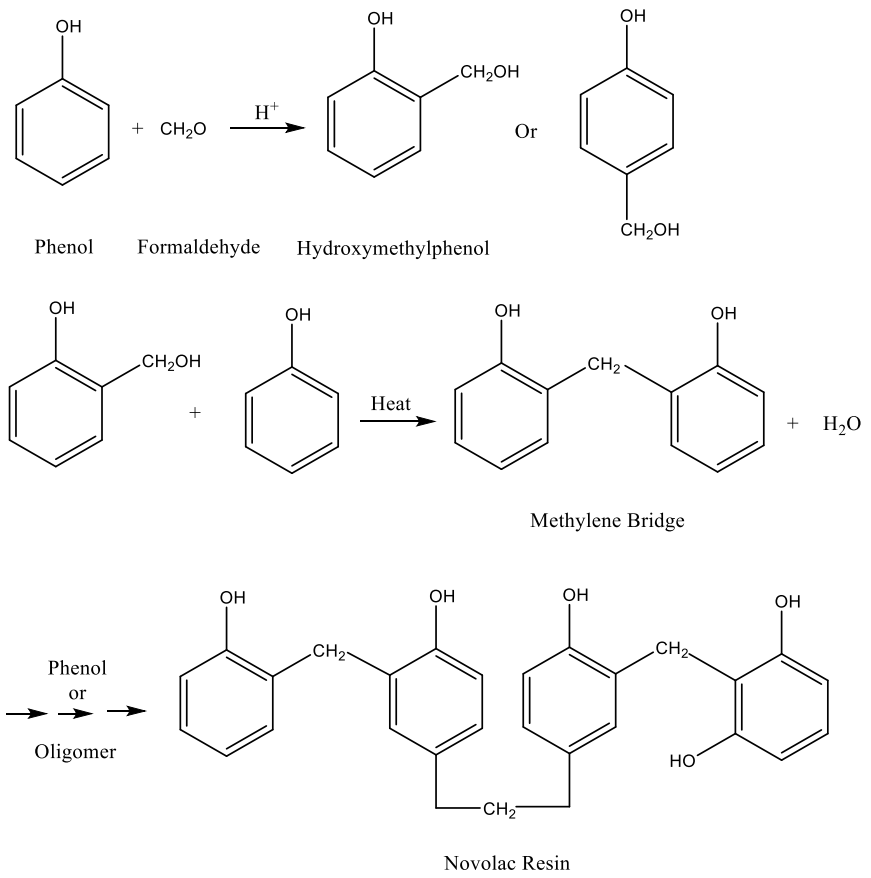

Figure 5. The synthesis mechanism of Novolac resin in acid media

Phenolic foams

Phenolic resoles can be formed into a cellular structure to obtain reduced density and additional desirable properties. To produce phenolic foams a phenolic resole is typically blended with blowing agents (hydrofluorocarbons, pentane or hexane), surfactant and a catalyst[107]. The liquid formulation is discharged into a mould or on a conveyor and expanded at an elevated temperature by the gasification of the blowing agents. Simultaneously the phenolic resole is cured. Phenolic foams with an open cell or closed cell structure can be obtained by precisely controlling the polymerisation temperature and the choice of surfactant[108, 109].

Closed-cell phenolic foams have very low thermal conductivity and, therefore, are suitable for thermal insulation of buildings, such as roofing, flooring, cavity walls and in other industrial applications, including heating and ventilation applications, such as insulating pipes, tanks and duct insulation. They also used in building applications and in the food processing industry for steel faced panels[110]. Due to their excellent flame-resistant properties[111], phenolic foams are superior in providing excellent thermal insulating as well as reducing fire risks as compared to other insulating polymer foams, such as PU, PE, and PS foams.[112].

Despite their excellent fire resistance and low smoke density and toxicity, and non-dripping behaviour during combustion[113], phenolic foams have some deficiencies, such as brittleness and low mechanical properties, which does limit their applications[114]. Therefore, researchers have attempted to address these deficiencies by incorporating modifiers, inert fillers and synthetic fibres into phenolic foams[115]. Auad et al.[116] used epoxy resin to modify phenolic foams to improve the compressive and shear properties and to reduce the friability of the foams. However, the flammability of the modified foams increased significantly. Shen and Nutt[113] produced phenolic foams with increased compressive properties by incorporating glass fibres into phenolic foams. Moreover, some nanomaterials have also been used to modify phenolic foams. Ma et al.[117] used elastomeric poly(nitrile butadiene) rubber (NBR) nanoparticles to toughen the phenolic resin, resulting in improved impact and flexural strengths. Yang et al.[118] reported the preparation of multi-walled carbon nanotubes (CNT) reinforced phenolic foams. The presence of CNTs in the phenolic foams improved their compressive strength, thermal stability and thermal conductivity.

2.4. POTENTIAL RESIN SYSTEMS: EPOXY RESIN

Epoxy resins or polyepoxides are obtained by the polymerisation of epoxide monomers[119]. They are characterized by the presence of two or more epoxide groups in their structure[120]. These materials possess high adhesiveness to many substrates, excellent mechanical properties and good chemical and thermal resistance after curing. Epoxy resins are intensively used for a various applications, such as matrix for fibre reinforced composites, high-performance coatings, adhesives, glue and bonding agents and encapsulating materials[121, 122]. Epoxy resin were discovered in 1936 by P. Castan, a Swiss chemist.[123] He synthesised epoxy resin from epichlorohydrin and bisphenol A; such diglycidyl ether of bisphenol A (DGEBA) is the most commercially used epoxy resin[124] (Figure 6).

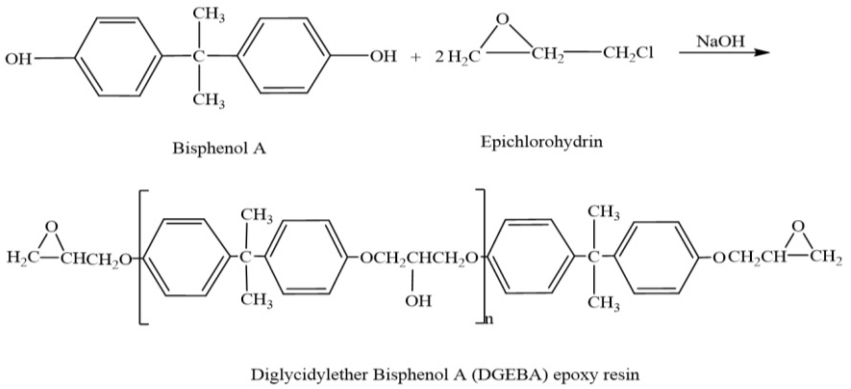

Figure 6. Synthesis of bisphenol A diglycidyl ether epoxy resin

The properties of DGEBA epoxy resins are highly dependent on the number of repeating units, which is dependent on the stoichiometry of synthesis reaction[125]. Usually, the repeating unit can range from 0 to 25 in many commercial products. Moreover, bisphenol F is obtained by the reaction of epichlorohydrin and diglycidylether bisphenol F (DGEBF) (Figure 7). Because of the absence of the methyl groups, the viscosity of bisphenol F resins is typically 1/3 (2,500-5,000 mPa s) of that of bisphenol A resins and thus they are used in applications requiring less viscous resins[126].

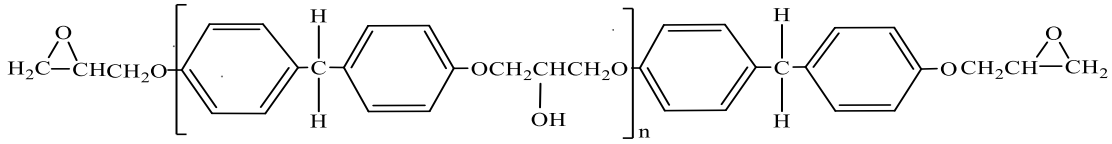

Figure 7. Diglycidylether Bisphenol F (DGEBF) epoxy resin

There are two main categories of epoxy resins, namely glycidyl epoxy and non-glycidyl epoxy resins[127]. Glycidyl epoxy resins are glycidyl ether, glycidyl ester and glycidyl amine resins[128] and non-glycidyl epoxy resins are either aliphatic or cycloaliphatic epoxy resins[129]. Glycidyl epoxies are prepared by the condensation of dihydroxy compounds, diacids or diamines and epichlorohydrin. Non-glycidyl epoxy are synthesised by peroxidation of olefinic double bonds[130]. Novolac epoxy resins are synthesised by reacting phenolic novolac resin with epichlorohydrin in the presence of NaOH as catalyst[131] (Figure 8). Novolac epoxy resins possess excellent mouldability, mechanical properties, excellent electrical properties, heat and humidity resistance[132].

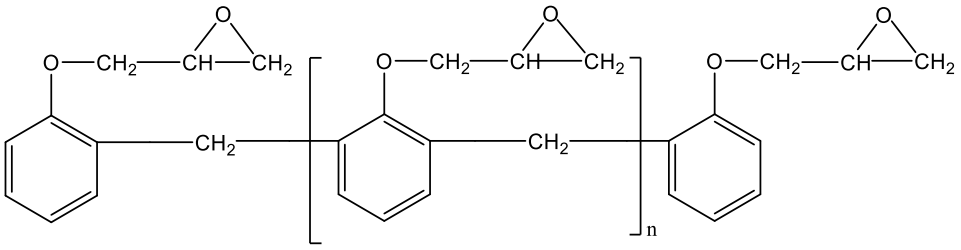

Figure 8. Structure of novolac epoxy resin

Epoxy resins can react with curing agents, which are usually called hardener, to produce epoxy polymers through a crosslinking process[133]. Since the reaction is an irreversible, exothermic polyaddition, the epoxy polymer cannot decompose into epoxy resin and hardener, and no by-products form during curing[123]. Typical curing agents are amines, amides, imidazoles, acid anhydrides, phenols, boron trifluoride complex, metal oxides and mercaptans[134, 135]. Some of these substances, such as amines, amides and some mercaptans, are able to react with epoxy resins at room temperature, while other curing agents usually need an elevated temperature to accelerate the curing process[136] (Figure 9).

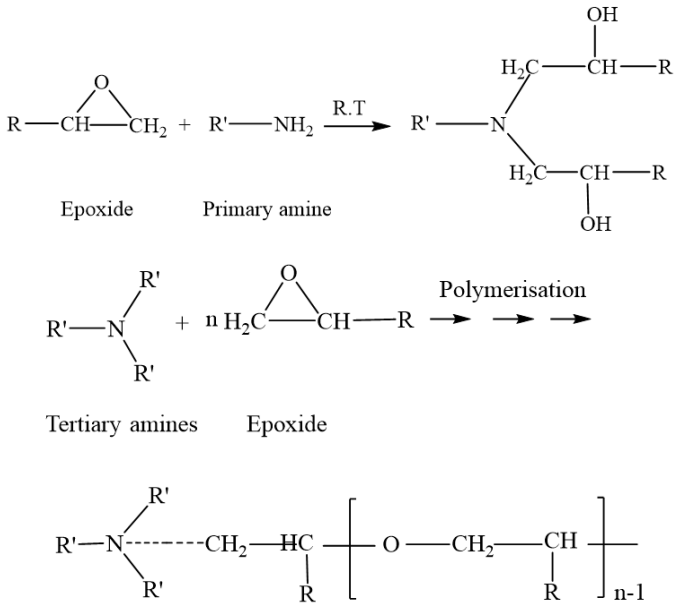

Figure 9. Curing process of epoxy with amine hardener

Gel point [137] or gel time, measured immediately after mixing epoxy resin with a hardener, is the time it takes for a mixed resin system to become so viscous that it can no longer be considered to be formed or shaped[138-140].

Below T_g epoxy polymers are in the glassy state, while above T_g epoxy polymers behave like rubbery materials[141]. Moreover the T_g is the temperature below which only vibrational motion of polymer molecules is present, whereas, above this temperature, individual molecule segments are able to move relative to each other[142]. The glass

transition temperature of epoxy resin increases as curing progresses[143]. In other words, the T_g is the onset of the verification process, and it happens when T_g is so close to the curing temperature[144,145]. T_g in cured epoxy is dependent on the molecular structure, such as crosslink density, the stiffness of the polymer backbone, and intermolecular interaction[146], that develops during curing. Therefore, it is closely related to the curing temperature. However, every resin system has an ultimate T_g, which is determined by the formulation that cannot be enhanced by an increase of the cure temperature[147].

In general, epoxy resins are versatile structural engineering materials because they provide a significant balance of chemical and mechanical properties combined with processing versatility[148]. Epoxy linings create a protective barrier in metal containers to prevent canned foods from becoming spoiled or contaminated with bacteria or rust[149]. In addition to this, epoxy resins with high molecular weight, must, as a rule, be dissolved in an organic solvent to be manageable which limits usage to paints and lacquers[150].

Epoxy foams

Creating epoxy foams by generating pores within the epoxy resin results in weight reduction but aims to conserve other properties. In some applications, for example in the automotive and aerospace sector, weight reduction of a component also results in the reduction of the total weight of vehicles, thus resulting a reduced fuel consumption and emission[151]. Epoxy foams, received particular attention in the composite sector because of their high strength[152], low water absorption[153], good dimensional stability, heat resistance and chemical resistance[154, 155]. Therefore, epoxy foams are widely used in applications requiring shock, thermal, vibration resistance and to insulate electronic components[156, 157]. Furthermore, epoxy foams are used in lightweight structures such as surfboards or as interior panels and crash-pads in the transportation industry [158].

Conventionally epoxy foams are produced by physical or chemical blowing. Blowing agents are blended into a mixture of epoxy resin, hardener and sometimes other stabilisers, such as surfactant and/or particles. The blowing agents result in gas formation during the exothermic curing process and consequently foam the resin during solidification. Stefani et al.[159] used a polysiloxane as a blowing agent to produce epoxy foams. An extra amino hardener was added to the formulation to allow a part of amino hardener to react with the polysiloxane, releasing hydrogen. However, these two reactions follow distinct kinetics, which makes the crosslinking/foaming process difficult to control. Sodium bicarbonate was also used as blowing agent for the production of

epoxy foams[160], since it thermally decomposes, releasing carbon dioxide and water. Wang et al.[161] prepared epoxy foams using a chemical blowing agent. The produced epoxy foams had a non-uniform pore structure when processed at a higher foaming temperature because of the migration of bubbles in the liquid resin. Unfortunately, the pore morphology affected the flexural strength more significantly. Epoxy foams can also be produced by phase separation techniques. Kiefer et al.[162] prepared a macroporous epoxy foams using chemically induced phase separation. Garcia-Loera et al.[163] synthesised porous epoxies by a polymerisation-induced phase separation process of a degradable thermoplastic polymer. Luo et al.[164] prepared porous epoxy foams with different pore morphologies using chemically induced phase separation. Tao and Anthamatten[165] produced a porous epoxy by controlling phase separation during vapour deposition polymerisation. This technique enabled control over the pore morphology of the epoxy foam.

Epoxy foams were also synthesised by emulsion templating; Wang et al.[166] used colloidal silica to stabilize concentrated emulsions containing epoxy resin/hardener and surfactant in the continuous phase of the emulsions, which were subsequently cured, resulting in macroporous epoxy. Furthermore, epoxy foams were also produced by using mechanically whipping air into a mixture of epoxy and hardener creating stable liquid epoxy froths, which could be cured. Lau et al.[167] frothed air in a viscous bio-based epoxy without surfactant or particles, and subsequently polymerised these froths producing macroporous epoxy. Song et al.[168] frothed the same bio-based epoxy resin and cured the froths at elevated temperatures. Due to the air bubbles expansion at higher temperatures, the bubbles in the froths expanded thus resulting in a higher porosity of the resulting epoxy foams.

2.5. LIGNIN

Lignin is a very complex aromatic biopolymer and is present in the cell walls of majority of land plants. It is the second most abundant natural polymer after cellulose on earth[169]. Lignin is the matrix for cellulose fibrils in the plant cell wall providing strength and rigidity to plant tissue[170]. Lignin consists of up to three different types of nine carbon structure (C_9-unit) or phenyl propane monomers, which contain a phenolic ring with three carbon side chains[171, 172] (Figure 10).

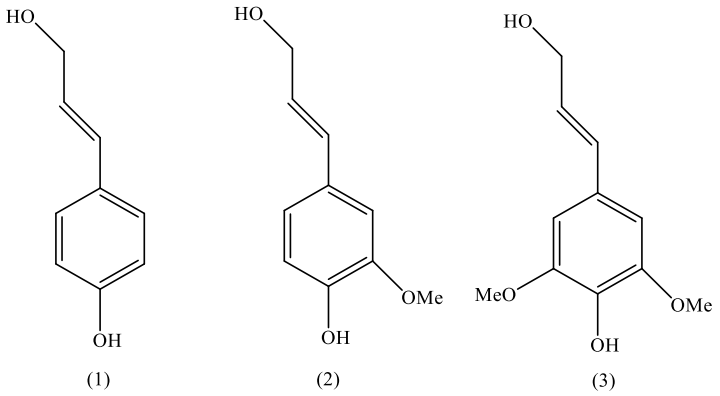

Figure 10. Examples of C_9 monomers: p-coumaryl alcohol (1), coniferyl alcohol (2), and syringyl alcohol (3).

Coniferyl alcohol is present in all species and is the main monomer in conifers (softwoods)[173]. Hardwood species contain up to 40% syringyl alcohol units, while grasses and crops may also contain coumaryl alcohol units[174]. Softwood lignins contain almost exclusively coniferyl alcohol and hardwood lignins both coniferyl and sinapyl alcohol and grasses lignins consisting of all three monomers[175].

The physical and mechanical properties of lignin depend on the botanic body from which the lignin is extracted, the extraction method used and secondary treatments[176]. Several methods are used to extract lignin, such as sulphite and kraft pulping as well as the soda process. The sulphite process has been replaced mainly by kraft (alkaline) pulping.[177] Nevertheless, lignosulfonates isolated from sulphite pulping liquors are still the largest source for commercial lignin with an annual global production of 1.8 million tonnes[178]. Lignosulfonates contain sulfonate groups and are, therefore, can be dissolved in water over a wide pH range. Lignosulfonates are typically used as binders, dispersants and emulsifiers as well as complexing agents[179].

Kraft pulping is now the most important chemical pulping process. It uses strong alkali in combination with a sodium sulphide catalyst to remove lignin from cellulose fibres[180]. The downstream solution with the lignin and hemicellulose removed during the pulping step is called “black liquor”. Black liquor is typically used as fuel and burned to produce energy to operate the mill and to regenerate the inorganic pulping reagents[181]. Different from lignosulfonates, kraft lignins do not contain sulfonate groups and, therefore, are only soluble in very alkaline solutions (pH > 10). Kraft lignin can be precipitated from black liquor by lowering the pH[182]. Figure 11 shows a representative kraft lignin fragment highlighting the typical bonding patterns.

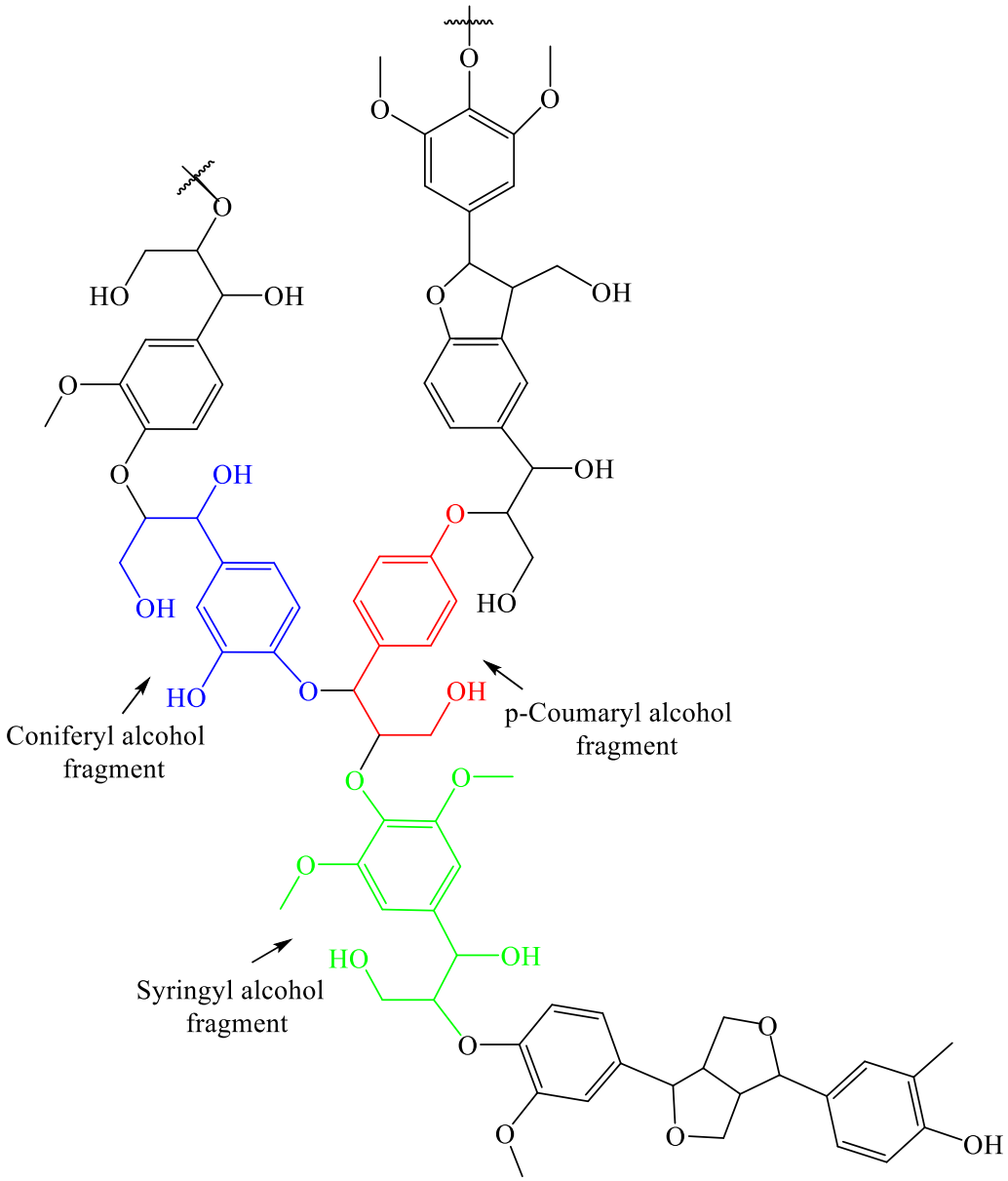

Figure 11. Fragment of the representative kraft lignin structure

In the soda process, lignin is extracted from the botanic body by using an alkaline solution; the pulping conditions are similar to kraft process but without the use of hydrogen sulfide. In this process the fibrous material dispersed in 13-16% sodium hydroxide (i.e. soda) is heated in a pressurised reactor to 140 – 170 °C. The ratio of liquid to dry fibre is typically 5:1. In the process, lignin is separated from cellulose, and is suspended in the liquid phase. The liquid phase (pulp) containing black liquor is separated from the solid phase containing cellulose fibres[183]. Soda process is preferable for chemical pulping of non-wood materials because of its economical viability on a small scale. Soda lignins are almost identical to kraft lignins and significantly different from lignosulphonates, as they have low molecular weight and contain only low amounts of sugar and ash contaminants and are insoluble in water[184].

Due to the absence of sulphur and closeness to lignin in nature, soda lignins have potential applications that are not available to kraft and sulphite lignins. For example, they can be used more readily as binder in thermosets. Moreover, they are used as a substitute for phenol[172] to produce phenolic resin or phenol formaldehyde (PF) resin used as binder in plywood[185].

Lignin foams

Lignin is not commonly used raw material for the production of solid foams. It has, however, been utilized as an additive for the manufacturing of PU foams and composites[186]. Lignin-based foams were described by Stevens et al.[187], they prepared a biodegradable foam panel from starch and kraft pine lignin. Such starch-lignin foams could be used as packaging/fill materials in containers for single or short-term use as biodegradable alternative to foamed polystyrene. Qu et al.[188] reported the use of lignin-phenol-formaldehyde (LPF) resin as precursors for the production of carbon foams. Lignin extracted from sedge grass has been used to replace 25 wt.-% of the phenol to prepare the LPF resin. A PU foam serving as template was impregnated with LPF resin and carbonised. The carbon foams possessed an open cell pore structure, a low bulk density and good water repellency. The most common use of lignin is to substitute petroleum derived polyols. It was shown that this results in improved compression properties of PU foams. Jeon et al.[189] prepared a flexible polyurethane foam using both kraft lignins and polyethylene glycol (PEG) as polyols. The results showed an improved compression modulus of PU foams when using a higher lignin to PEG ratio. Nevertheless, Liu et al.[190] concluded that the mechanical properties of lignin-based PU foams were not as good as those of their conventional counterparts. However lignin did contribute to the high thermal degradation temperatures and lower thermal conductivities to the lignin based PU foams. Xie et al.[191] produced bio-polyols from the microwave-assisted liquefaction of bamboo; lignin derivatives in the crude bio-polyols (CBP) were removed by the addition of water, which resulted in fractionated bio-polyols (FBP). Both lignin fractions were acceptable substitutes for polyols for the production of PU foams. The PU foam made from CBP had a superior thermal stability compared to that made from FBP. However, the presence of lignin derivatives in CBP affected the formation of PU foam, resulting in pores with irregular shapes containings cracks and more wrinkles. Aerogels are an important class of porous materials, which have a range of applications, including insulators, catalyst, adsorbent, etc.[192]. These materials are usually prepared by sol-gel polymerisation of resins, followed by solvent exchange to

recover the areogel. Phenolic resins such as resorcinol-formaldehyde are excellent precursors for the production of aerogels[193]. Chen et al.[194] have partially replaced resorcinol by lignin to produce resorcinol-lignin-formaldehyde resins in an aqueous solution of NaOH followed by subsequent drying to create aerogels.

Emulsion templated Lignin-based porous materials have also been produced using black liquor as a raw material[195]. The black liquor containing 40% lignin (w/v), epichlorohydrin as a crosslinker and a surfactant were used as continuous aqueous emulsion phase and castor oil was used as dispersed phase. Castor oil in black liquor emulsions with an emulsion phase volume ratio of 55% were successfully produced. The emulsion template was heated to crosslink the lignin present in the continuous phase with epichlorohydrin. The castor oil dispersed in crosslinked lignin monoliths was removed by extraction with ethanol, which resulted in a porous lignin foam with an interconnected pore morphology. Depending on the nature and amount of surfactant, the lignin foams had average pore sizes ranging from about 5 to 50 µm in diameter. Foulet et al.[196] prepared porous lignin monoliths by crosslinking the lignin in castor oil-in-black liquor and 1,2-dichloroethane-in-black liquor medium internal phase emulsion templates. The results of their experiment showed that using either castor oil or 1,2-dichloroethane as organic internal phase gave materials with similar morphology. However, using 1,2-dichloroethane allowed for the production of lignin foams with higher porosity and openness.

2.6 SUMMARY

Macroporous polymers have been widely explored in various industries due to their characteristic light weight as well as their tailor-made, outstanding physical, mechanical, chemical and biological properties. Conventionally, macroporous polymers can be produced using various methods; the majority of them does require different kinds of porogens, which cause problems to the environment and the production of the foams. Alternatively, mixing air into resins, dispersing it in bubble form thus creating froth templates, followed by polymerising the resins has been used to produce polymer foams. This air templating method is especially advantageous as it uses only air as templating phase. Moreover, purification of the polymerised or solidified macroporous polymers is not needed. Therefore, in this doctoral work, the air templating method will be further explored for the production of well-controlled polymer foams. Fundamentally it is aimed to investigate the applicability, scalability and versatility of air templating. Furthermore, manufacturing air templated polymer foams with practical applications is

also intended. Phenolic foams possess an excellent fire resistance and are great thermal insulators. However, such foams have so far only been produced using blowing agents or hollow spheres as porogens. Lignin is the second abundant biobased polymer. The lignin extracted from wood during the pulping process has hardly found high value-added applications but is used as fuel for energy recovery. Although lignin foams have been produced using the emulsion templating method, the purification of lignin foams and solvent reuse during the process are very energy consuming. Epoxy foams have been produced using chemical blowing agents; their good mechanical properties and light weight render them useful for applications as foam cores for sandwich composites. However, it remains an open question how to produce stable liquid epoxy foams suitable for air templating. Therefore, the previous research work on these materials motivated the material selection in this work; air templated phenolic foams, lignin foams and epoxy foams will be produced to reach the fundamental research goals and to explore their potential practical applications.

3. AIR TEMPLATED MACROPOROUS POLYMER FOAMS

Due to the easy production and stabilisation of aqueous froths this work started with formulation of phenolic froths and the synthesis of air templated phenolic foams. Furthermore, the scale up of the froth production was investigated. Furthermore, a potential application of the phenolic foams was demonstrated by using them as precursors for manufacturing large panels of carbon foams. An aqueous phenolic resole Cellobond J2027L and catalyst Phencat 382 was mechanically whipped using a 450 W egg beater. To start, about 10 g phenolic resole and 1 g catalyst were frothed for 10 min in a free-standing centrifuge (Falcon®) tube. However, this mixture of resole and catalyst could not be frothed. Therefore, a surfactant was added into the mixture to assist the frothing. Furthermore, in order to achieve a froth with maximum air volume in the aqueous resole solution, a group of surfactants, which are typically used to stabilise hydrophobic matter-in-hydrophilic matter systems, was screened. The screened surfactants included sodium dodecyl sulfate (SDS), 4-(1,1,3,3-tetramethylbutyl)phenyl-polyethylene glycol (Triton X-100), polyethylene glycol tert-octylphenyl ether (Triton X-405), sorbitane monooleate (Span 80), poly(ethylene glycol)-block-poly(propylene glycol)-block-poly(ethylene glycol) (Pluronic L-81) and two types of polyethylene glycol sorbitan monolaurates (Tween 20 and Tween 80). The surfactant concentrations were fixed to 14 wt.-% with respect to the phenolic resole. The phenolic formulation containing Tween 80 produced after mechanical whipping the froth with the highest volume increase, which was stable for more than 3 days, and therefore, was used in the following experiments.

After defining the formulation of the phenolic froths, the scalability of the frothing process to produce liquid phenolic froths and the subsequent phenolic foams was investigated. About 150 ml phenolic formulation can be whipped into froths of a volume of about 0.6 L using the 450 W egg beater. The liquid froths were transferred into a PTFE mould with a volume of 0.56 L. The mould was closed and to shorten the curing time placed in an oven with 50 °C, which resulted in phenolic foams with an interconnected porous structure and average pore sizes of 117 ± 62 µm. To scale up the production of phenolic froths further a large mixer was required. About 600 ml phenolic formulation was whipped using a 1400 W Kenwood mixer, which resulted in 3.3 L phenolic froths. In order to investigate the effect of whipping energy and time on the physical and morphological properties of the phenolic foams, the phenolic formulations were whipped at a power of 467 W, 933 W and 1400 W by adjusting the whipping mixing speed to 33%, 66% and 100% for a period of 10 min to 80 min. The

liquid froths were transferred into either a small PTFE mould with dimensions of 300 mm × 75 mm × 25 mm (0.56 L) and cured at 50 °C for 24 h. The phenolic foams had an interconnected pore structure with average pore sizes ranging from 120 µm to 480 µm. The density and pore sizes of the phenolic foams as a function of whipping time and energy input were investigated. Overwhipping occurred during prolonged whipping; the higher energy input led to overwhipping. By using the 1400 W mixer to produce larger amounts of phenolic froths allowed to manufacture phenolic foam panels with dimensions of 300 mm × 300 mm × 40 mm and a density of 0.18 ± 0.01 g/cm^3. These foam panels were pyrolysed to produce large carbon foam panels with a carbon yield of 48%. Unfortunately, in laboratory settings it was impossible to further scale up the process therefore scale up of the froth production was attempted using industrial mixers. The production of 1.5 kg phenolic froths was carried out using a 10 L vertical mixer at Henschel (Germany). Continuous production and spraying of phenolic froths was conducted using a continuously dynamic mixer at Delta Engineering (Belgium). The experiments and results are described in detail in **Publication I**.

Considering the rather expensive phenolic resole and the content of free phenol and free formaldehyde, a cheap, available biobased raw material was desired to test the air templating method. Crude black liquor (BL), a by-product from kraft pulping, which contains lignin and hemicellulose as the organic components and sodium, potassium salts as the inorganic components. The paste-like BL containing 70 wt.-% solute concentration was diluted with distilled water to reach solute concentrations of 40, 45, 50, 55 and 60 wt.-%. Hypermer 1083 (11 wt.-%) and epichlorohydrin (40 wt.-% with respect to the solute in the BL solutions) were added to 10 g BL solutions and mixed in 50 ml Falcon centrifuge tubes. A 450 W hand mixer was used to mechanically whip air into the mixture for either 6, 9 or 16 min to produce stable BL froths. The froths were placed in an oven at 50 °C to allow for the crosslinking of the lignin and hemicellulose. Afterwards, the solid lignin-based foams had to be washed with ethanol, HCl and water to completely remove all inorganic and organic impurities from the lignin foams. After drying the lignin foams possessed interconnected pore structures; the density of the lignin foams increased with increasing solute concentrations in the BL due to the increased viscosity of the BL more air could be beaten into the froth **(Publication II).** The lignin foams were pyrolysed in N_2 at 1000 °C to produce carbon foams with a carbon yield of 25 wt.-%. The carbon foams possessed an interconnected macropore structure with an average pore size of 67 ± 33 µm. The average pore size of the carbon foams determined by mercury intrusion porosimetry was 20 µm as compared to 40 µm

for the lignin foams. The surface area of the carbon foams was 18 m^2/g as compared to 1 m^2/g of the lignin foam.

After demonstrating the applicability of the air templating method for aqueous monomer/prepolymer systems it was attempted to produce stable non-aqueous froths. Contrary to aqueous foams, non-aqueous foam templates are difficult to stabilize and have been rarely studied. Epoxy resin (EPL) and hardener (GL1) were used in this work because of the low-cost, low curing temperature and adequate pot-life (about 40 min), which was required to produce epoxy resin froths. However, whipping the mixture EPL and GL1 did not produce any froths. Learning from conventional blowing processes used for the production of epoxy foams, using a surfactant could be a viable method to assist the frothing of the epoxy formulation. The non-ionic surfactant Pluronic L-81 was proved to be the "best" surfactant to aid frothing of this epoxy formulation during screening of a group surfactants, including Triton X100, Triton X405, Hypermer 2296, Hypermer 1083 and Tween 80. Literature[197] showed that the stability of non-aqueous froths does not depends on the reduction of the gas/liquid interface tension but on the rheology of the liquid films. Surfactants do not stabilize non-aqueous froths by reducing the surface tension of the liquid resin/gas interface. It was hypothesised that the surfactant, phase separates from the epoxy system driven by small surface tension differences between the epoxy resin/hardener and the surfactant. Hence, during whipping of the epoxy formulations, the rheology of the heterogeneous liquid films improved the stability of the froths. The liquid EPL/GL1/Pluronic L-81 froths produced were stable at room temperature and after 1 day, they solidified into solid epoxy foams. In an attempt to accelerate the curing of the froths, the prepared liquid froths were placed into an oven at 60 °C, but the liquid froths collapsed rapidly. To further increase the stability of the epoxy froths, silica particles were added into the epoxy formulations; the viscosity of the formulations increased with increasing silica loading from 0.2% to 10%. The resulting epoxy froths were stable and could be cured at 60 °C to produce epoxy foams. The density of the epoxy foams increased from 0.25 g/cm^3 to 0.55 g/cm^3 with increasing the silica particle loading. Furthermore, the silica concentration in the froths also affected the pore structure of the produced solid epoxy foams; the pore size distribution changed from a monomodal pore size distribution (epoxy foams containing no silica particles but cured at room temperature) to foams with a hierarchical pore structure, in which the large pores were surrounded by smaller pores. The epoxy foams with 5% and 10% silica particle loading possessed, however, non-regular shaped pores. The elastic moduli and crush strengths of the epoxy foams increased with increasing the foam density. The silica particles did not directly reinforce the epoxy resin. However,

the epoxy foams containing silica particles, showing a hierarchical porous structure, possessed higher specific elastic moduli and crush strengths than the epoxy foam with a monomodal pore size distribution. Nonetheless, increasing the silica particle loading to 5 and 10 wt.-% did not further increase the specific elastic moduli and crush strengths. This is because those foams contained non-spherical pores. The pore walls of irregularly shaped pores buckle much easier than the pore walls of spherical pores[94, 167]. Detailed results and discussion can be found in **Publication III.**

4. REFERENCES

[1] K.S. Sing, *Pure & Applied Chemistry* **1985**, *57*, 603.
[2] D.W. Hutmacher, *Biomaterials* **2000**, *21*, 2529.
[3] F. Yalcinkaya, D. Lubasova, *Polymers for Advanced Technologies* **2017**, *28*, 137.
[4] W. Busby, N. R. Cameron, C.A.B. Jahoda, *Biomacromolecules* **2001**, *2*, 154.
[5] R. Frind, M. Oschatz, S. Kaskel, *Journal of Materials Chemistry* **2011**, *21*, 11936.
[6] F. Svec, J. Frechet, *Analytical Chemistry* **1992**, *64*, 820.
[7] M. Ulbricht, *Polymer* **2006**, *47*, 2217.
[8] B. Wicklein, A. Kocjan, G. Salazar-Alvarez, F. Carosio, G. Camino, M. Antonietti, L. Bergström, **2014**, *10*, 277.
[9] X.Y. Liu, M.S. Zhan, K. Wang, *High Performance Polymers* **2012**, *24*, 646.
[10] L. J. Gibson, M. F. Ashby, "Cellular solids'', Second edition, *Cambridge university press,* **1999,** 21
[11] D.J. Kim, S.W. Kim, H.J. Kang, K.H. Seo, *Journal of Applied Polymer Science* **2001**, *81*, 2443.
[12] Á. Kmetty, K. Litauszki, D. Réti, *Applied Sciences* **2018**, *8*, 1960.
[13] M. Biron, "*Thermoplastics and thermoplastic composites"*, Third edition, *Elsevier,* **2018,** 787.
[14] H. Kataoka, S. Yamamoto, S. Narimatsu, *Chromatographia,* **2000**, *56,* 585.
[15] K. Ishizaki, S. Komarneni, M. Nanko, "*Porous Materials: Process technology and applications"*, First edition, Springer Springer US, **1998.**
[16] D. Eaves, "Handbook of polymer foams", *iSmithers Rapra Publishing* **2004**.
[17] A. Menner, A. Bismarck, *Macromolecular Symposia* **2006**, *242*, 19.
[18] M. Tebboth, A. Kogelbauer, A. Bismarck, *Chemical Engineering Science* **2015**, *137*, 786.
[19] M. S. Silverstein, N. R. Cameron, M. A. Hillmyer, "Porous Polymers*'', John Wiley & Sons,* **2011**, 176.
[20] J. Lee, J. G. Kim, J. Y. Chang, *Scientific Reports* **2017**, *7*, 13568.
[21] B. J. Scott, G. Wirnsberger, G. D. Stucky, *Chemistry of Materials* **2001**, *13*, 3140.
[22 M. Nandi, K. Okada, H. Uyama, *Functional Materials Letters* **2011,** *4,* 407.
[23] Y. Wang, Q. Zhao, N. Han, L. Bai, J. Li, J. Liu, E. Che, L. Hu, Q. Zhang, T. Jiang, S. Wang, *Nanomedicine: Nanotechnology, Biology and Medicine* **2015**, *11*, 313.
[24] A. Bajpai, S. Shukla, "Macroporous Polymeric Materials", in *Macroporous Polymers*, CRC Press, **2009**, 237.
[25] G. Pritchard, "*Plastics additives: an AZ reference"*, Springer Science & Business Media, **2012**.
[26] G. Wypych, ''Foaming and Blowing Agents'', First edition, *Elsevier* **2017**, 1.
[27] S. N. Singh, "*Blowing agents for polyurethane foams"*, iSmithers Rapra Publishing, 2002.
[28] H. Zhou, Z. Wang, G. Xu, X. Wang, B. Wen, S. Jin, *Cellular Polymers* **2017**, *36*, 167.
[29] J. C. Schubert, E. C. LeDuc, US4455272A, **1984**
[30] R. W. Johnson, *International Journal of Refrigeration* **2004**, *27*, 794.
[31] V. Baxter, S. Fischer, J. R. Sand, *ASHRAE journal* **1998**, *40*, 23.
[32] H. Stone, S. Lichvar, C. W. Bredbenner, R. Rupp, E. Minnich, US4906672A, **1990**.
[33] G. Pritchard, "Blowing agents", in *Plastics Additives: An A-Z reference*, G. Pritchard, Ed., Springer Netherlands, Dordrecht, **1998**, 142.
[34] S. Quinn, *Plastics, Additives and Compounding* **2001**, *3*, 16.
[35] J. A. Reglero Ruiz, M. Vincent, J. F. Agassant, T. Sadik, C. Pillon, C. Carrot, *Polymer Engineering & Science* **2015**, *55*, 2018.
[36] N. Sombatsompop, P. Lertkamolsin, *Journal of Elastomers & Plastics* **2000**, *32*, 311.
[37] J. Štěpek, H. Daoust, "Chemical and Physical Blowing Agents", in *Additives for Plastics*, Springer New York, New York, NY, **1983**, 112.
[38] H. Strathmann, K. Kock, *Desalination* **1977**, *21*, 241.
[39] Q. Cai, J. Yang, J. Bei, S. Wang, *Biomaterials* **2002**, *23*, 4483.
[40] C. A. Martínez-Pérez, I. Olivas-Armendariz, J. S. Castro-Carmona, P. E. García-Casillas, "Scaffolds for tissue engineering via thermally induced phase separation", in *Advances in Regenerative Medicine*, InTech, **2011**. 13.

[41] D. R. Lloyd, K. E. Kinzer, H. Tseng, *Journal of Membrane Science* **1990**, *52*, 239.
[42] D. R. Lloyd, S. S. Kim, K. E. Kinzer, *Journal of Membrane Science* **1991**, *64*, 1.
[43] P. van de Witte, P. J. Dijkstra, J. W. A. van den Berg, J. Feijen, *Journal of Membrane Science* **1996**, *117*, 1.
[44] J.W. Kim, K. Taki, S. Nagamine, M. Ohshima, *Langmuir* **2009**, *25*, 5304.
[45] F. Tasselli, "Non-solvent Induced Phase Separation Process (NIPS) for Membrane Preparation", in *Encyclopedia of Membranes*, E. Drioli and L. Giorno, Eds., Springer Berlin Heidelberg, Berlin, Heidelberg, **2015**, 1.
[46] Y. Xin, T. Fujimoto, H. Uyama, *Polymer* **2012**, *53*, 2847.
[47] C. Cohen, G. B. Tanny, S. Prager, *Journal of Polymer Science: Polymer Physics Edition* **1979**, *17*, 477.
[48] G. R. Guillen, Y. Pan, M. Li, E. M. Hoek, *Industrial & Engineering Chemistry Research* **2011**, *50*, 3798.
[49] P. Van de Witte, P. J. Dijkstra, J. Van den Berg, J. Feijen, *Journal of membrane science* **1996**, *117*, 1.
[50] O. Okay, *Progress in Polymer Science* **2000**, *25*, 711.
[51] J. Li, Z. Du, H. Li, C. Zhang, *Polymer* **2009**, *50*, 1526.
[52] J. Li, Z. Du, H. Li, C. Zhang, *Journal of Polymer Science Part B: Polymer Physics* **2010**, *48*, 2140.
[53] J. Kiefer, J. Hilborn, J. Hedrick, H. Cha, D. Yoon, J. Hedrick, *Macromolecules* **1996**, *29*, 8546.
[54] A. Della Martina, L. Garamszegi, J. G. Hilborn, *Journal of Polymer Science Part A: Polymer Chemistry* **2003**, *41*, 2036.
[55] Y. S. Nam, J. J. Yoon, T. G. Park, *Journal of Biomedical Materials Research: An Official Journal of The Society for Biomaterials, The Japanese Society for Biomaterials, and The Australian Society for Biomaterials and the Korean Society for Biomaterials* **2000**, *53*, 1.
[56] B. Mattiasson, A. Kumar, I. Y. Galeaev, "*Macroporous Polymers: Production Properties and Biotechnological/Biomedical Applications"*, CRC Press, **2009**.
[57] J. Reignier, M. A. Huneault, *Polymer* **2006**, *47*, 4703.
[58] S. Aizad, B. H. Yahaya, S. I. Zubairi, *Jurnal Teknologi* **2015**, *75*, 193.
[59] A. G. Mikos, J. S. Temenoff, *Electronic Journal of Biotechnology* **2000**, *3*, 23.
[60] J. Rojek, S. Nosewicz, M. Maździarz, P. Kowalczyk, K. Wawrzyk, D. Lumelskyj, *Procedia Engineering* **2017**, *177*, 263.
[61] R. J. Brook, "Sintering: An Overview", in Concise Encyclopedia of Advanced Ceramic Materials, Elsevier, **1991**, 438.
[62] K. Ishizaki, S. Komarneni, M. Nanko, "Sintering mechanisms and advanced sintering methods for porous materials", in Porous Materials: Process technology and applications, Springer US, Boston, MA, **1998,** *4,* 38.
[63] T. S. Pawatekar, R. B. Rode, *Asian Journal of Pharmacy and Technology* **2014**, *4*, 106.
[64] C. B. Park, M. Nofar, *EP2978801A1*, **2014.**
[65] E. Saiz, L. Gremillard, G. Menendez, P. Miranda, K. Gryn, A. P. Tomsia, *Materials Science and Engineering: C* **2007**, *27*, 546.
[66] Z. H. Zhao, J. N. Chen, *Composites Part B: Engineering* **2011**, *42*, 1306.
[67] B.G. Ahn, U.S. Choi, O.K. Kwon, *Polymer Journal* **1999**, *31*, 851.
[68] A. K. Datye, Q. Xu, K. C. Kharas, J. M. McCarty, *Catalysis Today* **2006**, *111*, 59.
[69] S. Matsumoto, Y. Kita, D. Yonezawa, *Journal of Colloid and Interface Science* **1976**, *57*, 353.
[70] S. Friberg, P. O. Jansson, E. Cederberg, *Journal of Colloid and Interface Science* **1976**, *55*, 614.
[71] J. Lim, S. Wong, M. Law, Y. Samyudia, S. Dol, *Journal of Applied Sciences* **2015**, *15*, 167.
[72] J. L. Knowlton, "Emulsion theory", in Poucher's Perfumes, Cosmetics and Soaps, H. Butler, Ed., Springer Netherlands, Dordrecht, **2000,** 601.
[73] V. H. Bartl, W. Von Bonin, *Die Makromolekulare Chemie: Macromolecular Chemistry and Physics* **1962**, *57*, 74.
[74] D. Barby, Z. Haq, *EP060138*, **1982**.
[75] H. Tai, A. Sergienko, M. S. Silverstein, *Polymer* **2001**, *42*, 4473.
[76] A. Barbetta, R. J. Carnachan, K. H. Smith, C. t. Zhao, N. R. Cameron, R. Kataky, M. Hayman, S. A. Przyborski, M. Swan, "Porous polymers by emulsion templating", in Macromolecular Symposia, Wiley Online Library, **2005,** 226.
[77] C. Stubenrauch, A. Menner, A. Bismarck, W. Drenckhan, Angewandte Chemie, **2018,** *57,* 10024.
[78] N. R. Cameron, D. C. Sherrington, "High internal phase emulsions (HIPEs) — Structure, properties and use in polymer preparation", Springer Berlin Heidelberg, Berlin, Heidelberg, **1996,** 163.

[79] D. Cummins, P. Wyman, C. J. Duxbury, J. Thies, C. E. Koning, A. Heise, *Chemistry of Materials* **2007**, *19*, 5285.
[80] M. Tebboth, A. Kogelbauer, A. Bismarck, *Industrial & Engineering Chemistry Research* **2015**, *54*, 7284.
[81] V. O. Ikem, A. Menner, A. Bismarck, *Langmuir* **2010**, *26*, 8836.
[82] P. Hainey, I. M. Huxham, B. Rowatt, D. C. Sherrington, L. Tetley, *Macromolecules* **1991**, *24*, 117.
[83] N. R. Cameron, *Polymer* **2005**, *46*, 1439.
[84] R. Owen, C. Sherborne, T. Paterson, N. H. Green, G. C. Reilly, F. Claeyssens, *Journal of the Mechanical Behavior of Biomedical Materials* **2016**, *54*, 159.
[85] Z. Bhumgara, Filtration & Separation **1995,** *32,* 245
[86] M. Ottens, G. Leene, A. A. C. M. Beenackers, N. Cameron, D. C. Sherrington, Industrial and Engineering Chemistry Research, **2000,** 39, 259.
[87] A. Barbetta, "Emulsion-derived (PolyHIPE) foams: optimization of properties and morphology for fluid flow applications", Thesis, Durham University, **2002.**
[88] K. Haibach, A. Menner, R. Powell, A. Bismarck, *Polymer* **2006**, *47*, 4513.
[89] W. Song, K. Barber, K.Y. Lee, *Polymer* **2017**, *118*, 97.
[90] J. J. H. Kelly, *US2261439A,* **1941.**
[91] J. C. Wong, E. Tervoort, S. Busato, U. T. Gonzenbach, A. R. Studart, P. Ermanni, L. J. Gauckler, *Journal of Materials Chemistry* **2009**, *19*, 5129.
[92] L. Marlin, A. J. Durante, E. G. Schwarz, *Journal of Cellular Plastics* **1975**, *11*, 317.
[93] R. Murakami, A. Bismarck, *Advanced Functional Materials* **2010**, *20*, 732.
[94] K.Y. Lee, L. L. C. Wong, J. J. Blaker, J. M. Hodgkinson, A. Bismarck, *Green Chemistry* **2011**, *13*, 3117.
[95] T. H. M. Lau, L. L. C. Wong, K.Y. Lee, A. Bismarck, *Green Chemistry* **2014**, *16*, 1931.
[96] A. Gardziella, L. A. Pilato, A. Knop, "Phenolic resins : chemistry, applications, standardization, safety, and ecology", Second illustrated Springer Science & Business Media, **2013.**
[97] A. Pizzi, K. Mittal, ''Adhesive technology'', Second edition, *Taylor & Francis Group, LLC,* **2003**, 541.
[98] A. Knop, L. A. Pilato, "Phenolic resins'', Second edition, *Springer-Verlag Berlin Heidelberg,* **2013**, 32.
[99] S. A. Song, Y. Lee, Y. S. Kim, S. S. Kim, *Composite Structures* **2017**, *173*, 1.
[100] A. Richard Horrocks, D. Price, Dennis Pricein, *''Fire Retardant Materials''*, Woodhead Publishing, illustrated, reprint, **2001**.
[101] P. W. Kopf, "Phenolic Resins", in *Encyclopedia of Polymer Science and Technology*, John Wiley & Sons, Inc., **2002,** 329.
[102] A. Gardziella, L. A. Pilato, A. Knop, "*Phenolic resins: chemistry, applications, standardization, safety and ecology"*, Springer Science & Business Media, **2013,** 33.
[103] R. Follensbee, J. Koutsky, A. Christiansen, G. Myers, R. Geimer, *Journal of applied polymer science* **1993**, *47*, 1481.
[104] W Hesse, J Lang, "Phenolic Resins", in *Ullmann's Encyclopedia of Industrial Chemistry*, Wiley-VCH Weinheim, Germany, **2004,** 46.
[105] F. Kassebi, B. Mammadov, S. Mohammadian-Gezaz, *International Journal of Polymeric Materials and Polymeric Biomaterials* **2012**, *61*, 323.
[106] A. Pizzi, "*Advanced wood adhesives technology"*, CRC Press, **1994,** 14.
[107] R. C. Clark, D. L. Kavanagh, US4900759A, **1990.**
[108] B. Wallaeys, P. Spanhove, US5444098A, **1995.**
[109] Q. Xu, R. Gong, M.Y. Cui, C. Liu, R.H. Li, *High Performance Polymers* **2015**, *27*, 852.
[110] G. Deshmukh, P. Birwal, R. Datir, S. Patel, *Journal of Food Processing & Technology* **2017**, *8*, 1.
[111] L. Costa, L. R. Di Montelera, G. Camino, E. D. Weil, E. M. Pearce, *Journal of Applied Polymer Science* **1998**, *68*, 1067.
[112] M. Le Bras, S. Bourbigot, G. Camino, R. Delobel, "*Fire retardancy of polymers: the use of intumescence"*, Royal Society of Chemistry, **1998,** 54.
[113] H. Shen, S. Nutt, *Composites Part A: Applied science and manufacturing* **2003**, *34*, 899.
[114] Y. J. Huang, C. H. Wang, Y. L. Huang, G. Guo, S. R. Nutt, *Polymer composites* **2010**, *31*, 256.
[115] H. Shen, A. J. Lavoie, S. R. Nutt, *Composites Part A: Applied Science and Manufacturing* **2003**, *34*, 941.
[116] M. L. Auad, L. Zhao, H. Shen, S. R. Nutt, U. Sorathia, *Journal of applied polymer science* **2007**, *104*, 1399.

[117] H. Ma, G. Wei, Y. Liu, X. Zhang, J. Gao, F. Huang, B. Tan, Z. Song, J. Qiao, *Polymer* **2005**, *46*, 10568.
[118] Z. Yang, L. Yuan, Y. Gu, M. Li, Z. Sun, Z. Zhang, *Journal of Applied Polymer Science* **2013**, *130*, 1479.
[119] Ha Q. Pham Maurice J. Marks, "Epoxy Resins", in *Ullmann's Encyclopedia of Industrial Chemistry*, **2005,** 164.
[120] E. Meijer, "Polyepoxides: formation and properties of their network structure", in *Philips Technical Review*, 1989, 44.
[121] S.J. Park, M.H. Kim, J.R. Lee, S. Choi, *Journal of Colloid and Interface Science* **2000**, *228*, 287.
[122] S.K. Ryu, B.J. Park, S.J. Park, *Journal of Colloid and Interface Science* **1999**, *215*, 167.
[123] C. May, "Epoxy resins: chemistry and technology", second edition CRC press, **1987.** 86.
[124] J. A. Gannon, "History and development of epoxy resins", in *High Performance Polymers: Their Origin and Development*, Springer, **1986,** 299.
[125] F.L. Jin, C.J. Ma, S.J. Park, *Materials Science and Engineering: A* **2011**, *528*, 8517.
[126] G. Ramilo, I. Valverde, J. Lago, J. M. Vieites, A. G. Cabado, *Archives of Toxicology* **2006**, *80*, 748.
[127] M. A. Boyle, C. J. Martin, J. D. Neuner, *ASM handbook* **2001**, *21*, 78.
[128] G. Gibson, "Chapter 27 - Epoxy Resins", in *Brydson's Plastics Materials (Eighth Edition)*, M. Gilbert, Ed., Butterworth-Heinemann, **2017,** 773.
[129] G. Tripathi, D. Srivastava, *International Journal of Organic Chemistry* **2011**, *1*, 105.
[130] S. T. Peters, "Handbook of composites", Second edition, Springer Science & Business Media, **2013.**
[131] C. Martín, G. Lligadas, J. C. Ronda, M. Galià, V. Cádiz, *Journal of Polymer Science Part A: Polymer Chemistry* **2006**, *44*, 6332.
[132] H. Ardebili, J. Zhang, M. Pecht, ''Encapsulation Technologies for Electronic Applications'', Second edition, William Andrew, 2**018,** 64.
[133] B. W. Randall, M. H. Macdonald, US3344117A, **1967.**
[134] G. Pritchard, ''Plastics Additives'', First edition, Springer Netherlands, **1998.**
[135] P. Sharma, V. Choudhary, A. Narula, *Journal of applied polymer science* **2006**, *101*, 3503.
[136] L. Matějka, K. Dušek, I. Dobáš, *Polymer Bulletin* **1985**, *14*, 309.
[137] D. J. Plazek, Z. N. Frund, *Journal of Polymer Science Part B: Polymer Physics* **1990**, *28*, 431.
[138] J. K. Fink, "Chapter 3 - Epoxy Resins", in *Reactive Polymers Fundamentals and Applications (Second Edition)*, J.K. Fink, Ed., William Andrew Publishing, Oxford, **2013**, 95.
[139] A. Shimkin, *Russian Journal of General Chemistry* **2016**, *86*, 1488.
[140] K. J. Abbey, D. J. Zalucha, "The Chemistry of Structural Adhesives: Epoxy, Urethane, and Acrylic Adhesives", in *Handbook of Industrial Chemistry and Biotechnology*, Springer, **2017,** 677.
[141] "5 - Acrylic Polymers and Copolymers", in *Chemical Resistance of Engineering Thermoplastics*, E. Baur, K. Ruhrberg, and W. Woishnis, Eds., William Andrew Publishing, **2016**, 249.
[142] H. Wang, K. S. Siow, *Polymer Engineering & Science* **1999**, *39*, 422.
[143] N.D. Danieley, E.R. Long Jr., *Journal of Polymer Science Part A,* **1981,** *19*, 2443.
[144] J. B. Enns, J. K. Gillham, *Journal of Applied Polymer Science* **1983**, *28*, 2567.
[145] G. Wisanrakkit, J. Gillham, J. Enns, *Journal of Applied Polymer Science* **1990**, *41*, 1895.
[146] A. T. DiBenedetto, *Journal of Polymer Science Part B: Polymer Physics* **1987**, *25*, 1949.
[147] J. M. Dean, N. E. Verghese, H. Q. Pham, F. S. Bates, *Macromolecules* **2003**, *36*, 9267.
[148] M. A. Boyle, C. J. Martin, J. D. Neuner, *ASM Handbook Volume 21 Composites* **2001**, 78.
[149] R. A. Rudel, J. M. Gray, C. L. Engel, T. W. Rawsthorne, R. E. Dodson, J. M. Ackerman, J. Rizzo, J. L. Nudelman, J. G. Brody, *Environmental health perspectives* **2011**, *119*, 914.
[150] J. Fan-Long, P. Soo-Jin, *Journal of Polymer Science Part B: Polymer Physics* **2006**, *44*, 3348.
[151] L. Santo, *Materials Science Forum* **2012**, *165,* 706.
[152] A. Bledzki, J. Gassan, W. Zhang, **1999**, *35,* 550.
[153] C. Soles, A. Yee, *Journal of Polymer Science part B: Polymer Physics* **2000**, *38,* 792.
[154] M. Alonso, M. Auad, S. Nutt, *Composites Part A: Applied Science and Manufacturing*, **2006**, 37, 1952.
[155] E.A. Baroncini, S. Kumar Yadav, G.R. Palmese, J.F. Stanzione III, *Applied Polymer Science*, **2016,** *133*, 44103.
[156] T.I. Wallow, M.C. Hunter, K.L. Krafcik, A.M. Morales, B. A. Simmons, L. A. Domeier, US7390377B1, **2005.**
[157] V. Kochetkov, R. Maksimov, *Mechanics of composite materials* **1996**, *32*, 61.

[158] J.P. Pascault, R.J.J. Williams, " *Epoxy Polymers: New Materials and Innovations'',* John Wiley & Sons, **2009,** 303.
[159] P. M. Stefani, A. T. Barchi, J. Sabugal, A. Vazquez, *Journal of Applied Polymer Science* **2003**, *90*, 2992.
[160] E. Mazzon, A. Habas-Ulloa, J.P. Habas, *European Polymer Journal* **2015**, *68*, 546.
[161] L. Wang, X. Yang, T. Jiang, C. Zhang, L. He, *Journal of Applied Polymer Science* **2014**, *131*.
[162] J. Kiefer, J. Hilborn, J. A. E. Månson, Y. Leterrier, J. L. Hedrick, *Macromolecules*, **1996**, *29,* 4158.
[163] A. Garcia-Loera, F. Cara, M. Dumon, J. Pierre Pascault, *Macromolecules*, **2002**, *35,* 6291.
[164] Y. S. Luo, K.C. Cheng, N. D. Huang, W. P. Chiang, S. F. Li, *Journal of Polymer Science Part B: Polymer Physics*, **2011**, *49,* 1022.
[165] R. Tao, M. Anthamatten, *Macromolecular rapid communications* **2013**, *34*, 1755.
[166] J. Wang, C. Zhang, Z. Du, A. Xiang, H. Li, *Journal of Colloid and Interface Science* **2008**, *325*, 453.
[167] T. H. Lau, L. L. Wong, K.Y. Lee, A. Bismarck, *Green Chemistry* **2014**, *16*, 1931.
[168] W. Song, K. Barber, K.Y. Lee, *Polymer* **2017**, *118,* 97.
[169] P. S. B. d. Santos, X. Erdocia, D. A. Gatto, J. Labidi, *Industrial Crops and Products* **2014**, *55*, 149.
[170] M. Abramson, O. Shoseyov, Z. Shani, *Plant Science*, **2010**, *178,* 61.
[171] O. Faruk, M. Sain, ''Lignin in Polymer Composites'', William Andrew, **2015.**
[172] A. Tejado, C. Pena, J. Labidi, J. Echeverria, I. Mondragon, *Bioresource Technology* **2007**, *98*, 1655.
[173] R. Mortimer, *Journal of Wood Chemistry and Technology* **1982**, *2*, 383.
[174] H. Chen, "*Chemical Composition and Structure of Natural Lignocellulose*", in Biotechnology of Lignocellulose, Springer, Dordrecht, **2014**, 25.
[175] F. S. Chakar, A. J. Ragauskas, *Industrial Crops and Products* **2004**, *20*, 131.
[176] A. García, M. Alriols, G. Spigno, J. Labidi, "*Lignin as natural radical scavenger. Effect of the obtaining and purification processes on the antioxidant behaviour of lignin*", **2012,** 173.
[177] H. Sixta,'' Handbook of Pulp'', First edition, **2008.**
[178] T. Stern, P. Schwarzbauer, *Forest products journal* **2008**, *58*.
[179] A. Thomas, F. Pedram, *ChemSusChem* **2017**, *10*, 1861.
[180] A. Vishtal, A. Kraslawski, "*Challenges in industrial applications of technical lignins*", **2011,** 3547.
[181] P. Tomani, F. Öhman, H. Theliander, P. Axegard, US8172981B2, **2008.**
[182] H. Loutfi, B. Blackwell, V. Uloth, *Tappi J* **1991**, *74*, 203.
[183] S.B. Knapp, J.D. Wethern, US2944929A, **1959.**
[184] W. O. S. Doherty, P. Mousavioun, C. M. Fellows, *Industrial Crops and Products* **2011**, *33*, 259.
[185] J. H. Lora, W. G. Glasser, *Journal of Polymers and the Environment* **2002**, *10*, 39.
[186] S. Laurichesse, L. Avérous, *Progress in Polymer Science* **2014**, *39*, 1266.
[187] E. Stevens, A. Klamczynski, G. Glenn, *Express Polymer Letters* **2010**, *4*, 311.
[188] J.Y. Qu, Q. Han, F. Gao, J.S. Qiu, *New Carbon Materials* **2017**, *32*, 86.
[189] H. Jeong, J. Park, S. Kim, J. Lee, N. Ahn, *Fibers and Polymers* **2013**, *14*, 1301.
[190] Z.M. Liu, F. Yu, G.Z. Fang, H.J. Yang, *Journal of Forestry Research* **2009**, *20*, 161.
[191] J. Xie, J. Qi, C.Y. Hse, T. F. Shupe, *Bioresources* **2013**, *9*, 578.
[192] L. W. Hrubesh, *Journal of Non-Crystalline Solids* **1998**, *225*, 335.
[193] T. Horikawa, J. i. Hayashi, K. Muroyama, *Carbon* **2004**, *42*, 169.
[194] F. Chen, M. Xu, L. Wang, J. Li, *Bioresources* **2011**, *6*, 1262.
[195] C. Forgacz, M. Birot, H. Deleuze, *Journal of Applied Polymer Science* **2013**, *129*, 2606.
[196] A. Foulet, M. Birot, G. Sonnemann, H. Deleuze, *Reactive and Functional Polymers* **2015**, *90*, 15.
[197] S. E. Friberg, *Current Opinion in Colloid & Interface Science* **2010**, *15*, 359.

5. LIST OF ABBREVIATIONS AND SYMBOLS

Abbreviations

AESO	acrylated epoxidised soyabean oil
ATRP	atom transfer radical polymerisation
BET	Brunauer, Emmett and Teller method
BL	black liquor
CBP	crude bio-polyols
CFCs	chlorofluorocarbons
CNT	carbon nanotube
CIPS	chemically induced phase separation
DGEBA	diglycidyl ether bisphenol A
DGEBF	diglycidyl ether bisphenol F
DSC	differential scanning calorimetry
DVS	dynamic vapour sorption
EHL	enzymatic hydrolysis lignin
EPL	epoxy L
FBP	fractionated bio-polyols
FRP	free radical polymerisation
HCFCs	hydrochlorofluorocarbons
HIPE	high internal phase emulsion
LPF	lignin phenol formaldehyde
NBR	nitrile butadiene rubber
OTFE	oligomeric tetrafluoroethylene
PE	polyethylene
PEEK	polyether ether ketone
PEG	polyethylene glycol
PEI	polyetherimide
PF	phenol formaldehyde
PLA	poly (lactic acid)
polyHIPE	polymerised high internal phase emulsion
polyLIPE	polymerised low internal phase emulsion
polyMIPE	polymerised medium phase emulsion

PP	polypropylene
PS	polystyrene
PTFE	polytetrafluoroethylene
PU	polyurethane
PVA	poly (vinyl alcohol)
PVDF	polyvinylidene difluoride
RH	relative humidity
ROMP	ring opening metathesis polymerisation
SDS	sodium dodecyl sulfate
SEM	scanning electron microscope
TGA	thermogravimetric analysis
TIPS	thermally induced phase separation
T_g	glass transition temperature
UV	ultraviolet
XPS	extruded polystyrene

Symbols

ε_f	flexural strain
ρ_f	foam density
ρ_s	skeletal density
σ	crush strength
σ_c	crush strength (in publication I)
σ_f	flexural stress
η	viscosity
μ	micron
A_s	specific surface area [$m^{-2}g$]
b	width
d	diameter
D	maximum deflection at the centre of the beam
d_p	average pore size
d_{pt}	average pore throat size
d_t	average pore throat size (publication II)

E_f	flexural modulus (publication I)
F	measured load
h	thickness
K	Kelvin
kHz	kilohertz
kN	kilonewton
kPa	kilopascal
kV	kilovolt
L	length of support pan
mA	milliampere (unit of electric current)
MPa	megapascal
P	porosity
Pa s	pascal-second
S	the volume increase
S	siemens (unit of electric conductance)
V	volume
V_0	original volume
V_f	secondary volume
W	watt
wt.%	weigh percent

6. PUBLICATIONS

6.1 PUBLICATION I

Mechanically whipped phenolic froths as versatile templates for manufacturing phenolic and carbon foams

Mohammad Jalalian, Qixiang Jiang, Arnaud Coulon, Martin Storb, Robert Woodward and Alexander Bismarck. Materials and Design, Volume 168, 2019, 107658. DOI: org/10.1016/j.matdes.2019.107658

Materials and Design 168 (2019) 107658

Contents lists available at ScienceDirect

Materials and Design

journal homepage: www.elsevier.com/locate/matdes

Mechanically whipped phenolic froths as versatile templates for manufacturing phenolic and carbon foams

Mohammad Jalalian [a], Qixiang Jiang [a,*], Arnaud Coulon [b], Martin Storb [b], Robert Woodward [c], Alexander Bismarck [a,c,**]

[a] Institute of Materials Chemistry and Research, Polymer & Composite Engineering (PaCE) Group, Faculty of Chemistry, University of Vienna, Währinger Strasse 42, A-1090 Vienna, Austria
[b] JSP, ZI Le Bois Chevalier, Route de Francières, 60190 Estrées Saint Denis, France
[c] Polymer & Composite Engineering (PaCE) Group, Department of Chemical Engineering, Imperial College London, South Kensington Campus, London SW7 2AZ, UK

HIGHLIGHTS

- Air was mechanically whipped in phenolic resole to produce stable liquid phenolic froths, resulting after curing in phenolic foams.
- By controlling the whipping power, the densities of the phenolic foams were tailored from 0.18 g/cm^3 to 0.44 g/cm^3.
- The phenolic foams were carbonised; the carbon foams retained the shape and the macroporous structure from the phenolic foams.

GRAPHICAL ABSTRACT

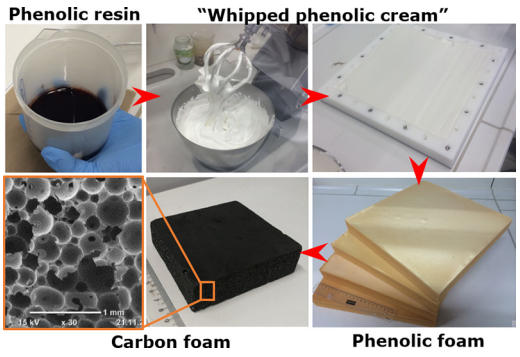

ARTICLE INFO

Article history:
Received 20 December 2018
Received in revised form 11 February 2019
Accepted 12 February 2019
Available online 16 February 2019

Keywords:
Phenolic foams
Froth templating
Carbon foams
Mechanical properties

ABSTRACT

Stable, liquid phenolic froths have been produced by whipping air into a mixture of phenolic resole, catalyst and surfactant. These liquid froths can be moulded into desired shapes and cured to produce open porous phenolic foams. This method, which we call froth templating, has been scaled to produce macroporous phenolic foam panels with a size of 400 mm × 400 mm × 50 mm. The density of the phenolic foams can be tuned from 0.44 g/cm^3 to 0.18 g/cm^3 by controlling the energy input into the liquid formulation, i.e. whipping speed and time. Accordingly, the phenolic foams had elastic moduli ranging from 200 MPa to 50 MPa. The phenolic foams were pyrolysed to produce carbon foams with a carbon yield of 48%. The carbon foams had an open porous structure replicating the phenolic foam precursor and electric conductivity of 17 S/m.

1. Introduction

Phenolic formaldehyde resins are produced by step-growth reactions between phenol and formaldehyde. The main attributes of phenolic formaldehyde resins are their excellent fire resistance and high stiffness while being electric insulators. Phenolic (formaldehyde) foams are commercially available since decades [1]. Closed-cell phenolic foams possess outstanding thermal insulating properties as well as fire resistance and, therefore, can be used as heat and fire barriers in

* Corresponding author.
** Correspondence to: A. Bismarck, Polymer & Composite Engineering (PaCE) Group, Institute of Materials Chemistry and Research, Faculty of Chemistry, University of Vienna, Währinger Strasse 42, A-1090 Vienna, Austria.
E-mail addresses: qixiang.jiang@univie.ac.at (Q. Jiang), alexander.bismarck@univie.ac.at (A. Bismarck).

https://doi.org/10.1016/j.matdes.2019.107658

buildings. Furthermore, because of their high stiffness, phenolic foams have also been commercialized as foam cores for sandwich composite structures, which can be used to protect equipment operating at high temperatures (e.g. ContraFlame® JF-120). The majority of phenolic foams is produced by physical blowing, where phenolic resoles, physical blowing agents, catalysts and surfactants are mixed and transferred into an oven; the heat causes the gasification and expansion of the blowing agents as well as the curing of the phenolic resoles, resulting in solid phenolic foams. However, only phenolic foam panels are usually produced using blowing agents. These panels still need to be machined into the desired shapes. Syntactic phenolic foams are produced by mixing hollow glass spheres into phenolic resoles together with catalysts followed by curing the resin [2]. The conventional methods for producing phenolic foams do require the use of blowing agents or suitable templating materials, which not only increase the cost of the phenolic foams but can also increase environmental burden (for instance, chlorofluorocarbons have been banned as blowing agents for the production of polymer foams) and risks during the production (e.g. pentane is an excellent physical blowing agent but flammable). Other methods to produce phenolic foams have been explored in research scale. Farhan et al. [3] impregnated open porous polyurethane foams with a mixture of pitch and phenolic resoles; the resoles were cured to produce templated porous materials, which were also utilized as precursors to produce carbon foams. Recently, Wu et al. [4] reported foaming and curing phenolic resoles by heating a phenolic resole with dispersed aluminosilicate particles. The pore size distribution of the resulting phenolic foams became narrower with increasing particle loadings from 3% to 7%, while the pore sizes increased with further increasing the particle loadings. Song et al. [5,6] dispersed active carbon, carbon nanotubes or graphene in phenolic resoles. The carbon nanoparticle-in-phenolic resoles were subsequently foamed and cured by microwave heating. The advantage of microwave heating is that the material is evenly heated. Kim and Lee [7] mixed small air bubbles into phenolic resoles and catalysts followed by microwaving the formulation. The small air bubbles nucleated the formation of air bubbles in the resole, while the phenolic resoles simultaneously cured. Although the procedure involved no blowing agents or templating materials, the use of microwave equipment rather than a conventional oven or furnace as a heating means rendered this procedure difficult to be scaled.

As an alternative to common foaming methods involving chemical or physical blowing agents, it is also possible to introduce air into liquid resins or monomers by mechanical whipping to produce stable liquid froths with the resin (or monomers) being the continuous foam phase surrounding the dispersed air bubbles acting as soft templating phase [8]. Curing these froths results in polymer foams whose porosity and morphology can be controlled by the air volume introduced and by air bubble size and geometry, respectively. Wong et al. [9] reported the preparation of air in ethanol/water solutions; polymer particles such as poly(tetrafluoroethylene), poly(vinylidene fluoride), poly(ether imide) and poly(ether ether ketone) were used to stabilise the bubbles in these foams. A group of closed-cell macroporous polymers was produced by drying the liquid froths followed by sintering and thus fusing the polymer particles together. However, the drawback of this method is the shrinkage of the foam associated with the drying and sintering process. A surfactant-stabilised liquid foam with an aqueous solution of polyvinyl alcohol and formaldehyde as the liquid phase was prepared [10] and cured resulting in an open-porous hydrogel. This porous hydrogel was further modified with glutaraldehyde and stearoyl chloride to obtain a hydrophobic surface for solvent absorption and separation purposes. Lee et al. [11] mechanically whipped air in to epoxidised acrylated soybean oil (AESO) with and without bacterial cellulose dispersed in the AESO. The high viscosity of AESO and addition of the bacteria cellulose resulted in kinetic stabilization of the froths hindering drainage of the monomer from the liquid films. However, after polymerisation the macroporous polymers had only a porosity of 59% and possessed non-spherical pores, indicating some instability of the froth templates. Continuing the line of mechanical whipping, Lau et al. [12] produced froths using a viscous bio-based epoxy, which did not contain any (surfactant or particle) stabilisers. These froths were subsequently cured to produce macroporous epoxy resins. The resulting epoxy resin foams had porosities ranging from 75% to 80% and compression moduli of 160 MPa to 88 MPa. In later work, elastomeric hollow spheres were added into the epoxy froths; the cured epoxy foams exhibited improved facture resistance and impact toughness without compromising the compressive moduli and strengths [13]. Renewable materials such as tannin [14] and lignin (black liquor) [15] have also been mechanically whipped into froths, which were cured to produce macroporous materials; these materials were used as precursors for producing carbon foams by pyrolysis.

Aiming for a simple and scalable method, we explored the foam templating route to produce phenolic foams. Air was frothed into formulated phenolic resole systems, which were subsequently cured to produce phenolic foams with well-defined physical, morphological and mechanical properties. In order to scale up froth templated phenolic foams the effect of the energy input, i.e. whipping speed and time, on the physical properties of the resulting phenolic foams was investigated. A potential application of the phenolic foams was demonstrated by using them as precursors for producing large carbon foams.

2. Experimental section

2.1. Materials

Phenolic resole (Cellobond J2027L, an aqueous dispersion containing 87 wt.-% resole) and catalyst (Phencat 382, a mixture of phosphoric acid and C3-C9 alky ester) were purchased from Caleb Technical Products Ltd. (Monmouthshire, UK). Polyoxyethylene (20) sorbitan monooleate (Tween 80) was purchased from Sigma-Aldrich. All chemicals were used as received.

2.2. Preparation of phenolic foams by froth templating

Phenolic resole, catalyst and Tween 80 were mixed in a 600 mL beaker using a 450 W egg beater equipped with a dual-whipping head to whip air into the mixture for 10 min. The liquid phenolic froths were transferred into a PTFE mould with dimensions of 300 mm × 75 mm × 25 mm (V = 0.56 L) and the mould was completely filled. The mould was closed and placed in an oven; the liquid phenolic froths were cured at 50 °C for 24 h.

2.3. Producing phenolic froths using a large mixer and phenolic foams therefrom

Phenolic resole, catalyst and Tween 80 were mixed in a mixer (Kenwood Chef Titanium with a maximum output power of 1400 W) equipped with a single-head whisk. The energy input for producing the froths was controlled to be 467 W, 933 W and 1400 W by adjusting the whipping speed to 33%, 66% and 100%; the whipping time ranged from 10 min to 80 min. The liquid froths were transferred into either a small PTFE mould with dimensions of 300 mm × 75 mm × 25 mm (0.56 L), which was completely filled, or a large PTFE mould of 310 mm × 310 mm × 60 mm (5.58 L), which was partially filled. The moulds were closed and placed in an oven, where the liquid phenolic froths were cured at 50 °C for 24 h. The formulations and whipping conditions of the phenolic froths are summarised in Table 1.

2.4. Preparation of carbon foams

Phenolic foams serving as templates for the preparation of carbon foams were placed into a furnace (Lenton ECF 12/30, Lenton, Hope, UK) and heated to 800 °C at a heating rate of 2 °C/min in a N_2 atmosphere. Once a temperature of 800 °C was reached, the samples were

Table 1
Composition, frothing conditions and curing temperature of phenolic froths.

	Phenolic resole [g]	Catalyst [g]	Tween 80 [g]	Mixer, energy input [W]	Whipping time [min]
A[a]	122.5	7	21.2	Hand mixer, 450	10
B-1	612.5	35	106	Bench mixer, 467	30
B-2	612.5	35	106	Bench mixer, 467	60
B-3	612.5	35	106	Bench mixer, 467	80
B-4	612.5	35	106	Bench mixer, 933	10
B-5	612.5	35	106	Bench mixer, 933	20
B-6	612.5	35	106	Bench mixer, 933	30
B-7	612.5	35	106	Bench mixer, 933	40
B-8	612.5	35	106	Bench mixer, 1400	10
B-9	612.5	35	106	bench mixer, 1400	20
B-10	612.5	35	106	Bench mixer, 1400	30
B-11	612.5	35	106	Bench mixer, 1400	40
C	612.5	52.5	106	Bench mixer, 1400	20

[a] Sample A was whipped using hand mixer, Sample B and C were whipped using bench mixer. Sample A and B were cured in small PTFE moulds (0.56 L); Sample C was cured in large PTFE mould (5.58 L).

held at this temperature for 1 h before the furnace was allowed to cool to room temperature overnight (remaining under a N_2 atmosphere).

2.5. Characterization of the phenolic and carbon foams

The morphology of the phenolic and carbon foams was investigated using scanning electronic microscopy (SEM, JCM-6000, JOEL, Germany). The samples were fixed onto carbon stubs; fracture surfaces of the phenolic foams were gold coated for 40 s at 30 mA using a sputter coater (JEOL Fine coater JF-1200, Germany). The SEM was operated in the secondary electron beam mode using an acceleration voltage of 15 kV. The software ImageJ was used to determine the average pore d_p and pore throat d_{pt} sizes of the macroporous phenolic and carbon foams for which the diameter of at least 150 pores and pore throats were measured.

The foam densities ρ_f were determined by weighing the foams and measuring the sample dimensions:

$$\rho_f = \frac{m}{V} \tag{1}$$

where m is the foam weight and V the foam volume. The skeletal density ρ_s of the phenolic foams was determined by measuring the volume of about 0.5 g powdered foam using a helium displacement pycnometer (Accupyc II 1340, Micrometrics Aachen, Germany). The porosity P of the foams was calculated:

$$P(\%) = \left(1 - \frac{\rho_f}{\rho_s}\right) \times 100 \tag{2}$$

Electrical conductivity of the phenolic and carbon foams was determined using a Potentiostat/Galvanostat/Zero-Resistance-Ammeter (GAMRY instruments reference 600, USA). Samples with dimensions of 16 mm × 16 mm × 7 mm were mounted between two copper electrodes. The measurements were conducted in a frequency range from 150 kHz to 1 kHz with an amplitude of the sinusoidal voltage of 5 mV at room temperature.

The specific surface area A_s of the phenolic and carbon foams was determined by measuring octane adsorption isotherms at 30 °C and 0% relative humidity using inverse gas chromatography (iGC-SEA, Surface Measurement Systems Ltd., London, UK). The flow rate of the vapour phase was set to 10 sccm (standard cubic centimeter per minute). The specific surface area of the samples was subsequently calculated from the corresponding adsorption isotherms, within a partial pressure range of 5 to 37% relative pressure.

Mechanical properties of the phenolic and carbon foams in compression were determined using a universal mechanical tester (Model 5969, Instron GmbH, Buckinghamshire, UK) equipped with a 50 kN load cell. The samples were cut into cubes with dimensions of 15 mm × 15 mm × 15 mm. The samples were compressed at a speed of 1 mm/min by 30% while recording stress-strain curves. Large test specimens with dimensions of 50 mm × 50 mm × 50 mm were also tested using the same test equipment. The samples were compressed at a speed of 5 mm/min following ISO 844. A minimum of five specimens for each sample type were tested to obtain statistically significant values for the elastic moduli E_c and crush strengths σ_c.

Three-point flexural tests on the phenolic and carbon foams were conducted using the same universal mechanical tester equipped with a 1 kN load cell; the tests followed the British standard BS EN ISO 178:2010 + A1:2013. The dimensions of all specimens were 75 mm × 13 mm × 4 mm; the span length was 64 mm. The crosshead speed was 1 mm/min. For each sample, at least five specimens were tested. The flexural stress σ_f was calculated using:

$$\sigma_f = \frac{3FL}{2bh2} \tag{3}$$

where F is the measured load, L the length of support span, b the sample width and h the sample thickness. The flexural strain ε_f was calculated using:

$$\varepsilon_f = \frac{6Dh}{L2} \tag{4}$$

where D is the maximum deflection at the centre of the beam. The flexural modulus E_f was determined from the slope of the initial linear region of the flexural stress-strain curve.

3. Results and discussion

Liquid phenolic froths were produced by mechanically beating air into a liquid mixture of phenolic resole, acid catalyst and surfactant for 10 min using a hand mixer operated at 450 W. The composition of the phenolic resole and the catalyst was suggested by the manufacturer's datasheet, while the surfactant and surfactant concentrations were optimised in order to obtain stable froths with as large froth volume increase as possible (ESI, S1). We identified the optimal surfactant and surfactant concentration to be: 14 wt.-% Tween 80, which resulted in stable liquid phenolic froths. This froths did not collapse at room temperature for three days (during which the liquid froths solidified, ESI, Fig. S3). To shorten the curing time, the liquid froths were transferred in to a PTFE mould and cured at 50 °C. The resulting phenolic foams possessed a skeletal density of 1.31 ± 0.01 g/cm^3 and a foam density of 0.33 ± 0.01 g/cm^3, resulting in a porosity of 75 ± 1%. The froth templated phenolic foams possessed an interconnected porous structure (Fig. 1) with pores of an average size of 117 ± 62 μm. The pores were templated

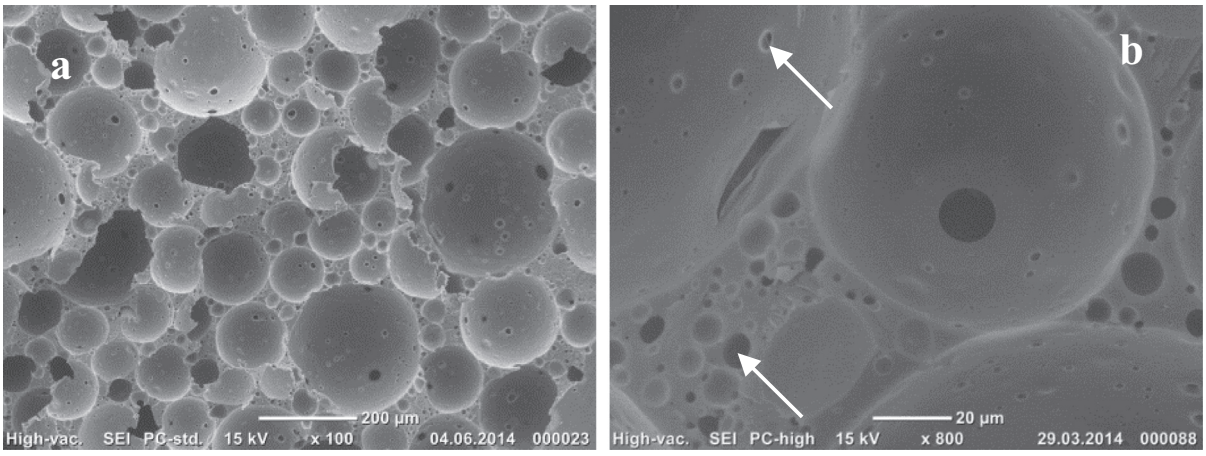

Fig. 1. Interconnected macroporous structure of froth templated phenolic foams produced by curing of froths produced using a hand mixer (a), which possessed a hierarchical pore structure (b).

by the air bubbles in the phenolic froth. The formation of interconnecting pore throats was attributed to the presence of surfactant, which allowed for the formation of thin liquid films compartmenting the air bubbles. During curing of the froths the liquid films contracted [16], leaving pore throats in the resulting phenolic foams or the polymer films thinning during curing raptured thus creating interconnects [17]. Furthermore, smaller closed-cell pores with dimensions less than 10 µm were observed in the plateau boarders; small pore throats of identical sizes were also observed in the pore walls (Fig. 1b, marked with white arrows). Both could be created by the release of volatile components, e.g. water, during the curing of the phenolic froths [18,19].

Scalability of the production of liquid phenolic froths and thus of froth templated phenolic foams was shown by beating air into 750 g of the optimised liquid formulation and curing the froths in small PTFE moulds (0.56 L). The energy input during mechanical whipping was controlled by adjusting the whipping speed and time. When whipping the resin formulation using only 467 W, air introduction into the liquid phenolic froths was very inefficient: 30 min whipping only doubled the volume of the froths approximately as compared to that of the initial liquid phase. Curing these froths resulted in a phenolic foam with a density of 0.44 ± 0.01 g/cm^3 and a porosity of 66 ± 1%. The phenolic foams possessed an interconnected macroporous structure (Fig. 3a) with an average pore size of 149 ± 62 µm. Increasing the whipping time of the resin formulations to 60 min and 80 min did result in reduced foam densities after curing. The resulting phenolic foams had densities of 0.2 g/cm^3 and 0.28 g/cm^3, respectively. Furthermore, these phenolic foams possessed larger pore sizes as compared to phenolic foams that were cured from a 30-min-whipped froth. This indicated that the continuous whipping helped to reduce the density of the phenolic froths and the subsequent foams by introducing more air into the froths and inflating the air bubbles. When doubling or tripling the whipping power of the bench mixer during frothing the resin formulation, we managed to obtain phenolic froths with equivalent density (resulting after curing in phenolic foams with similar densities as the aforementioned foams) within a much shorter time (Fig. 2a). This was as expected as that more vigorous beating is efficient to introduce more air into the liquid phenolic formulation, thus reducing the density of the phenolic froths in shorter (whipping) time. The phenolic foams possessed also an interconnected macroporous structure (Fig. 3b, c), where the pores were much larger than those in the phenolic foams produced by curing froths prepared by low-energy whipping (e.g. 30 min whipping, Fig. 2b). The aforementioned entrapment of large air bubbles during vigorous beating must be companied by the inflation of the air bubbles in the phenolic froths prepared with an energy input of 933 W or 1400 W, resulting after curing in phenolic foams with larger average pore sizes.

When frothing with 1400 W, the density of the phenolic foams increased with prolonging the whipping time, resulting in over-

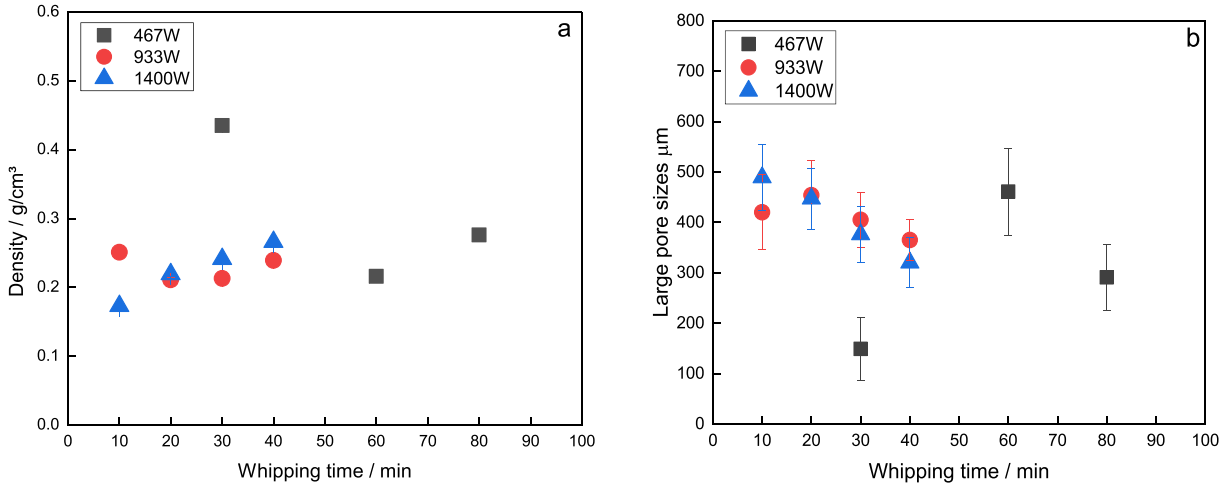

Fig. 2. Foam density (a) and average pore size (b) of the phenolic foams as a function of whipping energy and time used to prepare the phenolic froth templates.

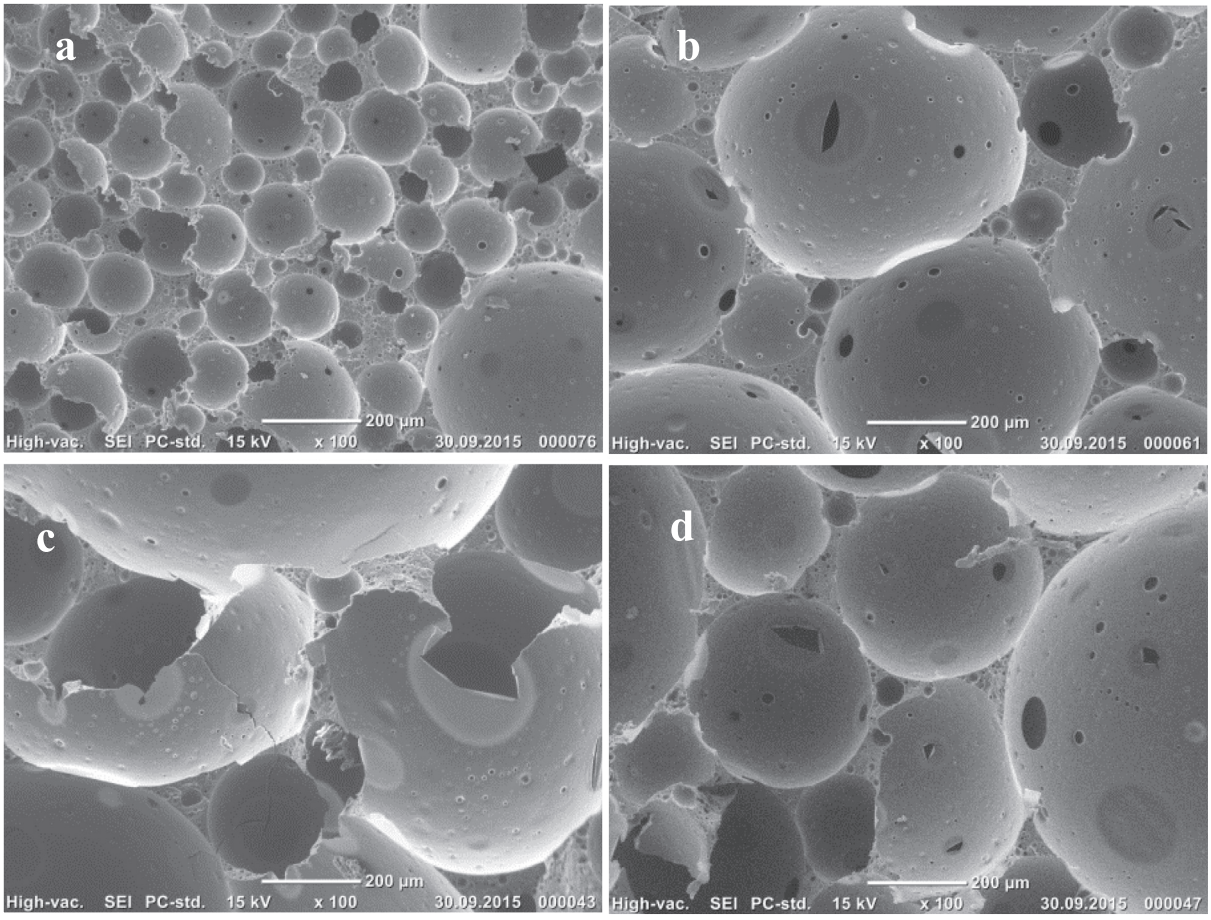

Fig. 3. Representative SEM images of froth templated phenolic foams, whose froth templates were prepared with a whipping energy of 467 W for 30 min (a), 933 W for 10 min (b), 1400 W for 10 min (c) and 1400 W for 20 min (d), respectively.

whipping[1] of the phenolic froths. During whipping the froths, the viscosity of the froths increased because of water evaporation from the resin phase and the onset of crosslinking of the phenolic resins. The increase in viscosity of the froths hindered the introduction of more air during whipping. Furthermore, with the loss of water and onset of crosslinking of the phenolic resin, the surfactant could become less soluble in the resin phase; this could lead to the rapture of liquid lamellas comparting air bubbles, causing release of air from the froths. Furthermore, over-whipping occurred regardless of the power input during whipping; it occurred after 60 min when using 467 W, after 20 min when using 933 W and after 10 min when using 1400 W. The increased power input (higher beating speed) during the frothing created more shear between the mixing head and the phenolic froths; the heat therefrom promoted water evaporation and phenolic resole crosslinking, which lead to over-whipping of the froths. The pore sizes of the phenolic foams reduced slightly for cured overwhipped froths (Fig. 2b and Fig. 3c, d). The decreased air bubble size was due to the air release from the froths during overwhipping.

Large phenolic foam panels were produced by curing froths, which were whipped at 1400 W for 20 min, in a large (5.8 L) PTFE mould. However, the resulting phenolic foam panels contained pores in the millimetre range, which could be either due to coalescence of air bubbles occurring during curing (or the unwanted air pockets introduced during pouring and casting of the liquid froths into the mould). During curing the heat transfer from the outside of the mould to the core of the froths was very slow. The core of the froths therefore cured at lower rate, thus allowing for a more time for the air bubbles to coalesce. In order to produce large phenolic foam panels with a comparable pore structure the curing time had to be reduced, the catalyst concentration in the phenolic froths was therefore increased by 50% as compared to the phenolic froths in group B (Table 1). About 3.3 L phenolic froths were transferred into the large (5.8 L) PTFE mould to be cured. The resulting phenolic panels had dimensions of about 300 mm × 300 mm × 40 mm (Fig. 4). The phenolic foams produced by curing froths prepared with identical whipping energy and curing temperature in a partially filled mould had a lower density of about 0.18 ± 0.01 g/cm^3 as compared to the samples produced in a completely filled mould (which had a density of 0.21 g/cm^3). The exothermal nature of the curing reaction of the phenolic resoles resulted in the expansion of the air bubbles which resulted in phenolic foams with lower density, [20] because we allowed room for expansion.

The mechanical properties of phenolic foams were measured by compression tests. Representative stress-strain curves of phenolic foams exhibit a typical linear elastic region ending in a yield point followed by some post-yield softening (Fig. 5a). In the following plateau region the small stress drops indicated failure of the local structure of the phenolic foams. The elastic moduli and crush strengths of the phenolic foams increased, as expected, with increasing foam density. The curves were fitted using power law equations (Fig. 5b and c) [21]:

$$E_c = a \times {\rho_f}^p \tag{5}$$

$$\sigma_c = c \times {\rho_f}^q \tag{6}$$

[1] Over-whipping is often observed when preparing whipped cream; the whipped cream will change from a soft and creamy to a grainy and broken consistency.

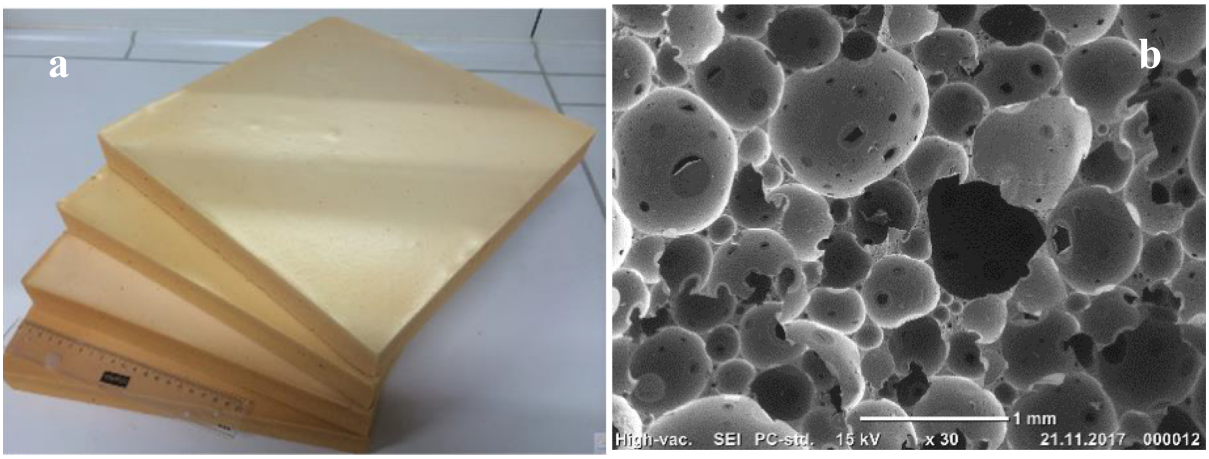

Fig. 4. Phenolic foam panels with dimensions of 300 mm × 300 mm × 40 mm (a). The ruler in the picture is 20 cm long. These phenolic foams possessed interconnected macroporous structure (b).

where a and c are material related coefficients, while p and q are structure related coefficients, describing the degree of the upward concave of the moduli/strength as function of density curves. Ashby [22] modelled and compared the deformation of pores of polymer foams and lattice structures. Lattice structures mainly fail due to stretching of the struts and dislocation of a rigid network; in this case p and q are close to 1. However, the pores in polymer foams (which is considered to be a more flexible structure as compared to a lattice), fail due to buckling or bending of the pore walls. Their stiffness decreases faster with increasing density as compared to lattice structures; this is represented by p and q values close to 2. In our work, p and q are 1.7 and 2.1, respectively, which indicated that our phenolic foams failed by bending and buckling of the pore walls.

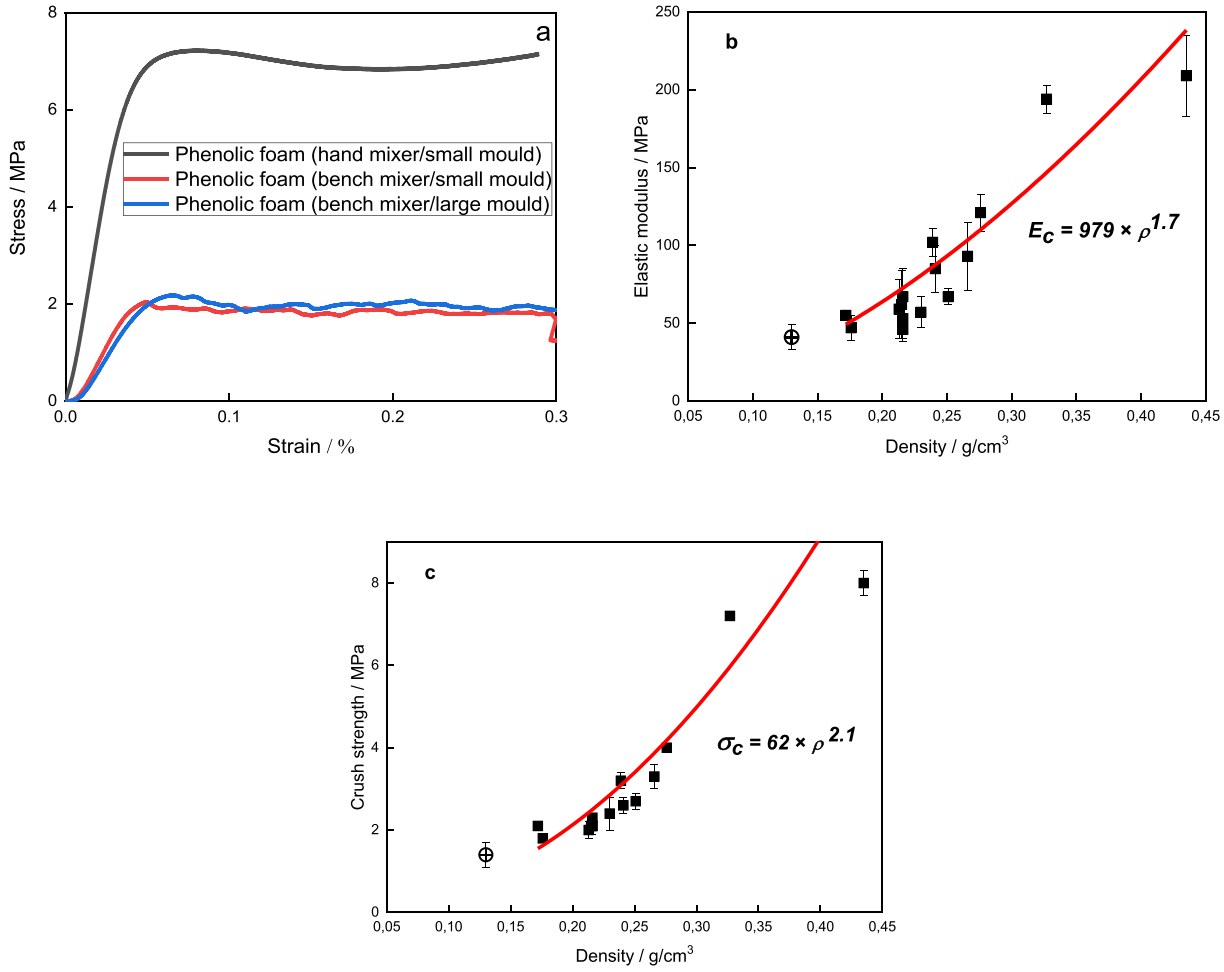

Fig. 5. Representative compressive stress-strain curves of phenolic foams (a), and elastic moduli (b) and crush strengths (c) of phenolic foams as a function of their density, the solid squares represent the test specimens with dimensions of 15 mm × 15 mm × 15 mm, while the crossed circles represent large 50 mm × 50 mm × 50 mm test specimens.

The elastic moduli and crush strengths of froth templated phenolic foams are compared with a group of polymer foams including closed cell phenolic foams. The elastic moduli of the froth templated open porous phenolic foams were lower than those of the closed cell phenolic foams (Fig. 6a). This could be due to the need of a rather high amount of surfactant (14 wt.-% compared to about 1–6 wt.-% typically used for physical blowing of phenolics [23]) necessary to prepare stable phenolic froths and the open porous nature of the resulting foams. The surfactant

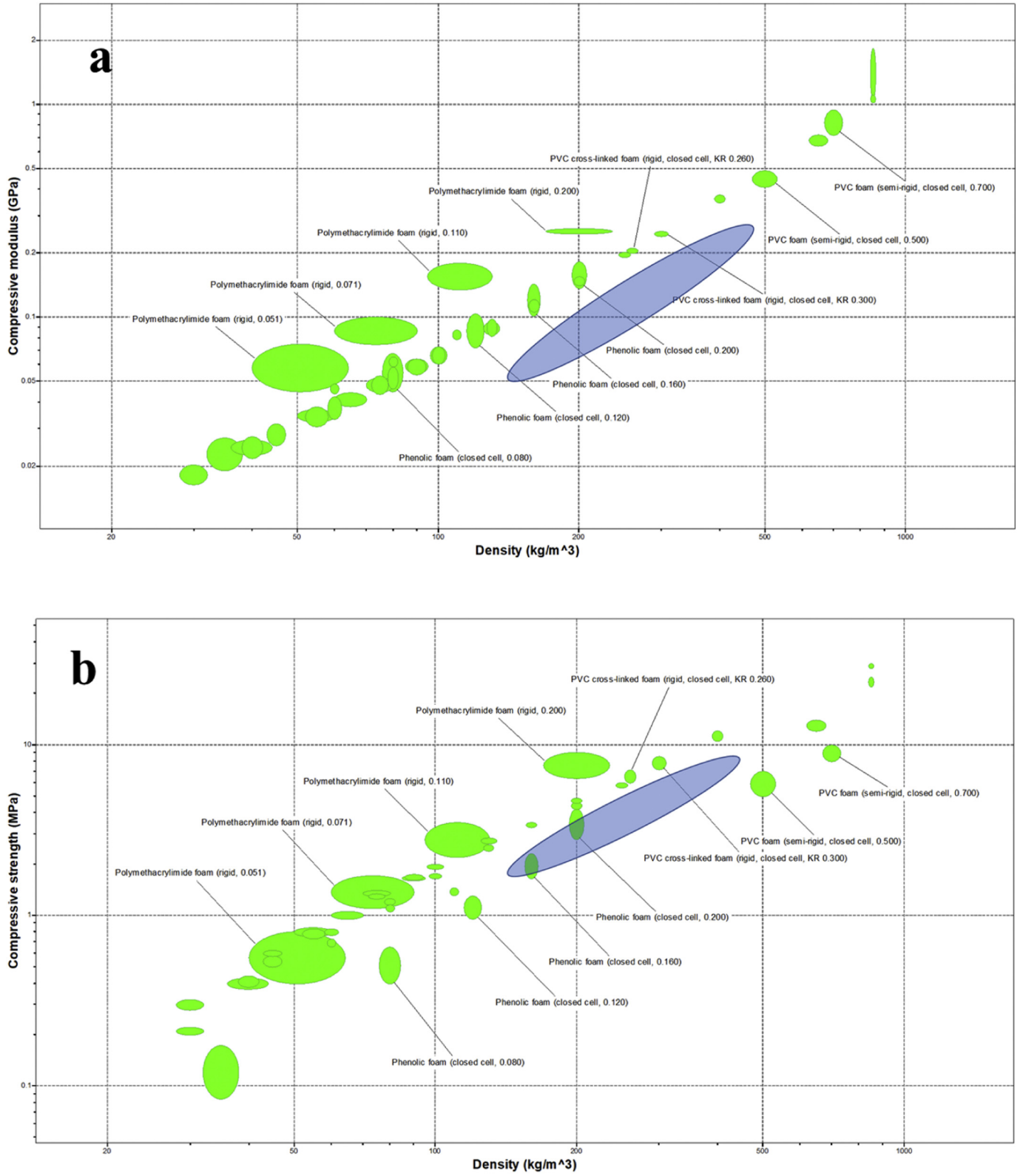

Fig. 6. Comparison of elastic moduli (a) and crush strengths (b) of froth templated phenolic foams with reported data of polymer foams including closed cell phenolic foams. The blue elliptic shapes represent our data obtained for froth templated phenolic foams.

was not removed from the cured phenolic foams, thus plasticising the polymer. However, the crush strengths of the froth templated phenolic foams are comparable to those of the other phenolic foams.

Also, flexural properties of the phenolic foams were investigated. The stress-strain curves (Fig. 7a) start with a liner region, from which the flexural moduli of the phenolic foams were determined. At the end of the first linear elastic region, the slope slightly decreased. This could be due to some local failure of the foam structure caused by compression from the upper pin of the three-point bending geometry. After the linear region the samples fail in a brittle manner at strains of 2% to 2.5%. The flexural moduli and strengths of the phenolic foams were also a function of the foam density; the relation between the flexural moduli and strengths and foam density was fitted using Eqs. (5) and (6). The value of p and q were 1.9 and 2, respectively, which were consistent with the structure related coefficients determined in compression.

We demonstrated that stable liquid froth templates can be produced by beating air into phenolic resole formulations in 50 mL free standing centrifuge tubes, 500 mL beakers and 4.7 L Kenwood mixer. However, 4.7 L was the maximum froth volume we could produce in our laboratory setting. A simple scale-up experiment was conducted at JSP (Estées-Saint-Denis, France) by mixing identical phenolic formulations in two 4.7 L Kenwood mixers. The phenolic froths were moulded and cured at 80 °C to produce phenolic foam panel with a size of 400 mm × 400 mm × 50 mm (Fig. 8). The large panels allowed compression tests on 50 mm × 50 mm × 50 mm specimens. The results in Fig. 5b and c showed that the elastic moduli and crush strengths of the large specimens were align with those of the small test specimens. This indicated the scaling process did not affect the mechanical properties of the froth templated phenolic foams. The large phenolic panels were also subjected for thermal conductivity test at the Building Research Establishment (Watford, UK). The phenolic foam with a density of 0.15 g/cm^3 possessed a thermal conductivity of 0.046 W m^{-1} K^{-1}. This value is similar to the thermal conductivity of Rockwool products, most likely due to their interconnected porous structure.

To demonstrate further scalability, phenolic froths were produced in the application laboratory of Zeppelin System, Henschel (Kassel, Germany). A 10 L vertical FML mixer was used to whip air into 1.5 kg phenolic formulation. A suitable mixing tool (Fig. 9a) was designed and used. Using this mixing tool we were able to produce stable froths with an air volume ratio of about 75% (Fig. 9c). The resulting froths were cured at 130 °C. The volume of the phenolic foams increased due to the thermal air bubble expansion and water evaporation at such high temperature during curing. The resulting phenolic foams had a density of about 0.03 g/cm^3 but, unfortunately, an irregular shape. The success of the froth templating trial using an industrial mixer, which is typically used for scale-up trials indicated the possibility for further scale up of this templating method to larger industrial mixers. Generally, large volumes of whipped liquid phenolic froths could be produced in analogy to whipped cream production in food industry.

However, we did encountered some challenges when producing phenolic froths in large batches, which including the heat generated from the mixers and the difficulty of transferring the highly viscous, compressible phenolic froths. As an alternative to batch production, we tested a continuous production method for phenolic froths, which does allow for on-site production and application of the froths. The

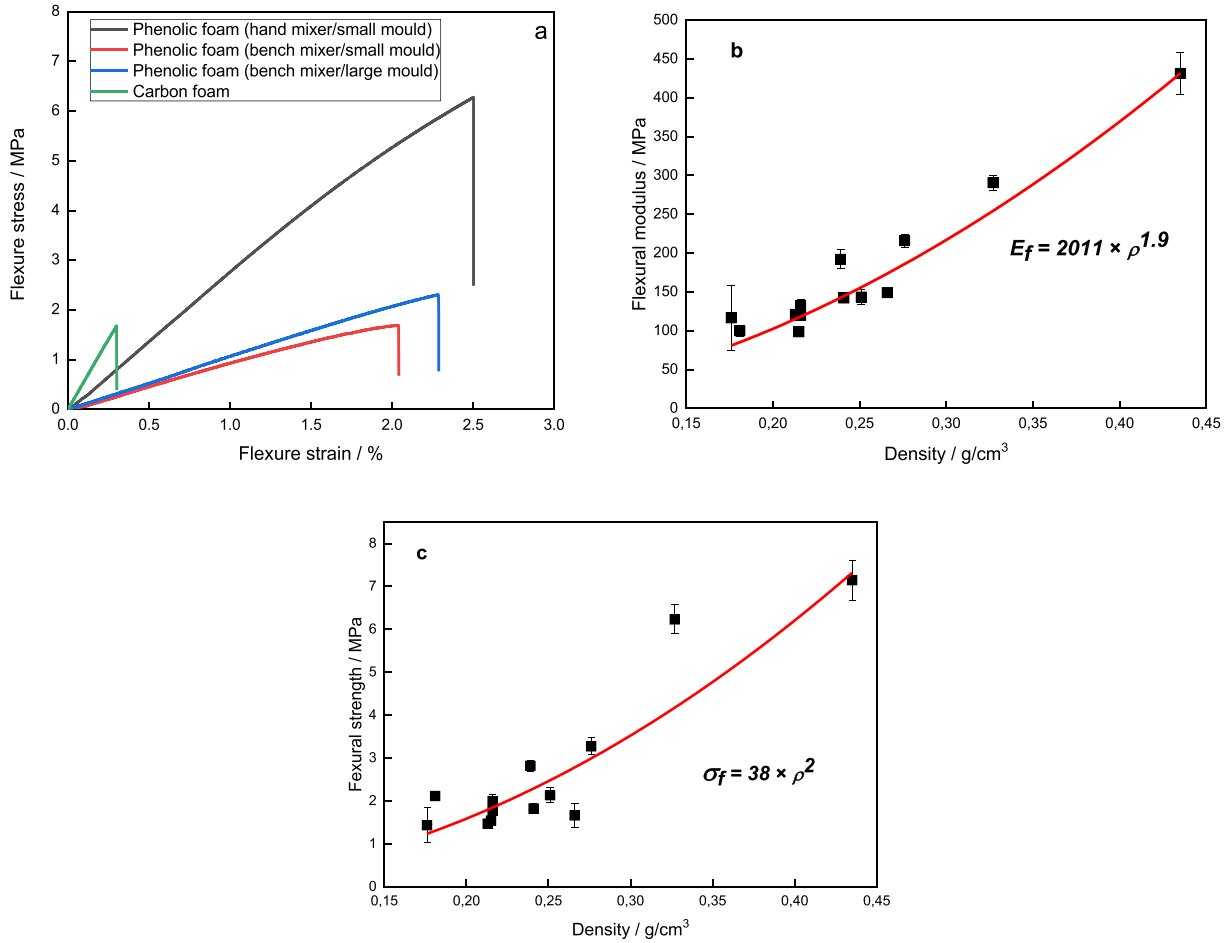

Fig. 7. Representative flexural stress-strain curves of phenolic and carbon foams (a), and flexural moduli (b) and strengths (c) of phenolic foams as a function of their density.

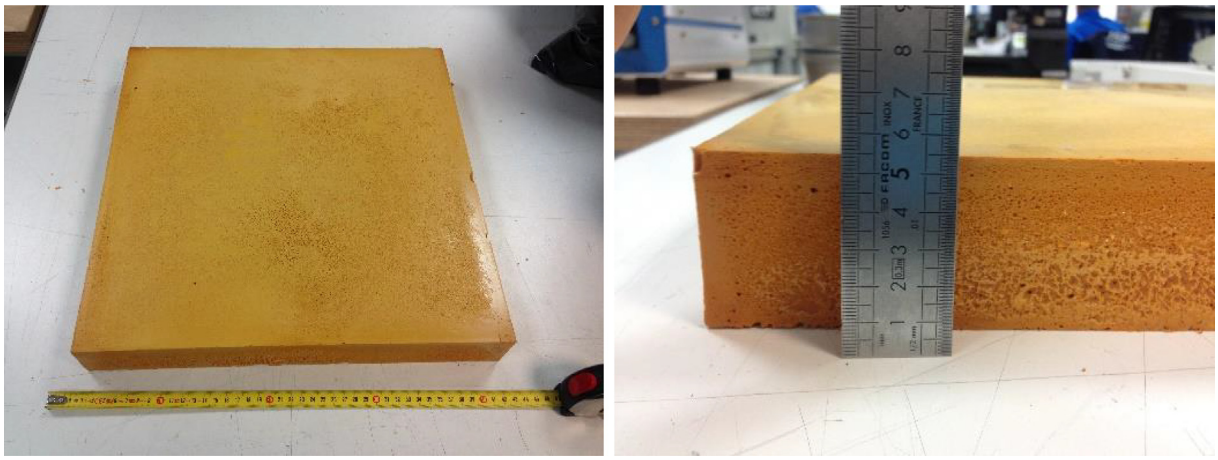

Fig. 8. Phenolic foam panels produced from two batches of phenolic froths.

Fig. 9. Whipping air in to phenolic formulations using a vertical FML Henschel mixer (Kassel, Germany): a) mixing tool, b) the phenolic formulation in the mixer, and c) phenolic froth.

continuous production of phenolic froths was attempted at Delta Engineering (Geraardsbergen, Belgium). The phenolic resole and a mixture of catalyst and surfactant stored in individual tanks as well as a compressed air were injected through a dynamic mixer continuously (Supporting video); the resulting phenolic froths could be sprayed out from a nozzle into a bucket. The phenolic froths possessed a density of about 0.5 g/cm^3. This preliminary work demonstrated the possibility of using continuous dynamic mixers to produce large quantities of phenolic froths, which can be sprayed to fill gaps or cover surfaces.

The attractiveness of the froth templating method is the liquid nature of the stable phenolic froths, which can be poured, casted or moulded into desired shapes. The subsequent curing of the moulded phenolic froths results in net-shaped functional phenolic foam parts, which do not need further machining. To demonstrate moulding, the produced phenolic froths were injected into polypropylene tubes with a diameter of about 8 mm; curing of the froth resulted in cylindrical phenolic foams embedded in the tube (Fig. 10a). Such phenolic foams with complex shapes or high aspect ratios are difficult to be produced by moulding, foaming and curing phenolic resoles with blowing agents, as the orientated expansion of froths during blowing does not guarantee complete filling of the moulds.

To demonstrate further applications of phenolic foams, panels were pyrolysed to produce large carbon foam panels replicating the shape of the initial phenolic foam precursors (Fig. 11a). The carbon yield after pyrolysis was 48%. The volume of the carbon foam as compared to the phenolic foam precursor decreased by 50%. The carbon foams had a skeletal

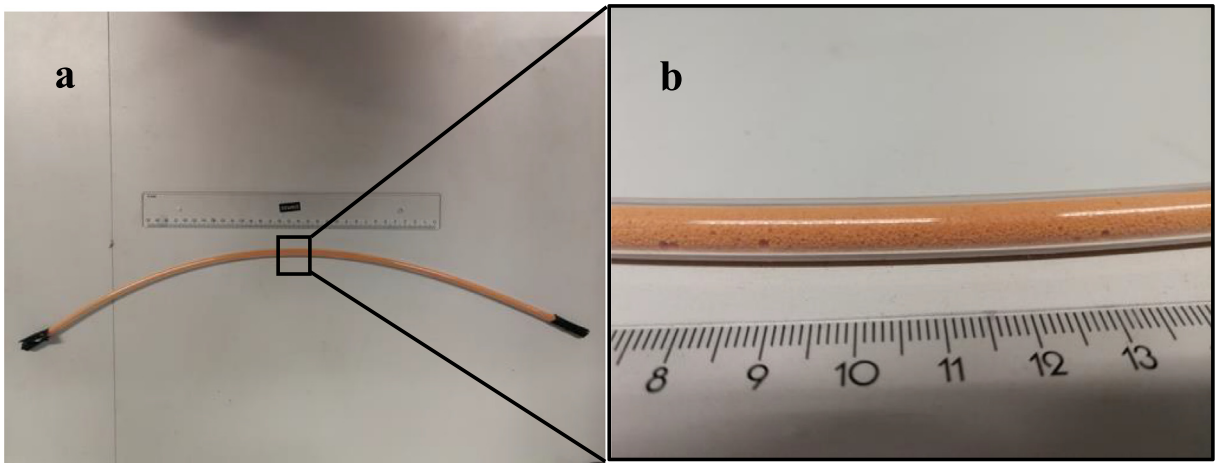

Fig. 10. Demonstration of the mouldability of phenolic froths; a liquid froth was injected into a polypropylene tube resulting after curing in a phenolic foam rod filling the tube.

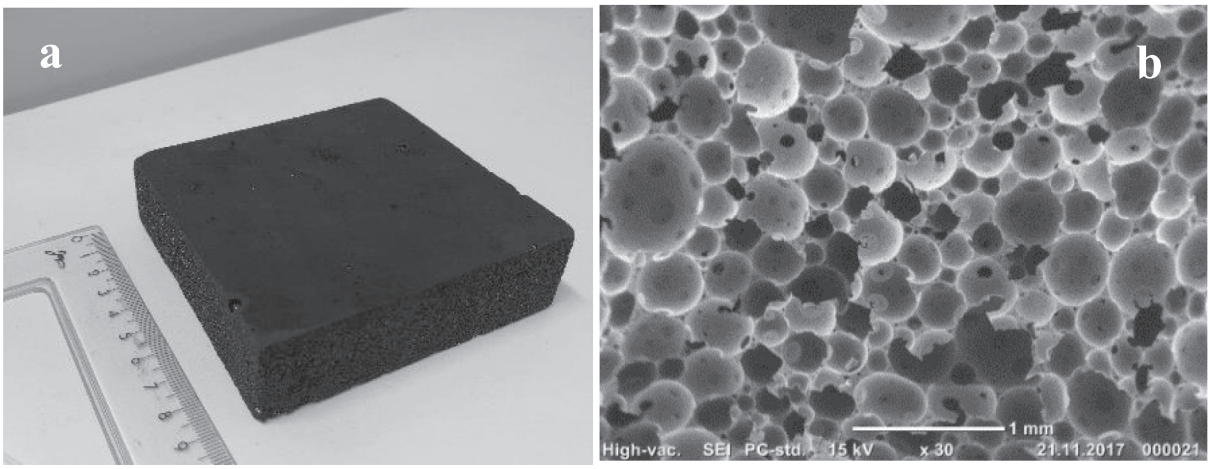

Fig. 11. Monolithic carbon foam (a), which were produced by pyrolysis of phenolic foams, possessed macroporous structure (b).

and foam density of 1.54 g/cm^3 and 0.19 g/cm^3, respectively, resulting in a porosity of 86%. The carbon foams retained the interconnected macroporous structure of the precursor foams (Fig. 11b); pores with an average size of 306 ± 19 μm were interconnected by the pore throats with an average size of 39 ± 25 μm. The smaller average pore size as compared to the phenolic foam precursors was due to the volume contraction during carbonisation. The specific surface area of the phenolic foam precursor was 0.17 m^2/g, while the specific surface area for the carbon foams increased to 17 m^2/g. Nevertheless, the specific surface area of the carbon foams was still much lower than those reported in previous studies [24,25]. This indicated that the carbon foams were not activated during pyrolysis. The electrical conductivity of the precursor phenolic foam was $3 \cdot 10^{-8}$ S/m but that of the produced carbon foam was 17 S/m, making the carbon foams excellent candidates for applications as porous electrodes.

The brittle nature of the carbon foams was demonstrated by flexural tests. The carbon foam specimens failed at only 0.5% strain (Fig. 7a) but their flexural modulus was 526 ± 32 MPa, which was 5 times higher than those of the phenolic foams with identical foam density. The compressive stress-strain curves (Fig. 12a) started with a linear elastic region. The compression modulus of the carbon foams was 76 MPa. After initial failure (crush strength of 3.2 ± 0.2 MPa), the stress dropped steeply, indicating progressive failure of the pore structure of the carbon foams. The stress-strain curves of the carbon foams were 'noisy' over the whole strain region, which was consistent with previous work [26,27]. The stress drops in the stress-strain curves indicated local failure of the carbon foams in mechanically weak regions. It was also observed that the foam structure failed in a layer by layer fashion from the bottom or top of the specimens during compression loading (Fig. 12b). During the compression failure of layers of pores the carbon foam did not

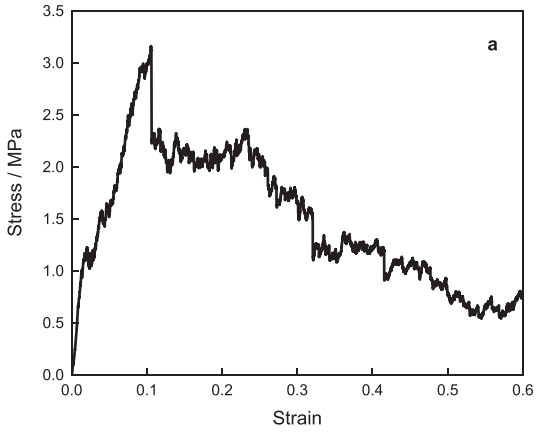

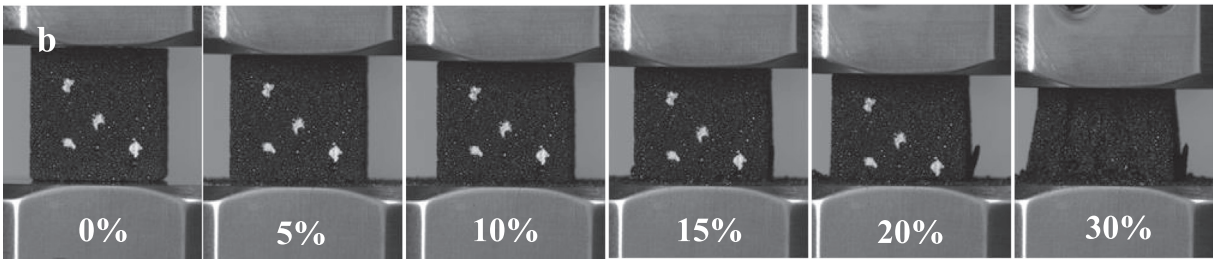

Fig. 12. Representative compressive stress-strain curve for a carbon foam (a) and a series of photographs showing progressive fragmentation of carbon foams with increasing strain (b).

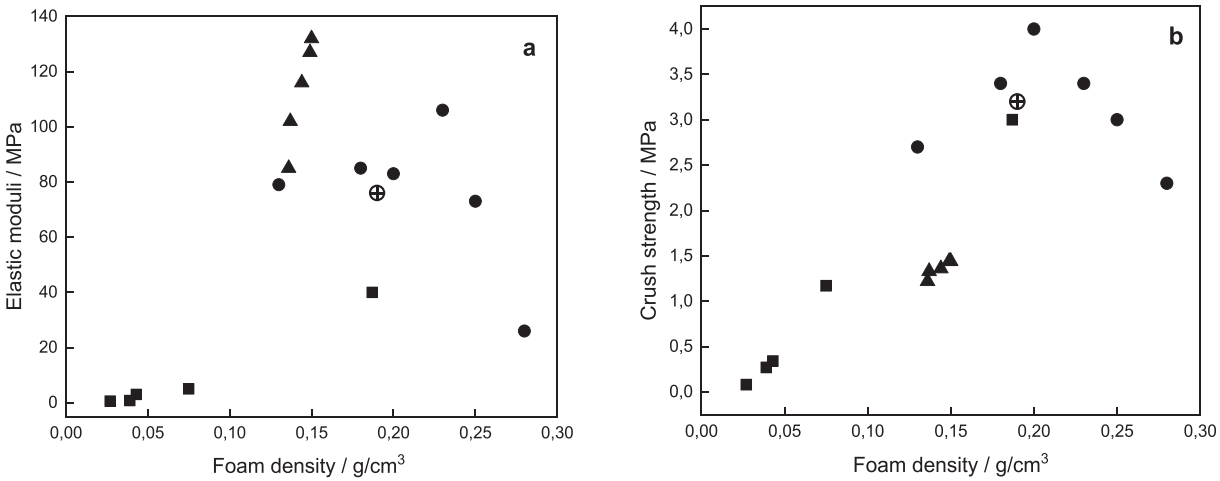

Fig. 13. Comparison of the elastic moduli (a) and crush strengths (b) of our carbon foams produced by carbonisation of froth templated phenolic foams (crossed circles) with literature data of other carbon foams. The solid squares, circles and triangles represent carbon foams produced by carbonisation of froth templated tannin [28], emulsion templated tannin [29] and emulsion templated poly(styrene-*co*-4-vinylbenzyl chloride-co-divinylbenzene) [30], respectively.

show any sign of buckling. The layered foam structure failure of the carbon foams can be explained by the brittleness of the carbon pore walls. Because of the high rigidity of the carbon foam, the stress created by compression accumulated rapidly in the bottom or top layers of the specimens; however, the stress cannot be redistributed over the specimen by buckling of pore walls. The local stress immediately exceeded the crush strengths of the carbon foams, leading to the fragmentation of pore layers in the samples. Subsequently the failure of the first pore layer in the foam structure enabled stress transfer to the next layer resulting in the progressive fragmentation of the samples until failure of the main foam structure.

The elastic moduli and crush strengths of carbon foams produced by carbonisation of froth templated phenolic foams were compared with other carbon foams reported in the literature (Fig. 13). Carbon foams produced from emulsion templated macroporous poly(styrene-co-4-vinylbenzyl chloride-co-divinylbenzene) possessed high elastic moduli but lower crush strengths as compared to our carbon foams, which was due to the different carbon source and much smaller pore sizes of the carbon foams produced by carbonisation of macroporous poly(styrene-co-4-vinylbenzyl chloride-co-divinylbenzene). On the other hand, our sample possessed a similar stiffness and strength compared to tannin based carbon foams [31].

4. Conclusions

Phenolic foams were successfully produced by mechanically whipping air into a phenolic resole resin, catalyst and surfactant formulation followed by curing the liquid froths. By controlling the energy input during whipping, i.e. speed and time, of the liquid froths we were able to adjust the foam densities from around 0.44 g/cm^3 to as low as 0.18 g/cm^3. The produced phenolic foams possessed an interconnected macroporous structure with average pore sizes ranging from 120 μm to 480 μm. The froth templating method was demonstrated to be scalable; we showed that phenolic foam panels with dimensions of 400 mm × 400 mm × 50 mm could be produced with ease. The mechanical properties of froth templated open porous phenolic foams are in line with other reported data of closed cell phenolic foams. The biggest advantage of the froth templating method is that the foam precursor is a liquid formulation, which can be moulded into desired shapes prior to curing without the need to remove a templating phase by drying or extraction. Our procedure provides a versatile method to produce phenolic foams with desired net-shapes. Large phenolic foam panels were pyrolysed resulting in carbon foams with a carbon yield of 48%. Despite significant shrinkage as a result of the carbonisation, the carbon foams retained the interconnected macroporous structure of the phenolic foam precursors and possessed excellent electric conductivity and mechanical properties.

CRediT authorship contribution statement

Mohammad Jalalian: Formal analysis, Investigation, Methodology, Resources, Writing - original draft. **Qixiang Jiang:** Conceptualization, Supervision, Writing - review & editing. **Arnaud Coulon:** Project administration, Resources, Visualization. **Martin Storb:** Project administration, Resources, Visualization. **Robert Woodward:** Formal analysis, Investigation, Methodology. **Alexander Bismarck:** Conceptualization, Supervision, Writing - review & editing, Funding acquisition.

Acknowledgement

The authors would like to acknowledge JSP and the University of Vienna for funding our research. Furthermore, we acknowledge the contributions in producing large phenolic foam samples at JSP, the thermal conductivity tests at BRE, the scale-up tests of phenolic froth production using industrial mixers at Henschel and the continuous production of phenolic froths at Delta Engineering.

Appendix A. Supplementary data

Supplementary data to this article can be found online at https://doi.org/10.1016/j.matdes.2019.107658.

References

[1] R.F. Shannon, C.A. Matuszak, L.G. Adams, G.W. Gillaum, Production of Phenolic Foams, US2979469A, 1961.
[2] K. Okuno, R.T. Woodhams, Mechanical properties and characterization of phenolic resin syntactic foams, J. Cell. Plast. 10 (1974) 237–244.
[3] S. Farhan, R.M. Wang, H. Jiang, N. Ul-Haq, Preparation and characterization of carbon foam derived from pitch and phenolic resin using a soft templating method, J. Anal. Appl. Pyrolysis 110 (2014) 229–234.
[4] X. Wu, Y.G. Liu, M. Fang, L. Mei, B. Luo, Preparation and characterization of carbon foams derived from aluminosilicate and phenolic resin, Carbon 49 (2011) 1782–1786.
[5] S.A. Song, H.J. Oh, B.G. Kim, S.S. Kim, Novel foaming methods to fabricate activated carbon reinforced microcellular phenolic foams, Compos. Sci. Technol. 76 (2013) 45–51.
[6] S.A. Song, Y.S. Chung, S.S. Kim, The mechanical and thermal characteristics of phenolic foams reinforced with carbon nanoparticles, Compos. Sci. Technol. 103 (2014) 85–93.
[7] B.G. Kim, D.G. Lee, Development of microwave foaming method for phenolic insulation foams, J. Mater. Process. Technol. 201 (2008) 716–719.

[8] C. Stubenrauch, A. Menner, A. Bismarck, W. Drenckhan, Emulsion and foam templating—promising routes to tailor-made porous polymers, Angew. Chem. Int. Ed. 57 (2018) 10024–10032.
[9] J.C.H. Wong, E. Tervoort, S. Busato, U.T. Gonzenbach, A.R. Studart, P. Ermanni, L.J. Gauckler, Designing macroporous polymers from particle-stabilized foams, J. Mater. Chem. 20 (2010) 5628–5640.
[10] Y. Pan, W. Wang, C. Peng, K. Shi, Y. Luo, X. Ji, Novel hydrophobic polyvinyl alcohol-formaldehyde foams for organic solvents absorption and effective separation, RSC Adv. 4 (2014) 660–669.
[11] K.Y. Lee, L.L.C. Wong, J.J. Blaker, J.M. Hodgkinson, A. Bismarck, Bio-based macroporous polymer nanocomposites made by mechanical frothing of acrylated epoxidised soybean oil, Green Chem. 13 (2011) 3117–3123.
[12] T.H.M. Lau, L.L.C. Wong, K.Y. Lee, A. Bismarck, Tailored for simplicity: creating high porosity, high performance bio-based macroporous polymers from foam templates, Green Chem. 16 (2014) 1931–1940.
[13] W. Song, V.L. Tagarielli, K.-Y. Lee, Enhancing the fracture resistance and impact toughness of mechanically frothed epoxy foams with hollow elastomeric microspheres, Macromol. Mater. Eng. 303 (2018), 1800363. .
[14] A. Szczurek, V. Fierro, A. Pizzi, A. Celzard, Mayonnaise, whipped cream and meringue, a new carbon cuisine, Carbon 58 (2013) 245–248.
[15] M. Jalalian, Q. Jiang, M. Birot, H. Deleuze, R.T. Woodward, A. Bismarck, Frothed black liquor as a renewable cost effective precursor to low-density lignin and carbon foams, React. Funct. Polym. 132 (2018) 145–151.
[16] N.R. Cameron, D.C. Sherrington, L. Albiston, D.P. Gregory, Study of the formation of the open-cellular morphology of poly(styrene/divinylbenzene) polyHIPE materials by cryo-SEM, Colloid Polym. Sci. 274 (1996) 592–595.
[17] A. Menner, A. Bismarck, New evidence for the mechanism of the pore formation in polymerising high internal phase emulsions or why polyHIPEs have an interconnected pore network structure, Macromol. Symp. 242 (2006) 19–24.
[18] L. Zhang, J. Ma, Processing and characterization of syntactic carbon foams containing hollow carbon microspheres, Carbon 47 (2009) 1451–1456.
[19] M. Rochefort, L. Ripley, P. Holland, V. Coppock, Phenolic Foam, US9896559B2, 2018.
[20] W. Song, K. Barber, K.Y. Lee, Heat-induced bubble expansion as a route to increase the porosity of foam-templated bio-based macroporous polymers, Polymer 118 (2017) 97–106.
[21] M.V. Alonso, M.L. Auad, S.R. Nutt, Modeling the compressive properties of glass fiber reinforced epoxy foam using the analysis of variance approach, Compos. Sci. Technol. 66 (2006) 2126–2134.
[22] M.F. Ashby, The properties of foams and lattices, Philos. Trans. R. Soc. 364 (2006) 15–30.
[23] V. Coppock, R. Zeggelaar, H. Takahashi, T. Kato, Phenolic Foam, US20110124257A1, 2014.
[24] X. Li, S. Liu, Y. Huang, Y. Zheng, D.P. Harper, Z. Zheng, Preparation and foaming mechanism of pyrocarbon foams controlled by activated carbon as the transplantation core, ACS Sustain. Chem. Eng. 6 (2018) 3515–3524.
[25] C.G. Lee, J.W. Jeon, M.J. Hwang, K.H. Ahn, C. Park, J.W. Choi, S.H. Lee, Lead and copper removal from aqueous solutions using carbon foam derived from phenol resin, Chemosphere 130 (2015) 59–65.
[26] A. Celzard, W. Zhao, A. Pizzi, V. Fierro, Mechanical properties of tannin-based rigid foams undergoing compression, Mater. Sci. Eng. A 527 (2010) 4438–4446.
[27] Q. Lin, L. Qu, B. Luo, C. Fang, K. Luo, Preparation and properties of multiwall carbon nanotubes/carbon foam composites, J. Anal. Appl. Pyrolysis 105 (2014) 177–182.
[28] A. Szczurek, V. Fierro, A. Pizzi, M. Stauber, A. Celzard, Carbon meringues derived from flavonoid tannins, Carbon 65 (2013) 214–227.
[29] A. Szczurek, V. Fierro, A. Pizzi, A. Celzard, Emulsion-templated porous carbon monoliths derived from tannins, Carbon 74 (2014) 352–362.
[30] D. Wang, N.L. Smith, P.M. Budd, Polymerization and carbonization of high internal phase emulsions, Polym. Int. 54 (2005) 297–303.
[31] G. Tondi, W. Zhao, A. Pizzi, G. Du, V. Fierro, A. Celzard, Tannin-based rigid foams: a survey of chemical and physical properties, Bioresour. Technol. 100 (2009) 5162–5169.

Electronic Supplementary Information for:

Mechanically Whipped Phenolic Froths as Versatile Templates for Manufacturing Phenolic and Carbon Foams

Mohammad Jalalian[1], Qixiang Jiang[*, 1], Arnaud Coulon[2], Martin Storb[2], Robert Woodward[3] and Alexander Bismarck[*, 1, 3]

[1] *Institute of Materials Chemistry and Research, Polymer & Composite Engineering (PaCE) Group, Faculty of Chemistry, University of Vienna, Währinger Strasse 42, A-1090 Vienna, Austria.*

[2] *JSP, ZI Le Bois Chevalier, Route de Francières, 60190 Estrées Saint Denis, France.*

[3] *Polymer & Composite Engineering (PaCE) Group, Department of Chemical Engineering, Imperial College London, South Kensington Campus, London, SW7 2AZ, UK*

[*] *Corresponding authors: qixiang.jiang@univie.ac.at, alexander.bismarck@univie.ac.at*

S1. Determining the surfactant type and surfactant concentration suitable for the preparation of stable phenolic froths

Whipping air into a phenolic resole and catalyst mixture without any other additives resulted in a liquid without any noticeable volume increase (Figure S1, a). Surfactant was needed to assist the entrapment of air and stabilisation of air bubbles in the phenolic froths. Aiming for a froth with maximum air volume in the aqueous resole solution we screened the following surfactants, typically used to stabilise hydrophobic matter-in-hydrophilic matter systems, sodium dodecyl sulfate (SDS), 4-(1,1,3,3-tetramethylbutyl)phenyl-polyethylene glycol (Triton X-100), polyethylene glycol tert-octylphenyl ether (Triton X-405), sorbitane monooleate (Span 80), poly(ethylene glycol)-block-poly(propylene glycol)-block-poly(ethylene glycol) (Pluronic L-81) and two types of polyethylene glycol sorbitan monolaurates (Tween 20 and Tween 80) (Figure S1. b-h). The surfactant concentrations were 14 wt.-%. The phenolic formulation containing Tween 80 produced after whipping the froth with the highest volume increase (Figure S1. h).

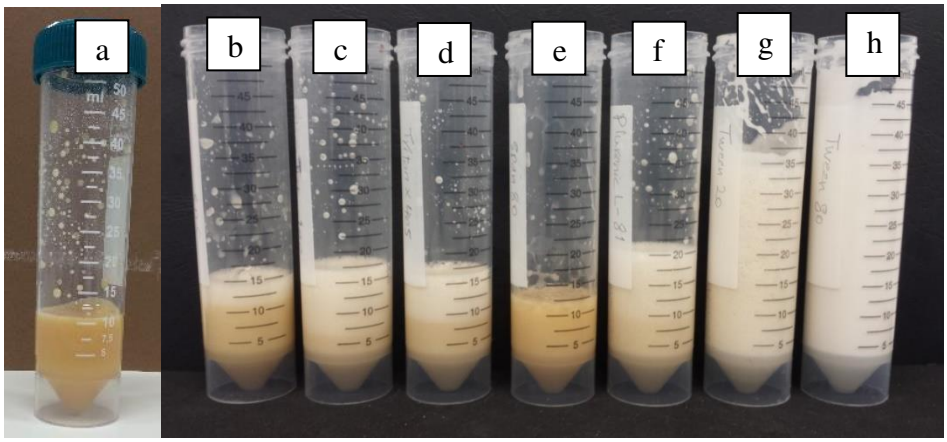

Figure S1. Phenolic formulation without surfactant cannot be mechanically frothed (a). In order to produce stable froths, screening of surfactants in phenolic formulations was carried out using the surfactants: SDS (b), Triton X-100 (c), Triton X-405 (d), Span 80 (e), Pluronic L-81 (f), Tween 20 (g), and Tween 80 (h).

To determine the optimum amount of surfactant needed to produce a froth with the highest froth volume, phenolic formulation containing 3.5 wt.-%, 7 wt.-% and 14 wt.-% Tween 80 were mechanically frothed, respectively (Figure S2, a-c). The phenolic froths produced were all stable and could be cured at 50°C, resulting in phenolic foams (Figure S2, d-f). However, the phenolic foams stabilised using 3.5 wt.-% and 7 wt.-% of surfactant exhibited large pores with pore diameters of 655 ± 204 µm and 440 ± 220 µm, respectively (Figure S2, g and h). As such large air bubbles did not exist in the corresponding phenolic froths (Figure S2, a and b), the cause of the large pores was likely coalescence of air bubbles during curing. However, when curing phenolic froths containing 14 wt.-% surfactant, the resulting phenolic foams possessed pores with a much smaller average pore diameter of 202 ± 112 µm (Figure S2, i). This indicated that increasing the surfactant concentration used to stabilise the phenolic froths hindered coalescence of air bubbles during curing. Furthermore, once we used 14 wt.-% surfactant in the phenolic formulation, the froths showed no sign of collapse over a period of 3 days, during which the froths already cured (Figure S3).

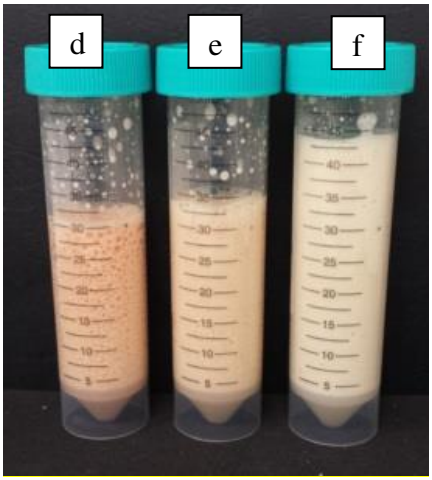

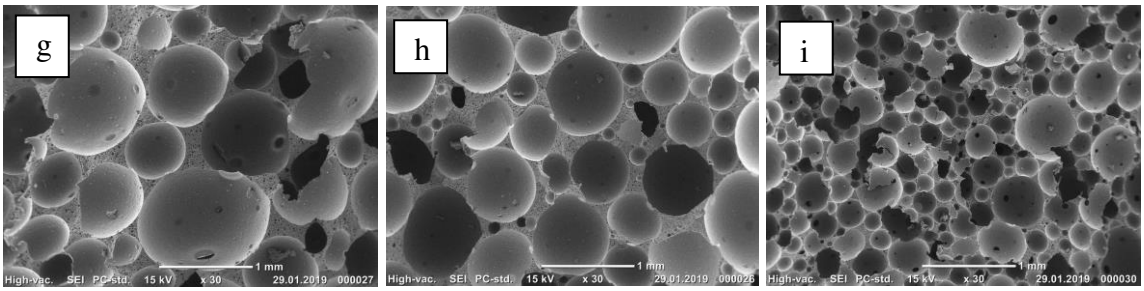

Figure S2. As-whipped phenolic froths stabilised using 3.5 wt.-% (a), 7 wt.-% (b) and 14 wt.-% (c) Tween 80 were cured to produce phenolic foams still containing 3.5 wt.-% (d), 7 wt.-% (e) and 14 wt.-% (f) Tween 80. The macroporous structure of these phenolic foams were determined by Tween 80 concentrations: 3.5 wt.-% (g), 7 wt.-% (h) and 14 wt.-% (i).

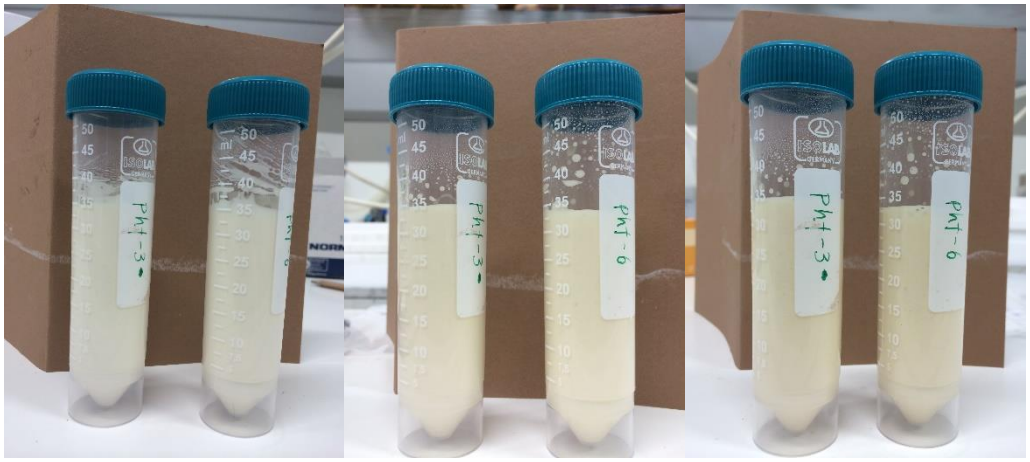

Figure S3. Photographs of phenolic froths stabilised using 14 wt.-%Tween 80 after room temperature storage for 0 h, 24 h and 72 h (from left to right).

S2: Table of physical and mechanical properties of air templated phenolic foams and thereafter pyrolysed carbon foams.

	ρ_s [g/cm^3]	ρ_f [g/cm^3]	P [%]	d_p [µm]	d_{pt} [µm]	E_c [MPa]	σ_c [MPa]	E_f [MPa]	σ_f [MPa]
A	1.31±0.01	0.33±0.01	74±1	117±62	8±5	194±9	7.2±0.2	290±10	6.2±0.2
B-1	1.26±0.01	0.44±0.01	65±1	149±62	11±6	208±26	8.0±0.3	431±26	7.1±0.5
B-2	1.27±0.01	0.22±0.01	83±1	461±86	67±36	55±8	2.3±0.1	131±7	1.9±0.2
B-3	1.26±0.01	0.28±0.01	78±1	291±65	43±26	121±12	4.0±0.1	216±8	3.2±0.2
B-4	1.24±0.01	0.25±0.01	80±1	420±74	46±30	94±22	2.7±0.2	143±10	2.1±0.2
B-5	1.26±0.01	0.21±0.01	83±1	454±68	48±34	68±12	2.1±0.1	98±4	1.5±0.1
B-6	1.22±0.01	0.21±0.01	84±1	405±56	38±25	54±14	2.0±0.2	121±2	1.4±0.1
B-7	1.22±0.01	0.24±0.01	80±1	365±41	38±22	105±4	3.2±0.2	192±12	2.8±0.1
B-8	1.23±0.01	0.17±0.01	86±1	479±65	75±63	47±8	1.8±0.1	116±30	1.4±0.5
B-9	1.23±0.01	0.22±0.01	82±1	447±71	76±61	72±12	2.1±0.2	120±7	1.7±0.1
B-10	1.23±0.01	0.24±0.01	80±1	374±66	51±31	85±14	2.6±0.2	142±3	1.8±0.1
B-11	1.23±0.02	0.27±0.01	79±1	320±50	42±25	95±26	3.3±0.3	149±3	1.6±0.3
C	1.26±0.01	0.18±0.01	85±1	404±64	58±20	54±2	2.1±0.1	99±7	2.1±0.1
C*	1.54±0.01	0.19±0.01	86±1	306±19	39±25	76±10	3.2±0.2	526±32	1.6±0.1

6.2 PUBLICATION II

Frothed black liquor as a renewable cost effective precursor to low-density lignin and carbon foams

Mohammad Jalalian, Qixiang Jiang, Marc Birot, Herve Deleuze, Robert T. Woodward and Alexander Bismarck. Reactive and Functional Polymers, Volume 132, 2018, Pages 145-151. DOI: org/10.1016/j.reactfunctpolym.2018.07.027

Reactive and Functional Polymers 132 (2018) 145–151

Contents lists available at ScienceDirect

Reactive and Functional Polymers

journal homepage: www.elsevier.com/locate/react

Frothed black liquor as a renewable cost effective precursor to low-density lignin and carbon foams

Mohammad Jalalian[a], Qixiang Jiang[a,*], Marc Birot[b], Hervé Deleuze[b], Robert T. Woodward[c], Alexander Bismarck[a,c,*]

[a] Institute of Material Chemistry and Research, Polymer & Composite Engineering (PaCE) Group, Faculty of Chemistry, University of Vienna, Währinger Strasse 42, Vienna 1090, Austria
[b] University of Bordeaux, Institut des Sciences Moléculaires, UMR-CNRS 5255, F-33405 Talence, France.
[c] Polymer & Composite Engineering (PaCE) Group, Department of Chemical Engineering, Imperial College London, South Kensington Campus, London SW7 2AZ, UK

ARTICLE INFO

Keywords:
Lignin
Froth templating
Foam
Carbonisation

ABSTRACT

By whipping air into a solution containing the pulp processing by-product black liquor, crosslinker and surfactant, stable air-in-black liquor froths were produced. The air volume in the froths was controlled by tuning the viscosity of the black liquor and the whipping time. By the selectively crosslinking the renewable lignin and hemicellulose content in the black liquor froths, lignin foams possessing a porosity of up to 88% have been produced. The porosity, pore and pore throat sizes decreased with increasing viscosity of the continuous liquid phase of the black liquor froths. The resulting lignin foams were pyrolysed to produce renewable carbon foams, which retained the shape and macropore structure of the lignin foam precursor well, opening the door to structurally designable carbon foams from lignin. The work demonstrated that froth templating using an industrial by-product is a viable low-cost method to produce both stable lignin and carbon foams.

1. Introduction

Lignin is the second most abundant renewable polymer existing in the botanic system. It is a structural polymer in the plant cell wall and acts as an adhesive binder for cellulose fibrils. Lignin is extracted from wood substrates during paper production *via* one of a number of pulping processes, including kraft, organosolv or soda processes. As a result, it is a by-product of the paper industry which is typically burnt to produce energy for the pulping plant. As a result, further valorization of lignin is sought, such as its utilisation as a platform to develop high value-added products [1]. Lignin has been blended with polypropylene and recycled polypropylene; owing to the antioxidative nature, the mixture showed increased onset oxidation temperature with increasing the lignin content to 10% [2]. Shankar et al. [3] have produced agar/lignin composite films, where the lignin improved the thermal resistance as well as the UV and water barrier properties, making the composite films suitable for food package applications. Lignin has been used in a cotton fiber reinforced poly(lactic acid) composites, where the lignin acted as a natural adhesive promoter to enhance the bonding between the matrix and the fibers, thus resulting in an improved tensile strengths and moduli [4]. The abundant functional groups in the molecules allow lignin or lignin derivatives to be chemically modified, making them versatile building blocks for various synthetic approaches [5, 6]. Polyurethane foams have been produced by partially substituting the polyol units with lignin to increase the renewable content in the foams [7, 8]. Similarly, due to its high phenolic content, lignin was used as a partial replacement for phenol in phenolic foams, where lignin can effectively increase the mechanical strengths of the phenolic foams while preserving the typical fire resistance of phenolic materials [9, 10]. Nevertheless, the production of primarily lignin foams has been scarcely investigated. Deleuze's research group [11 − 13] reported the synthesis of lignin foams *via* emulsion templating, in which emulsions containing black liquor (BL) in the continuous but minority phase and oil as the dispersed templating phase were produced. The lignin content was crosslinked and subsequent removal of the templating oil phase resulted in macroporous lignins. Furthermore, a series of work focused on both surfactant selection and emulsification technique [12, 13], recovery of the templating oil phase [11] and the carbonisation of the lignin foams [14] has been carried out. Although open-porous lignin foams have been produced, the purification and recovery of the oil phase, which occupied the majority of the volume of the emulsions, required a large amount of energy and solvents, meaning that scaling

* Corresponding authors at: Institute of Material Chemistry and Research, Polymer & Composite Engineering (PaCE) Group, Faculty of Chemistry, University of Vienna, Währinger Strasse 42, Vienna 1090, Austria.
E-mail addresses: qixiang.jiang@univie.ac.at (Q. Jiang), alexander.bismarck@univie.ac.at (A. Bismarck).

https://doi.org/10.1016/j.reactfunctpolym.2018.07.027
Received 2 May 2018; Received in revised form 30 July 2018; Accepted 31 July 2018
Available online 03 August 2018
1381-5148/

up such process is not a practical option.

Air-in-liquid froths have been used as templates to produce highly porous polymers, whose pores are templated from an internal air phase in the form of bubbles [15]. Murakami and Bismarck [16] utilised oligomeric tetrafluoroethylene particles to stabilise air bubbles in a continuous polymerisable phase, which was then polymerised to produce macroporous closed-cell polymers. Marlin et al. [17] produced macroporous polyurethane *via* the reaction of isocyanate, polyols, and catalyst, which were mechanically frothed and stabilised using surfactant, prior to the reaction. Lee et al. [18] prepared frothed epoxidised acrylated soybean oil (AESO) in the presence of bacterial cellulose. The high viscosity of AESO and bacterial cellulose promoted the stability of the froth by hindering the drainage of liquid from the films; however, after curing, the macroporous polymers possessed non-regular shaped pores and a porosity of only 59%. In later work, Lau et al. [19] used a viscous bio-based epoxy which could be frothed and subsequently polymerised without the use of emulsifiers to produce a macroporous epoxy resin. The resultant epoxy foams possessed a porosity ranging from 75% to 80% and elastic moduli of 88 to 160 MPa. Szczurek et al. [20] whipped air into an aqueous tannin solution; the crosslinking of the tannin resulted in macroporous materials with porosities of up to 98%. The porous materials could be pyrolysed to produce carbon foams. More recently, Merle et al. [21–23] improved the process for frothing tannin solution by the addition of lignosulfonate and kraft black liquor in the liquid phase; highly porous foams were generated by crosslinking the liquid phase of the froths.

Herein, we report the production of macroporous lignins by the whipping of air into BL solutions, followed by crosslinking the lignin and hemicellulose present in the continuous BL phase. By the production and subsequent crosslinking of stable froths, no template removal step is required, leading to significant reductions in energy and solvent consumption during the workup process in comparison to the previous example of emulsion-templated macroporous lignins [11]. Aiming to produce highly porous lignin foams, the effect of formulation and whipping conditions on froth volume, as well as the physical properties of the resulting macroporous lignin, were investigated. In order to demonstrate the stability of the lignin foams, they were used as precursors for the production of designable highly porous carbon foams.

2. Experimental

2.1. Materials

Crude Kraft black liquor (BL) with 70 wt.-% solute, including lignin and hemicellulose as the organic components and sodium, potassium salts as the inorganic components, was kindly supplied by a paper mill (Smurfit Kappa Cellulose du Pin Kraft paper mill, Facture, France). Epichlorohydrin, ethanol and HCl were purchased from Sigma–Aldrich. Hypermer 1083 was kindly provided by CRODA (Spain). All the chemicals were used as received.

2.2. Production of lignin foams by crosslinking of BL froths

The received BL with 70 wt.-% solute concentration was diluted with distilled water to reach solute concentrations of 40, 45, 50, 55 and 60 wt.-%. The Hypermer 1083 surfactant (11 wt.-%) and epichlorohydrin (always 40 wt.-% with respect to the solute in the BL solutions) were added to 10 g BL solutions and mixed in a 50 ml Falcon centrifuge tube. The mixture was approximately 13 ml; the volume could guarantee the engagement of the mixture with the whipping head and leave enough space in the Falcon tube to allow the volume increase of the froths during whipping. A 450 W hand mixer equipped with a dough kneading head (which has a diameter of about 2 cm and fit in the Falcon tube with a diameter of 2.5 cm) was used to mechanically whip air into the mixture for either 6, 9 or 16 min. The compositions of the BL froths are summarised in Table 1. The resulting froths were placed in an oven at 50 °C for 48 h to allow for crosslinking of lignin/hemicellulose. Afterwards, the foams were washed in water for 24 h, followed by ethanol for 24 h and lastly in aq. HCl (pH = 1) for another 24 h. The lignin foams were dried in air for 24 h and in oven at 50 °C for 5 h.

Table 1
Composition and whipping time of the BL mixture.

Sample	BL[b] (wt.-%)	Epichlorohydrin (wt.-%)	Hypermer 1083 (wt.-%)	Whipping time (min)
BL-40-1[a]	76	13	11	6
BL-40-2	76	13	11	9
BL-40-3	76	13	11	16
BL-45-1	75	14	11	6
BL-45-2	75	14	11	9
BL-45-3	75	14	11	16
BL-50-1	74	15	11	6
BL-50-2	74	15	11	9
BL-50-3	74	15	11	16
BL-55-1	73	16	11	6
BL-55-2	73	16	11	9
BL-55-3	73	16	11	16
BL-60-1	72	17	11	6
BL-60-2	72	17	11	9
BL-60-3	72	17	11	16

[a] The number after BL refers to the solute concentration in the BL solution.
[b] The concentrations of BL, epichlorohydrin and Hypermer 1083 were with respect to the mass of the mixture.

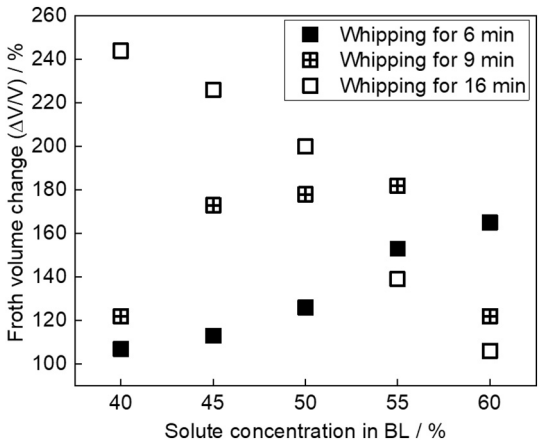

Fig. 1. Volume change from a solution consisting of BL, crosslinker and surfactant to BL froths as a function of solute concentrations at different whipping time.

2.3. Characterisation of BL, solid lignin and carbon foams

The original volume V_0 of the BL, crosslinker and surfactant mixture was determined by summing up the volume of each components, which were combined prior to whipping. After whipping the mixture in a graduated 50 ml free standing polypropylene Falcon centrifuge tube, the volume of the whipped BL froths V_f could be read from the Falcon tube. The volume increase S of the BL froths is given by:

$$S = (V_f - V_0)/V_0$$

Elemental analysis of BL and lignin foams was performed using a Eurovector EA 3000 (CHNS-O Elemental Analyser). The dry samples (2 mg) were ground into powder and weighed in a vial. Digestion/mineralisation of the samples was conducted by flash combustion in 25 kPa oxygen atmosphere at 1000 °C. The resulting combustion gases passed through a reduction furnace and were flowed into the gas chromatographic column by the helium carrier gas. The gases were separated in the column and detected by the thermal conductivity detector, which provided an output signal proportional to the

Table 2
Composition of elements (at. %) in dry solute in BL and lignin foams.

	C	H	N	S	O	Cl	K	Na	Br	Rest
Dry solute in BL	32.39	3.28	0.11	4.05	37.17	0.3	1.86	17.95	< 0.02	2.87
Lignin foam washed in water	61.2	7.48	0.16	2.67	25.57	2.71	0.105	1.81	< 0.02	–
Lignin foam washed in water and EtOH	55.2	6.98	0.15	2.65	25.44	2.29	0.231	4.45	< 0.02	2.58
Lignin foam washed in water, EtOH and HCl	63.96	7.89	0.18	2.46	23.32	0.37	0.05	0.05	< 0.02	1.71

Table 3
Foam ρ_f and skeletal ρ_s density, porosity P, average pore d_p and pore throat d_t size as well as specific BET surface area A_s of the lignin foams.

Sample	ρ_s/g/cm^3	ρ_f/g/cm^3	P/%	d_p/μm	d_t/μm	A_s/m^2/g
BL-40-3	1.30 ± 0.01	0.15 ± 0.02	88 ± 1	165 ± 49	32 ± 14	0.80
BL-45-3	1.32 ± 0.01	0.19 ± 0.01	86 ± 1	138 ± 40	28 ± 10	0.86
BL-50-3	1.31 ± 0.01	0.25 ± 0.03	81 ± 1	107 ± 27	20 ± 7	1.01
BL-55-3	1.31 ± 0.01	0.37 ± 0.05	72 ± 1	66 ± 18	14 ± 3	1.63
BL-60-3	1.33 ± 0.01	0.49 ± 0.07	63 ± 1	97 ± 35	9 ± 3	1.40
				23 ± 8[a]	4 ± 1	

[a] BL-60-3 foams possessed bi-model pore size distributions, large and small pore sizes were quantified separately.

concentration of the individual components in the gas mixture.

The lignin foam densities ρ_f were determined by weighing the samples and measuring the dimensions. The foam densities were calculated by:

$$\rho_f = m/V$$

where m and V are the mass and volume of the lignin foams. The skeletal density ρ_s was determined by measuring the volume of about 0.5 g sample powder using a helium displacement pycnometer (Accupyc 1350, Micrometrics Aachen, Germany). The porosity P of the lignin foams were calculated by:

$$P = (1 - \rho_f/\rho_s)$$

The surface area (A_s) of the lignin foams was measured using a TriStar II 3020 Surface Area and Porosity System (Micromeritics instrument corporation, USA). Pieces of lignin foam (0.2 g) were degassed at 60 °C for 24 h in N_2 prior to the measurement. The N_2 adsorption-desorption isotherms of the samples were analysed using the Brunauer, Emmett and Teller (BET) method.

The moisture adsorption of the lignin foams was investigated using dynamic vapour sorption (DVS Intrinsic, Surface Measurement System Ltd. UK). Samples (10 mg) were exposed to 0, 90 and 0% relative humidity for 24 h, respectively. The weight change of the samples was monitored as a function of time.

The morphology of the lignin foams was investigated using scanning electron microscopy (SEM, JCM-6000, JOEL, Germany). The SEM was operated under a secondary electron beam mode with an electron voltage of 15 kV. Prior to SEM, the lignin foams were fixed onto SEM stubs using carbon tabs and gold coated for 30 s at 30 mA using a sputter coater (JEOL Fine Coater JFC-1200). The SEM images were further analysed using the software ImageJ; to give an accurate representation of macropore diameters (d_p) and pore throat diameter (d_t) of the lignin foams at least 150 pores were measured.

Compression tests were performed on lignin foams using a universal mechanical tester (Model 5969, Instron GmbH, Buckinghamshire, UK) equipped with a 1 kN load cell. Cylindrical test specimens with a diameter of 25 mm and a height of 10 mm were compressed between two flat plates at a speed of 1 mm min^{-1}. The lignin foams were compressed by 30% and the stress-strain curves of the samples were recorded. Five specimens for each sample type were tested to obtain statistically significant values for the elastic moduli and crush strengths.

Mercury intrusion porosimetry was carried out in a Micromeritics Autopore IV 9500 porosimeter (Micromeritics Instrument Corp. USA) at intrusion pressures from 0.0003 to 124.0000 MPa. The pore diameter distribution of each sample was determined from the incremental intrusion curves assuming a contact angle of Hg on the substrate of 130° and Hg surface tension of 485 mN/m. The porosity of samples was determined from the volume of Hg pushed into the samples. Sample BL-50-3 was characterized by the Hg porosimetry, before and after carbonisation.

3. Results and discussion

Stable air-in-BL froths were produced by mechanical mixing followed by the whipping of air into solutions of BL, crosslinker and surfactant. As the resulting BL froths were intended to be used as templates for production of lignin foams, the internal air volume of the froths, which determines the porosity of the resulting lignin foams, needed to be well-controlled. The air volume fraction in the froths was anticipated to be influenced by the viscosity of the liquid phase and the energy input during the whipping. Unfortunately, we were unable to quantify the viscosity of the BL solutions because of the highly alkaline nature (pH > 12) of the BL solution, which damaged the measuring geometry of our rheometer (the detailed information can be found in ESI, S1). However, it is safe to say that the viscosity of the BL solutions increased with increasing solute concentrations from 40 to 60 wt.-%. The energy input was adjusted by controlling the whipping time while keeping the power output of the mixer constant. The volume increase due to air entrapment within the BL solution was then plotted as a function of the BL solute concentrations (Fig. 1). With just 6 min of whipping time the volume of the BL froths increased with increasing solute concentrations in the liquid phase. The BL liquid phase with higher solute concentration, thus higher viscosity, promoted the kinetic stability of the froths by hindering liquid film drainage between air bubbles, therefore allowing the froths to entrap a larger amount of air. In contrast, when the formulations were whipped for 16 min the volume of the resulting BL froths was decreased with increasing solute concentration, despite the increasing viscosity of the liquid phase. The increasing air volume in the froths, coupled with increased water evaporation during the extended whipping process, meant that the viscosity of the froths increased further and as a result it became more difficult to introduce air into the systems. Furthermore, whipping BL-55 for more than 12 min or BL-60 for more than 6 min also led to decreased liquid foam volumes. This indicated the existence of an optimal whipping time (which is proportional to the energy input) to produce froth with maximum air volume fraction as overwhipping[1] led to the

[1] When whipping cream “overwhipping” is often observed: it describes the transition of a soft cream to a stiff and grainy matter.

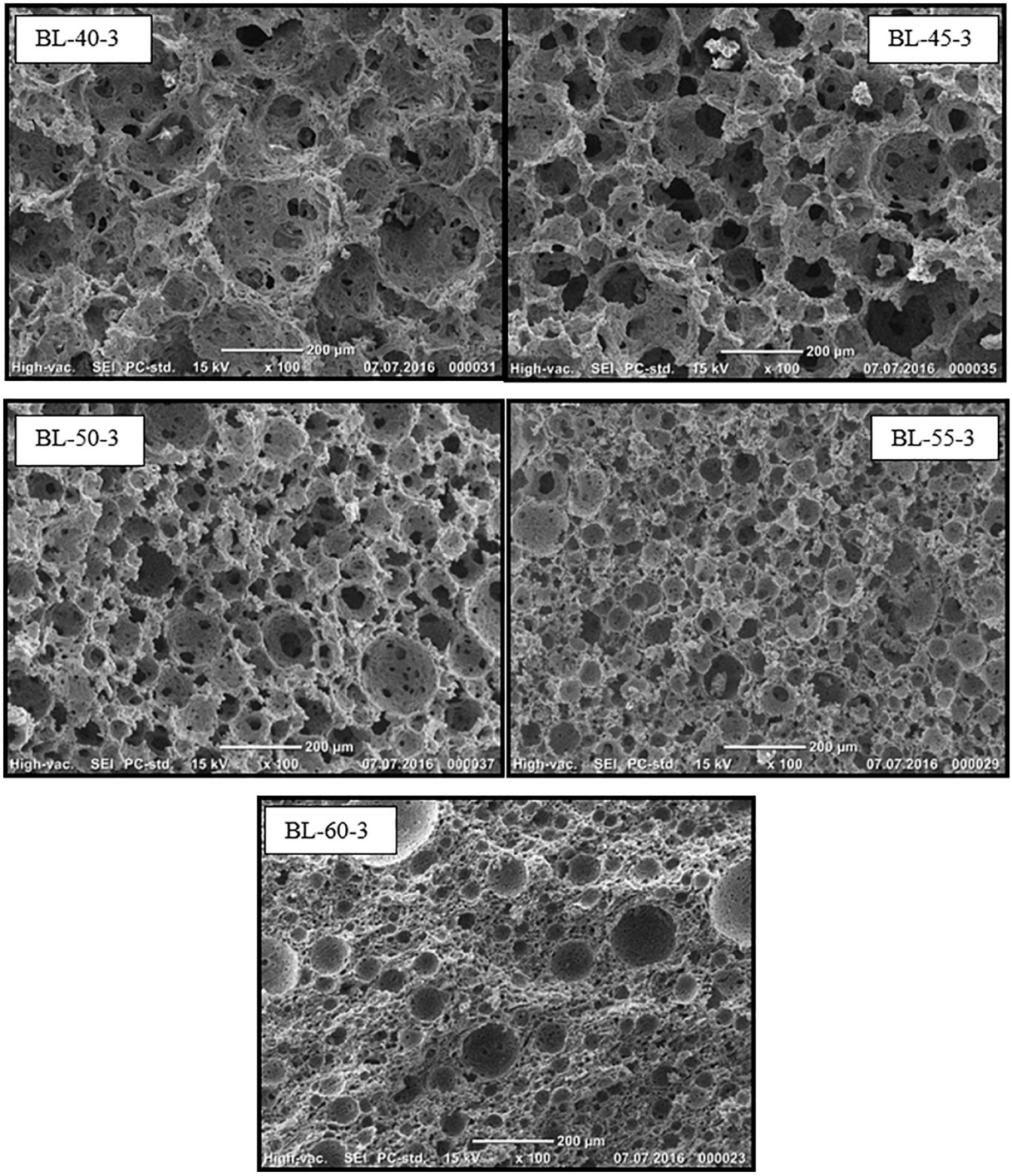

Fig. 2. Characteristic SEM images of froth templated macroporous lignin foams. The lignin foams were produced from BL froths with 40, 45, 50, 55 and 60 wt.-% solute.

decrease of the froth volume. Overwhipping can cause aggregation of particles in the froths, leading to the rupture of the lamellae enclosing the air bubbles and the release of air from the froths [24]. Furthermore, overwhipping can also cause phase separation of the surfactant from the liquid phase of the froths due to accelerated water evaporation. Although the surfactant concentration was identical in all BL solutions, froths with lower water content (*e.g.* BL-60) were more prone to overwhipping.

It was previously described by Forgacz et al. [12] that the crosslinking of lignin and hemicellulose was possible in the presence of epichlorohydrin at elevated temperatures. BL froths whipped for 16 min were placed in oven at 50 °C to crosslink the lignin and hemicellulose. The 16 min-whipped BL froths were employed to produce lignin foams as the froths covered a wide range of volume increase; curing such BL froths allowed us to produce lignin foams of varying densities. Furthermore, as 16 min whipping did cover the overwhipped BL froths, the effect of the overwhipping on the morphology and mechanical properties of the resulting after curing lignin foams could be investigated. The resulting solid foams were washed with water in order to purify the materials; they did not disintegrate during this washing process, indicating the successful crosslinking. However, after the lignin foams were dried, they started to adsorb moisture from the environment and

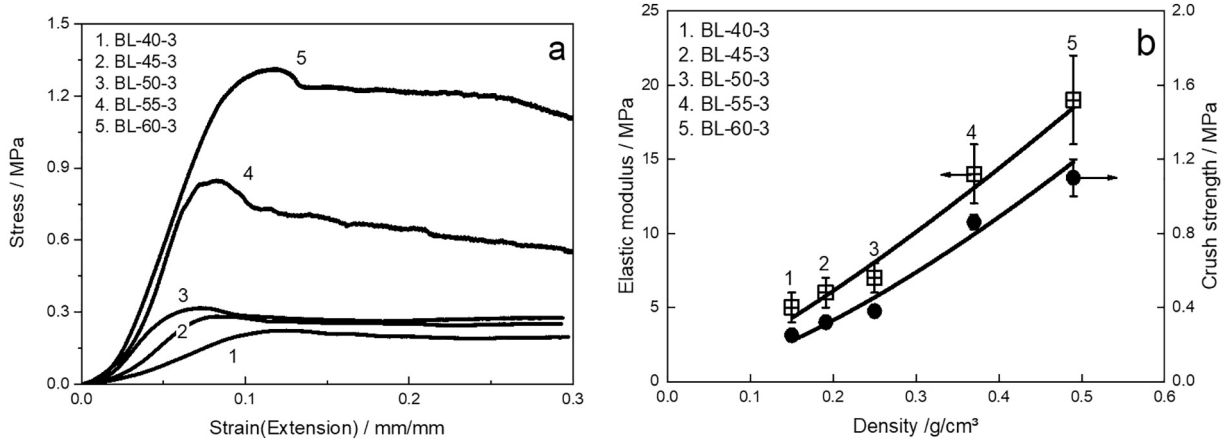

Fig. 3. Stress-strain curves of lignin foams (a) and elastic moduli and crush strengths of lignin foams as a function of their foam density (b).

became soft after being left in air for about 1 day. Water vapour sorption showed that the lignin foams took up 41% moisture at 90% RH. A further wash of the lignin foams in ethanol resulted in the reduction of the moisture uptake to 29% at 90% RH. Correspondingly, the C, H and Cl elemental content in the lignin foam washed in water and ethanol reduced as compared to those washed in water only (Table 2). This can be explained by the removal of surfactant and unreacted epichlorohydrin during the washing process, thus changing the hygroscopic nature of the lignin foams. A further wash of the lignin foams in HCl (pH = 1) resulted in the removal of inorganic material from the foams as indicated by decreased content of Cl, K and Na. Accompanied by the removal of the hydrophilic components, the moisture uptake of the lignin foams dropped to 12% at 90% RH.

The crosslinked lignin foams did not show a glass transition temperature (ESI, S2, Supplementary Fig. S1) within the temperature range from -19 °C to 300 °C. This could be due to the high degree of crosslinking of the lignin. All the lignin foams possessed a skeletal density of about 1.3 g/cm^3. Lignin foams produced by crosslinking the lignin and hemicellulose content in the froth produced from a BL solution with only 40 wt.-% solute concentration had a foam density of 0.15 g/cm^3, resulting in a porosity of 88% (Table 3). The porosity calculated from the volume change, *i.e.* the introduced air volume fraction, of the as-whipped liquid froth was only 63%; the higher porosity of the lignin foam was due to the removal of water from the crosslinked lignin phase during purification. The surface area of all the lignin foams was low, indicating that the removal excess and unreacted material from the continuous lignin phase did not introduce any additional (micro)porosity in the pore walls. The foam densities of the lignin foams increased with increasing solute concentrations in the BL solutions, which were mechanically whipped to create the froth templates. As a result, the porosity of the lignin foams decreased from 88% to 63%. This was, on one hand, due to the decreased air volume fraction of the produced BL froths caused by the difficulty to beat more air into the viscous system. On the other hand, the decreased water content in the BL solutions also resulted in a lower porosity of the produced lignin foams as less water was removed from the foam.

The produced solid lignin foams have open-porous structures (Fig. 2) in which the pores are interconnected by pore throats. In contrast to air-templated closed-cell polymer foams reported by Lee et al. [18] and Lau et al. [19], the formation of the interconnected porous structure of these lignin foams was due to the use of a surfactant to stabilise the aqueous BL froths. The presence of the surfactant possibly resulted in the thinning of the liquid films separating bubbles in the froths. During the crosslinking step, the liquid films contracted, resulting in the formation of pore throats between adjacent bubbles [25]. The average pore sizes of the lignin foams produced by crosslinking the lignin/hemicellulose in the BL-40 solutions were 160 µm; the increased solute concentration in BL-60 systems caused the average pore sizes of the solid lignin foams to decrease to about 100 µm (Table 3). The BL solutions with higher solute concentrations and, thus higher viscosity, promoted the stability of the froth containing smaller air bubbles by retarding the liquid drainage from the films [26]. The average pore dimensions of the solid lignin foams inherited by the bubbles therefore decreased with increasing BL solute concentrations. BL-60 derived lignin foams possessed a bimodal pore size distribution: large pores were surrounded by smaller ones. The formation of larger bubbles, and thus pores after crosslinking, is likely due to the rupture of lamellae caused by overwhipping, which allowed for air transport though the ruptured liquid films, causing some of the bubbles to grow at the expense of the shrinkage of the surrounding ones.

The mechanical properties of lignin foams were measured using compression tests. The stress-strain curves of the lignin foams exhibit a linear region ending in a yield point followed by some post-yield softening, especially for the stronger lignin foams produced from BL-55 and BL-60 systems (Fig. 3a). This region is followed by a plastic plateau in which progressive failure of the pore walls occured as indicated by the decreasing plateau stress with increasing strain. The elastic moduli and crush strengths of the lignin foams increased with increasing foam density (Fig. 3b) as predicted by Gibson and Ashby [27]. The dependency of E and σ = f (ρ_f) can be fitted by power law equation:

$$E = a \times \rho_f^m$$

$$\sigma = b \times \rho_f^n$$

where E and σ are the elastic moduli and crush strengths, a and b are material related constants and m and n are 1.2 and 1.4, respectively. The m- and n-values indicate that the failure of the lignin foams was due to the bending and buckling of the pore walls in the foams [28].

BL-50-3 lignin foams were pyrolysed in N_2 at 1000 °C to produce carbon foams with a carbon yield of 25 wt.-%. The carbon yield was in agreement with the thermal degradation tests of the lignin foams in nitrogen atmosphere (ESI, S3, Supplementary Fig. S2). The monolithic carbon foams retained a similar shape to their corresponding lignin foam precursors but shrank in volume by about 80% (Fig. 4). The carbon foams possessed an interconnected macroporous structure with an average pore size of 67 ± 33 µm; the smaller average pore size of the carbon foams was due to the shrinkage of the foam structure during carbonisation. The average pore size of the carbon foams determined by mercury intrusion porosimetry was 20 µm as compared to 40 µm for the lignin foams. The surface area of the carbon foams increased to 18 m^2/g as compared to 1 m^2/g of the lignin foam. The retention of the shape and porous structure of the lignin foam precursors after carbonisation highlights the potential of lignin foams from liquid froths templates, which can be moulded into a net shape, to produce carbon foams in a

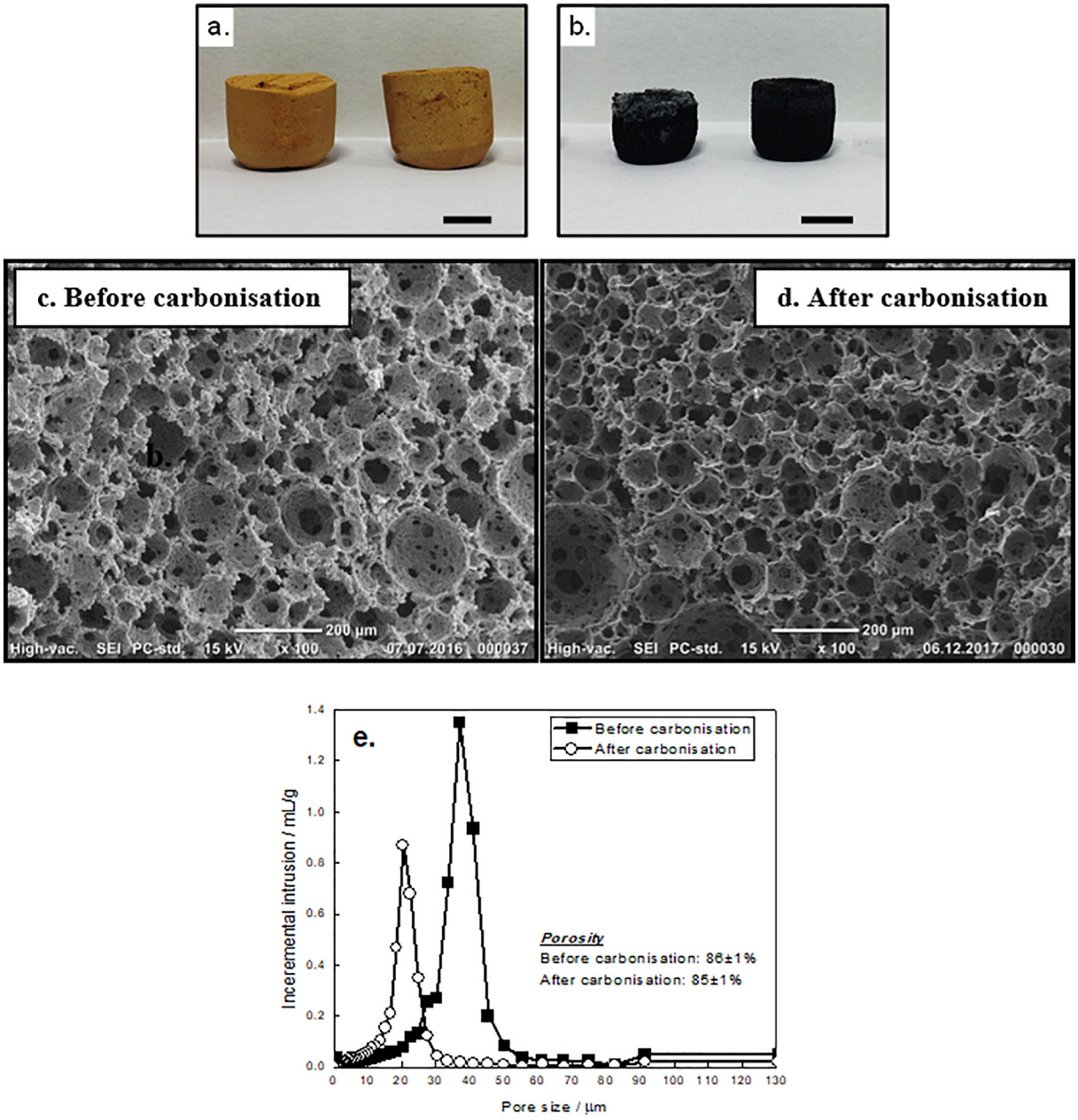

Fig. 4. Lignin foams pyrolysed at 1000 °C in N_2 resulting in carbon foams, which retained the shape (a. prior- and b. post-pyrolysis, scale bar = 1 cm) and macroporous structure (c, d) of the lignin foam precursors. The carbon foams possessed smaller pores than the lignin foam precursors (e).

desired 3D shape.

4. Conclusions

Stable BL froths were successfully prepared by mechanically whipping air into black liquor solutions which also contained crosslinker (epichlorohydrin) and surfactant. The air volume which can be introduced into the froths was determined by the viscosity of the liquid phase and whipping time, *i.e.* the energy input. The viscosity of the froths depended on the solute (lignin and hemicellulose) concentration. Overwhipping of the froths was observed when highly viscous BL solutions were whipped, causing the air volume fraction of the froths to decrease with increasing whipping time. The crosslinking of the lignin and hemicellulose by epichlorohydrin within the BL solution resulted in rigid lignin foams upon heating at relatively low temperatures. However, the as produced dried foams were hygroscopic, resulting in significant moisture adsorption from the environment. In order to reduce the moisture adsorption, the lignin foams had to be washed in ethanol and HCl solution to remove hydrophilic components from the foams. The lignin foams possessed an open-porous structure; the pore and pore throat sizes decreased with increasing BL solute concentration. The porosity of the lignin foams could be tailored to range from 63% up to 88%.

Finally, the pyrolysis of lignin foams to produce highly porous carbon foams was demonstrated. The resulting carbon foams retained the shape and interconnected macroporous structure of the lignin foam precursors and gave char yields of around 25%. This highlights the potential of mouldable lignin foams, which were produced by crosslinking the continuous phase of liquid BL froths, to produce highly porous carbon foams.

Supplementary data to this article can be found online at https://doi.org/10.1016/j.reactfunctpolym.2018.07.027.

Acknowledgements

The authors would like to acknowledge JSP for funding our research.

References

[1] J. Zakzeski, P.C.A. Bruijnincx, A.L. Jongerius, B.M. Weckhuysen, The catalytic valorization of lignin for the production of renewable chemicals, Chem. Rev. 110 (2010) 3552–3599.
[2] A. Gregorová, Z. Cibulková, B. Košíková, P. Šimon, Stabilization effect of lignin in polypropylene and recycled polypropylene, Polym. Degrad. Stab. 89 (2005) 553–558.
[3] S. Shankar, J.P. Reddy, J.-W. Rhim, Effect of lignin on water vapor barrier, mechanical, and structural properties of agar/lignin composite films, Int. J. Biol. Macromol. 81 (2015) 267–273.
[4] N. Graupner, Application of lignin as natural adhesion promoter in cotton fibre-reinforced poly(lactic acid) (PLA) composites, J. Mater. Sci. 43 (2008) 5222–5229.
[5] S. Laurichesse, L. Avérous, Chemical modification of lignins: towards biobased polymers, Prog. Polym. Sci. 39 (2014) 1266–1290.
[6] D. Stewart, Lignin as a base material for materials applications: chemistry, application and economics, Ind. Crop. Prod. 27 (2008) 202–207.
[7] J. Bernardini, I. Anguillesi, M.-B. Coltelli, P. Cinelli, A. Lazzeri, Optimizing the lignin based synthesis of flexible polyurethane foams employing reactive liquefying agents, Polym. Int. 64 (2015) 1235–1244.
[8] B.L. Xue, J.L. Wen, R.C. Sun, Lignin-based rigid polyurethane foam reinforced with pulp fiber: synthesis and characterization, ACS Sustain. Chem. Eng. 2 (2014) 1474–1480.
[9] L. Hu, Y. Zhou, M. Zhang, R. Liu, Chracterization and properties of a lingosulfonate-based phenolic foam, Bioresources 7 (2011) 554–564.
[10] B. Del Saz-Orozco, M. Oliet, M.V. Alonso, E. Rojo, F. Rodríguez, Formulation optimization of unreinforced and lignin nanoparticle-reinforced phenolic foams using an analysis of variance approach, Compos. Sci. Technol. 72 (2012) 667–674.
[11] A. Foulet, M. Birot, G. Sonnemann, H. Deleuze, The potential of Kraft black liquor to produce bio-based emulsion-templated porous materials, React. Funct. Polym. 90 (2015) 15–20.
[12] C. Forgacz, M. Birot, H. Deleuze, Synthesis of porous emulsion-templated monoliths from a pulp mill by-product, J. Appl. Polym. Sci. 129 (2013) 2606–2613.
[13] C. Forgacz, S. Caubet, Y. Le Guer, B. Grassl, K.E. Omari, M. Birot, H. Deleuze, Synthesis of porous emulsion-Templated monoliths using a low-energy emulsification batch mixer, J. Polym. Environ. 21 (3) (2013) 683–691.
[14] A. Foulet, M. Birot, R. Backov, G. Sonnemann, H. Deleuze, Preparation of hierarchical porous carbonaceous foams from Kraft black liquor, Mater. Today Commun. 7 (2016) 108–116.
[15] C. Stubenrauch, A. Menner, A. Bismarck, W. Drenckhan, Emulsion & foam templating: promising routes to tailor-made porous polymers, Angew. Chem. 57 (2018) 10024–10032.
[16] R. Murakami, A. Bismarck, Particle-stabilized materials: dry oils and (polymerized) non-aqueous foams, Adv. Funct. Mater. 20 (2010) 732–737.
[17] L. Marlin, A.J. Durante, E.G. Schwarz, Mechanically frothed urethane: a new process for controlled gauge, high density foam, J. Cell. Plast. 11 (1975) 317–322.
[18] K.-Y. Lee, L.L.C. Wong, J.J. Blaker, J.M. Hodgkinson, A. Bismarck, Bio-based macroporous polymer nanocomposites made by mechanical frothing of acrylated epoxidised soybean oil, Green Chem. 13 (2011) 3117–3123.
[19] T.H.M. Lau, L.L.C. Wong, K.-Y. Lee, A. Bismarck, Tailored for simplicity: creating high porosity, high performance bio-based macroporous polymers from foam templates, Green Chem. 16 (2014) 1931–1940.
[20] A. Szczurek, V. Fierro, A. Pizzi, A. Celzard, Mayonnaise, whipped cream and meringue, a new carbon cuisine, Carbon 58 (2013) 245–248.
[21] J. Merle, P. Trinsoutrot, F. Charrier-El Bouhtoury, Optimization of the formulation for the synthesis of bio-based foams, Eur. Polym. J. 84 (2016) 577–588.
[22] J. Merle, M. Birot, H. Deleuze, P. Trinsoutrot, H. Carré, Q. Huyette, F. Charrier-El Bouhtoury, Valorization of Kraft black liquor and tannins via porous material production, Arab. J. Chem. (2016).
[23] J. Merle, M. Birot, H. Deleuze, C. Mitterer, H. Carré, F.C.-E. Bouhtoury, New bio-based foams from wood byproducts, Mater. Des. 91 (2016) 186–192.
[24] Q. Zhao, W. Kuang, Z. Long, M. Fang, D. Liu, B. Yang, M. Zhao, Effect of sorbitan monostearate on the physical characteristics and whipping properties of whipped cream, Food Chem. 141 (2013) 1834–1840.
[25] N.R. Cameron, D.C. Sherrington, L. Albiston, D.P. Gregory, Study of the formation of the open cellular morphology of poly(styrene/divinylbenzene) polyHIPE materials by cryo-SEM, Colloid Polym. Sci. 274 (1996) 592–595.
[26] E. Seguineau De Preval, D. Fabrice, M. Gilles, C. Gérard, M. Samir, Influence of surface properties and bulk viscosity on bubble size prediction during foaming operation, Colloids Surf. A Physicochem. Eng. Asp. 442 (2014) 88–97.
[27] L.J. Gibson, M.F. Ashby, Cellular Solids: Structure and Properties, Cambridge University Press, Cambridge, 1999.
[28] M.F. Ashby, The properties of foams and lattices, Philos. Trans. R. Soc. A 364 (2006) 15–30.

The following are the supplementary data related to this

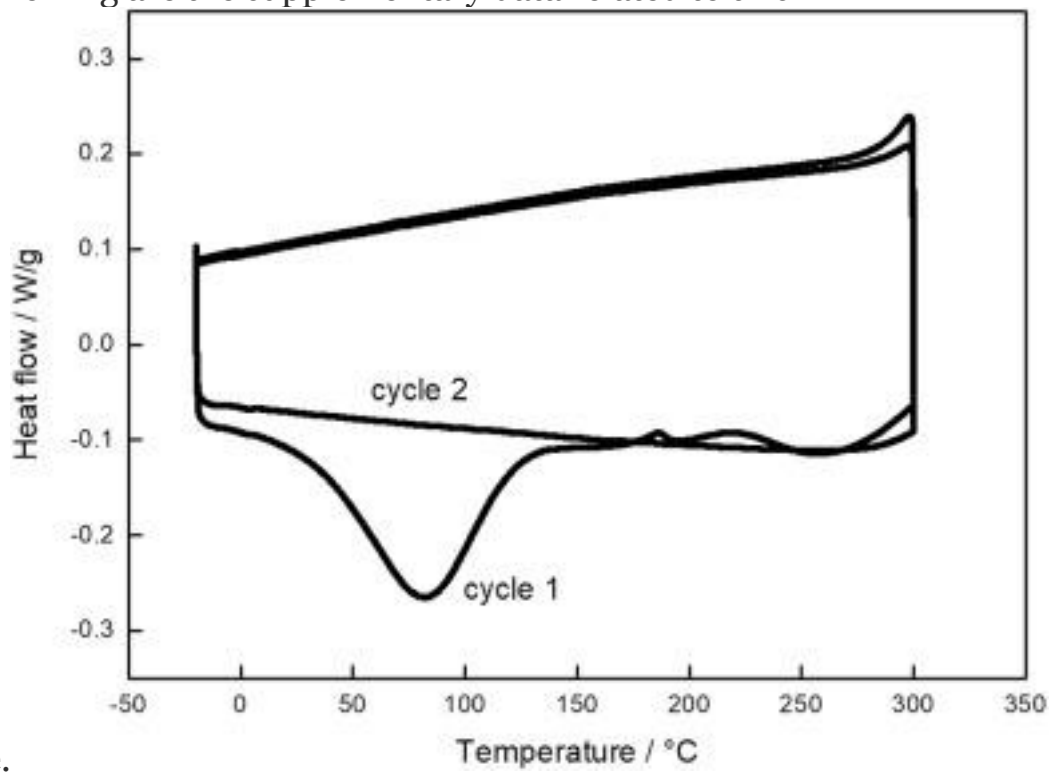

article.

1. Download high-res image (60KB)
2. Download full-size image

Supplementary Fig. S1. Heat flow of the crosslinked lignin upon heating and cooling.

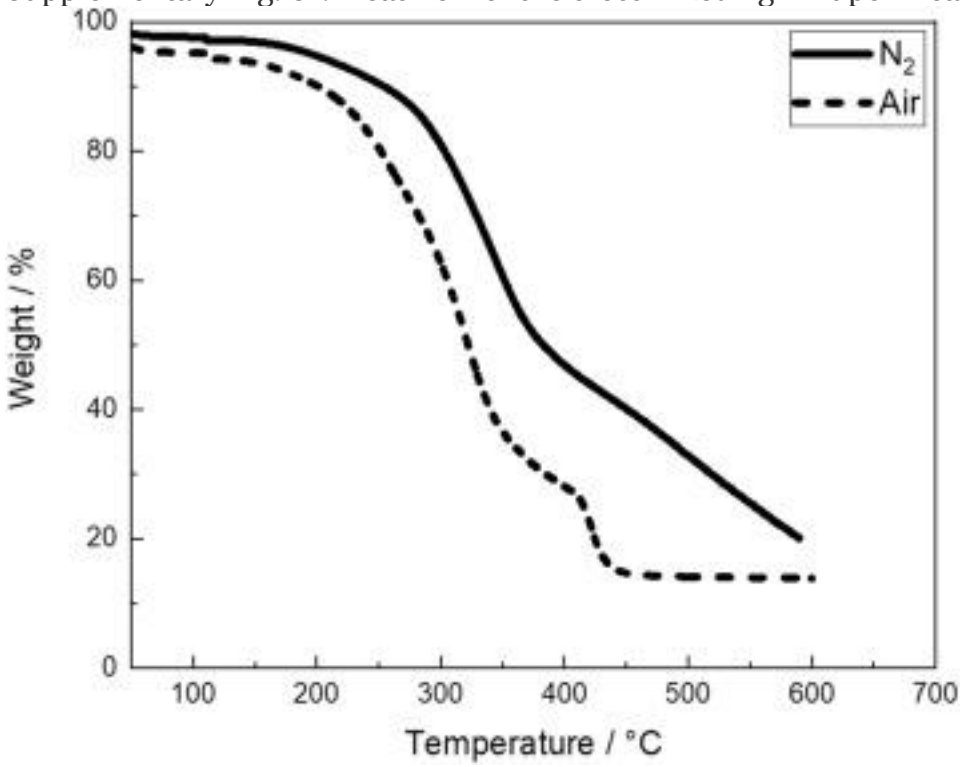

1. Download high-res image (56KB)
2. Download full-size image

Supplementary Fig. S2. Thermal degradation of BL-50-3 foam in air and N_2, respectively.

6.3 PUBLICATION III

Air templated macroporous epoxy foams with silica particles as property-defining additive

Mohammad Jalalian, Qixiang Jiang, and Alexander Bismarck. ACS Applied Polymer Materials, Volume 1, 2019, Pages 335-343. DOI: 10.1021/acsapm.8b00084

ACS APPLIED POLYMER MATERIALS

March 2019
Volume 1
Number 3
pubs.acs.org/acsapm

ACS Publications
Most Trusted. Most Cited. Most Read.

www.acs.org

ACS APPLIED POLYMER MATERIALS

Article

Cite This: ACS Appl. Polym. Mater. 2019, 1, 335−343

pubs.acs.org/acsapm

Air Templated Macroporous Epoxy Foams with Silica Particles as Property-Defining Additive

Mohammad Jalalian, Qixiang Jiang,* and Alexander Bismarck*

Institute of Material Chemistry and Research, Polymer & Composite Engineering (PaCE) Group, Faculty of Chemistry, University of Vienna, Währinger Strasse 42, 1090 Vienna, Austria

Supporting Information

ABSTRACT: Nonaqueous foams were successfully produced by mechanically beating air into liquid epoxy resin, surfactant, and silica particle mixtures and used as templates to produce macroporous polymers. The air bubbles introduced into the epoxy formulations served as templates for the pores of the cured epoxy foams. The addition of silica particles into the resin mixture resulted in an increased viscosity of the formulation, thus enhancing the stability of the liquid epoxy froths, which could then be thermally cured at 60 °C. Increasing the silica loading in the formulation resulted in an increase of the foam density and decrease of the average pore size of the epoxy foams. The epoxy foams containing silica exhibited a hierarchical pore structure, where large pores were surrounded by smaller pores, and enhanced stiffness as compared to the control epoxy foams with a monomodal pore size distribution.

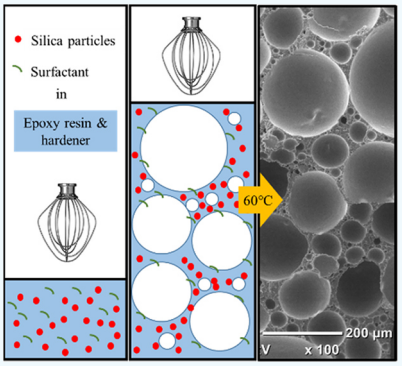

KEYWORDS: *epoxy foam, nonaqueous foams, frothing, hierarchical porous structure, templating*

1. INTRODUCTION

Epoxy foams exhibit excellent properties, including low shrinkage, low moisture uptake,[1] good thermal and chemical stability, as well as mechanical properties even at low foam density.[2] These properties have resulted in many applications of epoxy foams in structural materials, such as sandwich composites,[3] in construction and the automotive industry.[1]

Epoxy foams are produced using various methods. Physical blowing agents, such as hexane or cyclohexane, can be mixed into epoxy resin and hardener formulations.[4] During the exothermic curing reaction between resin and hardener, the physical blowing agents expand and foam the still liquid but curing epoxy formulations. Chemical blowing agents have been widely used to foam epoxy resins both in research[1,5,6] and production of commercial epoxy foams, such as for instance the PB series epoxy foams (Sicomin, France).[7] Chemical blowing agents react with components in the epoxy resin, usually the amino hardener,[1,5] and generate gas to expand the resin/hardener mixture. Syntactic epoxy foams have been produced by mixing the resin and hardener with hollow (or expanding) spheres followed by curing of the resin.[2,8,9] Syntactic epoxy foams have a controllable density, but their density is usually higher compared to that of epoxy foams produced by either chemical or physical blowing.[10] Epoxy foams produced by emulsion templating were also reported.[11,12] Emulsions whose continuous but minority phase consisted of a mixture of epoxy resin/hardener and an internal aqueous templating phase have been produced; curing of the resin phase and the subsequent removal of the internal aqueous phase led to macroporous epoxies, whose density and pore size can be controlled by tuning the emulsion phase volume ratio and the droplet size of the emulsions, respectively.

Air templating is an alternative method to produce polymer foams from nonaqueous foam precursors. Air is mechanically whipped or beaten into liquid monomers or resins,[13−15] and the introduced air forms spherical bubbles which are kinetically stable if the liquid viscosity is high enough. The polymerization/curing of the monomers or resins results in macroporous polymer foams, where the pores are templated by air bubbles. One advantage of air templating as compared to the conventional blowing or syntactic methods is that no costly porogens are needed. Furthermore, nonaqueous foam templating does not require the removal, i.e. by drying, of any liquid templating phase from the resulting polymer foams, making it superior to emulsion templating. Contrary to nonaqueous foams, aqueous foam templates are much easier to be stabilized[16] and were used as templates for the fabrication of various porous materials.[17,18] Porous polymers were made from aqueous liquid foams consisting of a continuous aqueous solution of poly(vinyl alcohol) and formaldehyde;[19] the foam was subsequently cured to produce open-porous hydrogels. Aqueous tannin solutions were mechanically frothed and cured to produce macroporous tannin, which was subsequently pyrolyzed to produce carbon foams.[15] Black liquors, a by-produce from Kraft-mill,[20] have also been mechanically

Received: November 8, 2018
Accepted: January 28, 2019
Published: January 28, 2019

DOI: 10.1021/acsapm.8b00084
ACS Appl. Polym. Mater. 2019, 1, 335−343

whipped into froths, and the lignin was cured to produce macroporous materials; these materials were also used as precursors for the production of carbon foams by pyrolysis. Schueler et al.[21] introduced foamed (styrene-in-water) emulsion templates; the polymerization of the styrene droplets dispersed in the continuous aqueous phase resulted in macroporous polystyrene.

Air templated epoxy foams were disclosed earlier in a patent by Simpson et al.[22] In the disclosed example, nitrogen gas was injected and whipped into a mixture of epoxy resin, hardener, and surfactant. After molding and curing of the liquid epoxy froths, epoxy foams with a foam density in the range of 288 kg/m^3 to 689 kg/m^3 were produced. Lau et al.[23] reported mechanical whipping of air using a kitchen blender into a liquid epoxy resin/hardener mixture, resulting in liquid epoxy froths; subsequent curing of the froths produced macroporous epoxy resins. The authors claimed that the viscous nature of the resin reduced the drainage of liquid resin from the films separating the entrapped bubbles in the epoxy froths, thus preventing froths from collapsing; a highly viscous epoxy/hardener mixture without surfactant was therefore used. More recent work by Song et al.[24] demonstrated the possibility to control the pore size of the epoxy foams by controlling the curing temperature of the liquid froth templates. Increasing the curing temperature of the epoxy resin caused thermal expansion of the entrapped air bubbles in the froth, which simultaneously resulted in a further decrease of the foam density.[24] However, it was necessary to precure all liquid epoxy froth templates at room temperature, which is not a time efficient method to produce epoxy foams.

Many types of additives have been added to conventional epoxy foams to tailor the properties of the resulting foams. Carbon nanotubes were added to epoxy foams to enhance their electrical conductivity.[9] Because a foam structure consists of mainly high aspect ratio polymer walls, the percolation threshold of the carbon nanotubes in polymer phase of the epoxy foam was reduced; therefore, a low nanotube loading resulted already in percolation of the nanotubes and thus boosted the electrical conductivity of the solid foam. Rice husk ash has been used in a chemical blowing process for the production of foamed epoxy composites.[25] The addition of the rice husk ash, due to its nucleation effect, resulted in a reduced average pore size of the epoxy foams. Furthermore, white rice husk ash has been found to result in improved mechanical properties of the epoxy foams. Silica particles have also been found to enable the nucleation of gas bubbles during conventional blowing processes; they contributed to small pore sizes in the resulting epoxy foams or, when the silica loading exceeded a certain weight fraction, led to epoxy foams with a bimodal pore size distribution.[10] Furthermore, the presence of silica particles in the cured epoxy resin resulted in an increased glass transition temperature of the epoxy.

Here, we describe a method to produce epoxy foams using the nonaqueous foam templating method. The addition of silica particles to liquid resin formulations was shown to increase the viscosity of epoxy resin formulations,[26] which was hypothesized to be the key in stabilizing liquid epoxy froths.[23] Using silica particles to tune the morphology of blown epoxy foams has been reported. We aimed to produce low density epoxy foams with a fine cell structure using silica particles as property-defining additives in a commercial liquid epoxy formulation. We also anticipate that the incorporated silica particles will act as reinforcement[27,28] and thermal stabilizers[29] of epoxy foams.

2. EXPERIMENTAL DETAILS

2.1. Materials. Epoxy L (EPL) and hardener GL1, purchased from R&G Faserverbundwerkstoffe GmbH (Waldenbuch, Germany), were used as matrix, and poly(ethylene glycol)-*block*-poly(propylene glycol)-*block*-poly(ethylene glycol) (Pluronic L-81) (Sigma-Aldrich) was used as surfactant. Pyrogenic silica particles HDK H18 were kindly supplied by Wacker Co. (Germany). The fumed silica particles have a primary particle size of about 5−30 nm as determined by scanning electronic microscopy.[30] The size of the fumed silica particles was determined by measuring the particles in tetrahydrofuran by dynamic light scattering (DLS, Malvern Zetasizer Nano ZS, Malvern, UK). The particle size was 120 μm with a polydispersity index of 0.16. All chemicals were used as received.

2.2. Preparation of Epoxy Foam. EPL, GL1, and Pluronic L-81 were mixed with or without silica particles in 50 mL of free-standing polypropylene centrifuge tubes using a 450 W hand mixer equipped with a dough kneading head (Figure S1). The mixing also simultaneously introduced air into the mixture by mechanical whipping. The produced epoxy froths were subsequently cured either at room temperature or in an oven at the desired curing temperatures for 24 h (following the suggested curing protocol of the manufacturer). The formulations, frothing time, and curing conditions are summarized in Table 1. In general a "foam" can be both liquid and solid; in this paper, the solid macroporous epoxy resin is called epoxy foam, while the liquid precursor is called epoxy froth.

Table 1. Resin Formulation, Frothing Time, and Curing Temperature of Epoxy Froths

	EPL (vol %)[a]	GL1 (vol %)[a]	L-81 (vol %)[a]	SiO_2 (w/v %)[b]	frothing time (min)	curing temperature (°C)
1A	68	20	12	0	12	21
1B	68	20	12	0	12	60
2A	68	20	12	0.2	12	60
2B	68	20	12	0.5	12	60
2C	68	20	12	1	12	60
2D	68	20	12	2	12	60
2E	68	20	12	2.5	12	60
2F	68	20	12	5	12	60
2G	68	20	12	10	12	60
3A	68	20	12	2.5	2	60
3B	68	20	12	2.5	6	60
3C	68	20	12	2.5	24	60
4A	68	20	12	2.5	12	80
4B	68	20	12	2.5	12	100

[a]Volume ratio of the liquid components is expressed with respect to the total volume of the liquid phase. [b]Silica particle loading with respect to the liquid phase volume.

2.3. Characterization of Liquid Epoxy Froths and Solid Epoxy Foams. The viscosity η of the liquid mixture of epoxy resin, hardener, surfactant, and silica particles was determined using a rotational rheometer (Discovery Hybrid Rheometer RH2, TA Instruments, Germany). The liquid epoxy resin, hardener, surfactant, and silica particles were mixed in a centrifuge tube until the silica particles were dispersed. A stainless-steel geometry with cone angle of 1° and 40 mm diameter was used. The viscosity of the resin mixture was measured as a function of shear rate in the range from 0.01 to 100 s^{-1} at 25 °C.

To investigate morphology of the epoxy foams, the epoxy foams were hand-broken; small pieces of fragments were fixed on carbon stickers. The fracture surface of the epoxy foams was gold-coated for 40 s at 30 mA in a sputter coater (JEOL Fine Coater JFC-1200,

DOI: 10.1021/acsapm.8b00084
ACS Appl. Polym. Mater. 2019, 1, 335−343

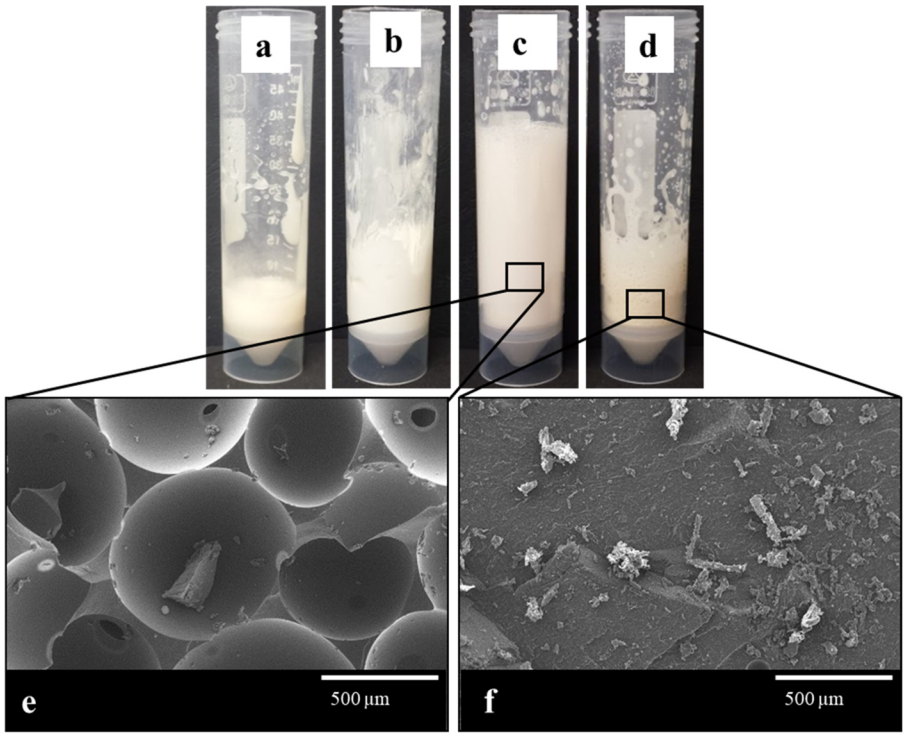

Figure 1. Preliminary formulation trials: (A) epoxy resin/hardener; (B) epoxy resin/hardener/silica particles; (C) epoxy resin/hardener/surfactant, cured at 23 °C; (D) epoxy resin/hardener/surfactant, cured at 60 °C. Curing the epoxy froth at room temperature resulted in epoxy foams with a semiopen porous structure (e), while curing the identical epoxy froths at 60 °C led to nonporous epoxy polymers (f).

Germany). SEM was carried out in the secondary electron beam mode using an electron acceleration voltage of 15 kV. ImageJ was used to analyze the SEM images of the epoxy foams; to obtain an average pore size with statistical significance, at least 150 pores were measured.

The foam density ρ_f of solid epoxy foams was quantified on cut samples, whose diameter d and height h were measured. The foam densities were calculated:

$$\rho_f = \frac{m}{V} = \frac{4m}{\pi d^2 h} \quad (1)$$

where m is the mass of the epoxy foam sample. To measure the skeletal density ρ_s of the cured epoxy foam, about 0.5 g of ground powder of epoxy foams was subjected to helium displacement pycnometry (AccuPyc II 1350, Micrometrics Aachen, Germany). The porosity P of the epoxy foams was calculated:

$$P = \left(1 - \frac{\rho_f}{\rho_s}\right)100\% \quad (2)$$

A universal mechanical tester (Model 5969, Instron GmbH, Buckinghamshire, UK) was used to perform compression tests on epoxy foams. A 50 kN load cell was attached to the mechanical tester. The test method was adapted from standard BS ISO 844. Test specimens with a diameter of 25 mm and a height of 10 mm were placed between two Teflon coated flat compression plates. The test speed was 1 mm min^{-1}. The epoxy foams were compressed by 30% while recording stress−strain curves. The elastic moduli E of the epoxy foams were determined from the slope of the first linear region of the stress−strain curves; the crush strength σ of the epoxy foams was the strength at the end of the first linear region. A minimum of at least five specimens of each sample was tested to obtain elastic moduli and crush strengths with statistical significance.

The curing kinetics of the epoxy formulation was investigated by differential scanning calorimetry (DSC, Discovery DSC, TA Instrument, Germany). Ten milligrams of mixtures of epoxy resin, hardener, and surfactant with or without silica particles were heated to 60 °C at a heating rate of 20 °C/min and isothermal for 3 h. The heat flow curves were plotted as a function of time. Glass transition temperatures (T_g) of the cured epoxy foams were also determined by DSC. Ten milligrams of epoxy foam powder was heated/cooled/heated/cooled between 20 and 150 °C at a ramping rate of 10 °C/min. The heat flow curves were plotted as a function of temperature.

Dynamic mechanical thermoanalysis (DMTA) was performed using a RSA-G2 (TA Instruments, United States) to determine glass transition temperatures T_g of the epoxy foams. Rectangular shaped specimens with dimensions of 10 × 10 × 5 mm were prepared and tested in compression mode at a frequency of 1.0 Hz from 30 to 150 °C at a heating rate of 2 °C/min and an oscillation amplitude of 0.1%.

3. RESULTS AND DISCUSSION

Whipping simply a mixture of epoxy resin/hardener did not result in a froth. However, it was possible to mechanically whip air into epoxy/hardener/silica formulations, resulting in a froth with a limited foam volume. Therefore, following earlier patented work[4,22,31] disclosing foamed epoxy resins, we identified a suitable surfactant to aid foaming of our formulation. With surfactant liquid epoxy froths were successfully produced by mechanically beating air into a liquid epoxy formulation. Friberg[16] in his review stated that the stability of nonaqueous froths depends not on the reduction of the gas/liquid interface tension but on the rheology of the liquid films. Therefore, surfactants do not stabilize nonaqueous froths by reducing the surface tension of the liquid resin/gas interface. In some cases, surfactants do form crystals and stabilize nonaqueous froths;[32] however, we did not observe the formation of a crystalline phase in the liquid resin. Our hypothesis is that the surfactant (Pluronic L-81) phase separated from the epoxy system driven by small surface tension differences between the epoxy resin/hardener and the surfactant. During whipping of the epoxy formulations, the

DOI: 10.1021/acsapm.8b00084
ACS Appl. Polym. Mater. 2019, 1, 335−343

rheology of the heterogeneous liquid films improved the stability of the froths. The liquid froths were stable at room temperature; after storing the epoxy froths for 1 day at room temperature, they solidified into solid epoxy foams. These epoxy foams had a semiopen porous structure with spherical pores, which were templated by the air bubbles in the froths; some pores were connected by pore throats (Figure 1e). However, once the as-prepared liquid froths were placed into an oven at 60 °C, in an attempt to accelerate the curing of the froths, the liquid froths collapsed rapidly, resulting after curing in a nonporous epoxy block (Figure 1f). The elevated temperature resulted in a decrease of the viscosity of the liquid resin phase of the froth, which accelerated the drainage of the liquid from the films separating the air bubbles, resulting in coalescence of air bubbles.

To accelerate the production of epoxy foams by curing liquid froths at an elevated temperature, the viscosity of the liquid phase in the froth had to be increased to slow the drainage from the liquid froth at elevated curing temperatures. Therefore, silica particles were added into the epoxy resin/hardener/surfactant mixture. The viscosity of the mixtures containing increasing silica loadings was measured. The pure liquid phase containing no and 0.2 wt % silica particles exhibited slight shear thinning; the viscosity decreased with increasing shear rate from 0.01 to 100 s^{-1}, while the resin phase containing 0.5 to 10 wt % silica particles exhibited a more significant shear thinning behavior. Furthermore, the zero-shear viscosity of the mixtures increased with increasing silica loadings (Figure 2). The increased zero-shear viscosity of

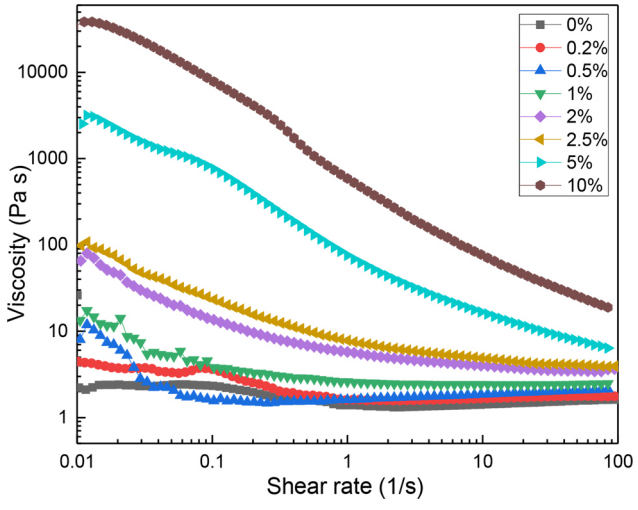

Figure 2. Viscosity of liquid resin phase consisting of epoxy, hardener, and surfactant with increasing silica particle loading as a function of shear rate.

the liquid phase with increasing silica particle loading is expected to favor the formation of stable froths, especially at elevated temperatures.

Epoxy foams were successfully produced by curing the liquid epoxy froths containing silica particles at 60 °C, during which the silica containing froths were all stable, i.e. the froth volume did not decrease. The epoxy froth containing 0.2 wt % silica particles was surprisingly stable during curing at 60 °C even though the zero-shear viscosity of the liquid resin phase with such low amount of silica was only 4 Pa·s as compared to 2 Pa·s for the pure resin without silica particles. A reduction of the percolation threshold of fillers in polymer foams as compared to bulk polymer has been reported;[33,34] this has been explained by fillers being concentrated in the plateau regions in the liquid phase due to the relocation of the fillers during the frothing process. Therefore, regardless of the rheological behavior of the bulk liquid, the presence of silica particles in the plateau regions could arrest liquid film drainage and stabilize air bubbles against coalescence.[35] The curing behavior of the epoxy froths was investigated by holding the liquid formulations at 60 °C for 3 h in a DSC. The epoxy foams were fully cured in 90 min (a detailed discussion can be found in the Supporting Information, Figure S2) irrespectively of silica particle loading. The skeletal and foam density of the epoxy foams (Figure 3a) containing 0.2 wt % silica was 1.18

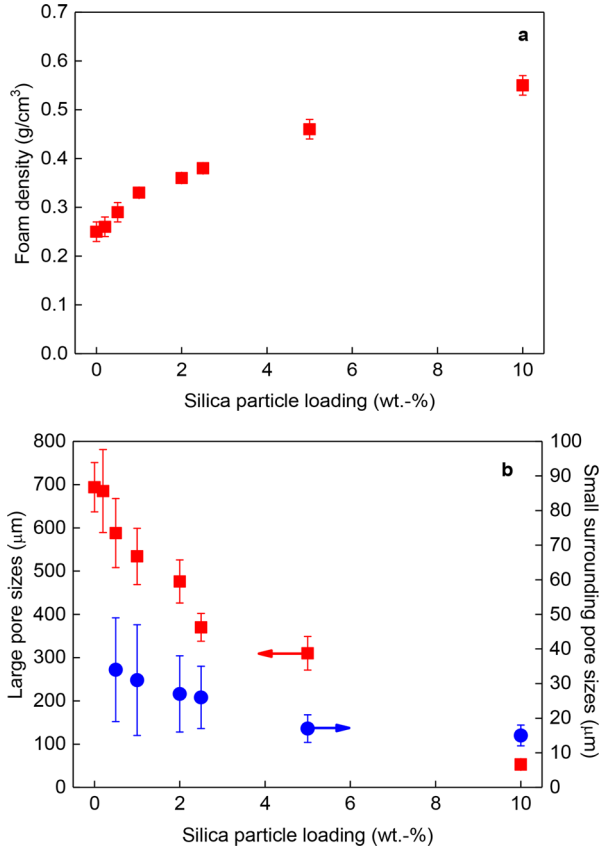

Figure 3. Foam density (a) and average pore size of large and small pores (b) of solid epoxy foams as a function of silica particle loading.

and 0.25 g/cm^3, respectively, resulting in a porosity of 79% (the physical, morphological, and mechanical properties of all epoxy foams are summarized in the Supporting Information, Table S1). Epoxy foams with silica particles possessed a closed-cell structure (Figure 4). This can be explained by the presence of the silica particles, which retarded liquid film drainage in the epoxy froths during curing. As a result, the liquid films separating the air bubbles were not thin enough to allow pore throats to form during curing. Epoxy foams containing 0.2 wt % silica particles had an average pore size of about 700 μm: hardly any smaller pores with a diameter of about 100 μm existed in the pore walls or plateau regions. With increasing silica loadings, the skeletal density of the epoxy foams was identical within error, which was 1.18 ± 0.02 g/cm^3. However, the foam densities of the epoxy foams increased to about 0.55

DOI: 10.1021/acsapm.8b00084
ACS Appl. Polym. Mater. 2019, 1, 335−343

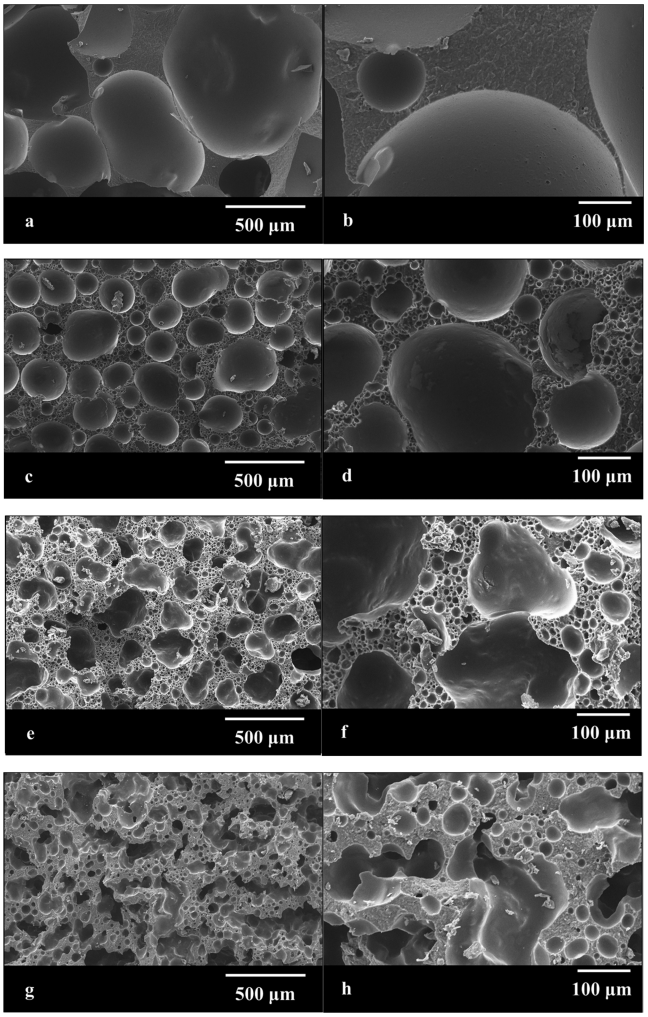

Figure 4. Characteristic SEM images of macroporous epoxy foams containing increasing amounts of silica particles: 0.2 (a, b), 2.5 (c, d), 5 (e, f), and 10% (g, h) silica particles. With increasing silica particle loading, the morphology of the epoxy foams changed from a semiopen porous structure to a closed cell but hierarchical pore structure to a hierarchical pore structure with irregular pores.

g/cm^3 (Figure 3a), leading to a decrease of the porosity from 79 to 54%. Because all liquid froths in this group were produced with identical energy input (identical mixer and mixing tool, whipping time, and initial liquid phase volume), the liquid phase containing more silica particles, thus having a higher viscosity, was more difficult to be mechanically whipped, resulting in the froths with smaller froth volumes and thus lower air content. Moreover, the silica concentrations in the froths also affected the pore structure of the produced solid epoxy foams; the pore size distribution changed from a monomodal pore size distribution (epoxy foams containing no silica particles but cured at room temperature and 0.2 wt % silica particles, Figure 1A and Figures 4a and b) to foams with a hierarchical pore structure, characterized by large pores with average diameters of hundreds of micrometers being surrounded by many smaller pores having an average pore diameter approximately one order of magnitude smaller (Figure 3b and Figures 4c–h show representative SEM images). Silica particles could function as nucleating agents to help regulate and stabilize gas bubbles during foaming polymers:[4,10] such nucleation from silica particles must be in a foaming process, which starts from small gas bubbles (usually caused by phase separation of blowing agents) and bubble growth. However, in our case, the air bubbles were introduced by mechanical whipping; the air was entrained through the spout, and bubble break up occurred only later by shear. Therefore, in our case, the function of the silica particles was not to aid nucleation. Instead, the silica particles most likely formed a network or packed in the liquid films in the epoxy froths; the network or packed silica particles hindered the small air bubbles to coalesce, therefore stabilizing the froths with small bubbles in the liquid films. The curing of such froths therefore resulted in a hierarchical pore architecture containing both large and small pores. The epoxy foams produced by curing froths containing 5 and 10 wt % silica particles contained nonspherical pores (Figures 4e–h). Liquid films containing a high silica loading thus having an increased rigidity did not permit the bubbles, after being deformed during whipping, to relax into their equilibrium spherical shape,[14] therefore resulting after curing in epoxy foams with irregular pores, e.g. channel-like or elliptical pores. We determined the size of the constrictions in these channel-like pores separating them in to smaller joined pores; the pore sizes for each of the individual pores was determined. Once the large pores had elliptical shapes, the average size of these pores was determined by measuring and averaging the long and short axis of the ellipse. Both the large and small pore sizes of the epoxy foam decreased with increasing silica particle loading (Figure 3b), as the silica particles hindered the drainage from the liquid film and bubble coalescence in the initial epoxy froths.

Solid epoxy foams were rigid but not brittle, characterized by compressive stress–strain curves without failure up to strains of 30% (Figure 5a); the specimens buckled but exhibited no visible cracks during mechanical testing. As expected, the elastic moduli and crush strengths of the epoxy foams depended on the foam density; epoxy foams with higher foam densities had higher elastic moduli and crush strengths. To compare foams with different porosities and investigate the effect of the silica particles on the mechanical properties of the epoxy foams, the elastic moduli and crush strengths of the epoxy foams were normalized with respect to their foam density. The epoxy foams without silica particles had a specific elastic modulus of 348 ± 32 MPa/(g/cm^3) and a specific crush strength of 16 ± 2 MPa/(g/cm^3). With increasing the silica particle loading from 0.2 to 2.5 wt %, the specific stiffness and crush strengths of the epoxy foams increased from 420 MPa/(g/cm^3) to 520 MPa/(g/cm^3) (Figure 5b). Despite the incorporation of silica particles into pore walls of the epoxy foams, the reinforcing efficiency of silica particles at such low concentrations is low as predicted by the Guth–Gold relation.[36] The glass transition temperature T_g, determined by DMTA, of all epoxy foams was about 88 °C, indicating that the silica particles did not chemically interact with the epoxy matrix. The incorporation of silica particles, however, did affect the pore morphology and structure of the epoxy foams, which also affects the mechanical properties. For instance, Wong et al.[37] reported that cross-linked polystyrene foams with a hierarchical pore structure produced by emulsion templating have a higher stiffness as compared to foams with a monomodal pore size distribution. Therefore, the increase of the specific elastic moduli and crush strengths could also be due to the change of the pore morphology of the epoxy foams from a single modal pore size distribution to a hierarchical pore structure. Increasing the silica particle loading to 5 and 10 wt %

DOI: 10.1021/acsapm.8b00084
ACS Appl. Polym. Mater. 2019, 1, 335–343

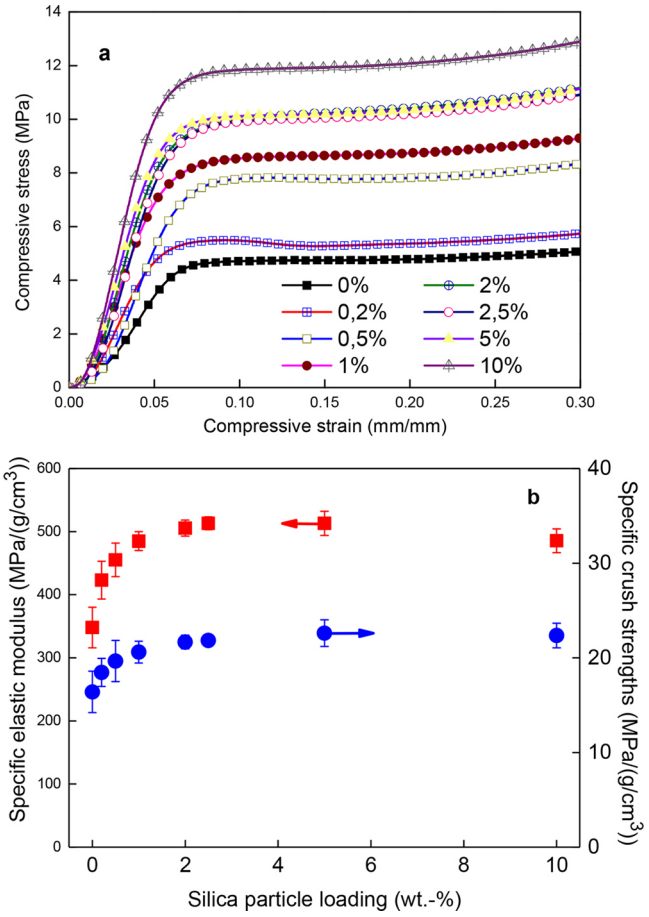

Figure 5. Stress–strain curves of epoxy foams (a) and specific elastic moduli and crush strengths of epoxy foams as a function of silica particle loading (b).

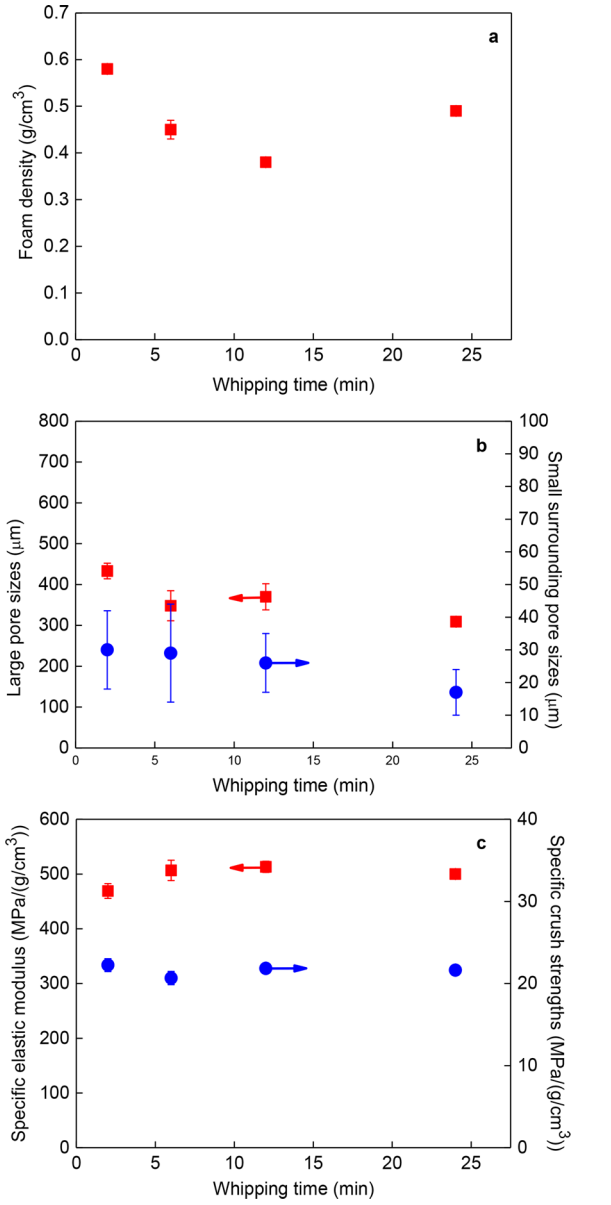

Figure 6. Foam density (a), average pore size (b), and specific elastic moduli and crush strengths (c) of the epoxy foams as a function of whipping time used to produce the epoxy froths.

did not further increase the specific elastic moduli and crush strengths as compared to the epoxy foams containing smaller amounts of silica particles. However, the mechanical properties of the epoxy foams containing 5 and 10 wt % silica particles could be affected because those foams contained nonspherical pores;[14,23] the pore walls of irregular shaped pores buckle much easier in compression as compared to the pore walls of spherical pores.

To investigate the introduction of air bubbles into the liquid phase, epoxy froths were produced using identical formulations (all with 2.5 wt % silica particles) but with increasing whipping times (and thus energy input) from 2 to 24 min. The epoxy foams produced by curing froths whipped for 2 min possessed hierarchical porous structures with larger pores of an average size of 440 μm and smaller pores with sizes of about 30 μm, while the epoxy foams obtained by curing 6 and 12 min whipped froths had smaller average pore sizes (Figure 6b). This finding supports our hypothesis that the air bubbles initially whipped into the liquid phase were large and that these larger air bubbles initially introduced into the template were broken up into smaller ones. Increasing the whipping time (from 2 to 12 min) of the froths resulted in epoxy foams with a lower density. This was consistent with our observation that the volume of the froths increased with increasing whipping time from 2 to 12 min, evidencing that an increasing amount of air was continuously entrapped into the liquid froths. However, when the froth was whipped for 24 min, the froth volume decreased again. After curing this template, the resulting epoxy foam had a higher density than the foams synthesized by curing froths produced with shorter whipping times (Figure 6a). This indicated that "overwhipping" occurred between 12 to 24 min. "Overwhipping" is a well-known phenomenon when preparing whipped cream and is studied by food scientists.[38] In our case, the reason for overwhipping could be the onset of the reaction between epoxy and hardener, resulting in an increase of the viscosity of the liquid froth phase or phase separation of the surfactant, which reduces the capability of the liquid phase to entrap more air, thus leading to a reduced froth volume. The average pore size of the large pores in epoxy foams produced by curing the overwhipped froths was further reduced to 309 μm as compared to the epoxy foams prepared from froths whipped for 2, 6, and 12 min (Figure 6b). This indicated that although air is gradually removed from the froths during overwhipping, larger air bubbles were still being broken. The

DOI: 10.1021/acsapm.8b00084
ACS Appl. Polym. Mater. 2019, 1, 335−343

epoxy foams produced from 2, 6, 12, and 24 min froths possessed hierarchal pore structures (Figure S4); they also exhibited similar specific elastic moduli and crush strengths because they had the same composition (Figure 6c).

The effect of curing temperature on the properties of the epoxy foams was investigated by curing epoxy froths of identical formulation and whipping time at 60, 80, and 100 °C, respectively. Increasing the curing temperature from 60 to 80 and 100 °C resulted in epoxy foams with lower foam densities (Figure 7a). The increased curing temperature caused larger average pore sizes by thermal expansion of air bubbles before complete solidification of the liquid phase in the epoxy froths (Figure 7b).[24] The specific elastic moduli and the crush strengths of the epoxy foams produced by curing the liquid froths at 80 and 100 °C were slightly lower than those of the epoxy foam cured at 60 °C (Figure 7c). The thermal expansion of the air bubbles in the froths caused the liquid films to stretch during air bubble growth, which resulted after curing in epoxy foams with thinner polymer walls and thus lower resistance to buckling in compression.

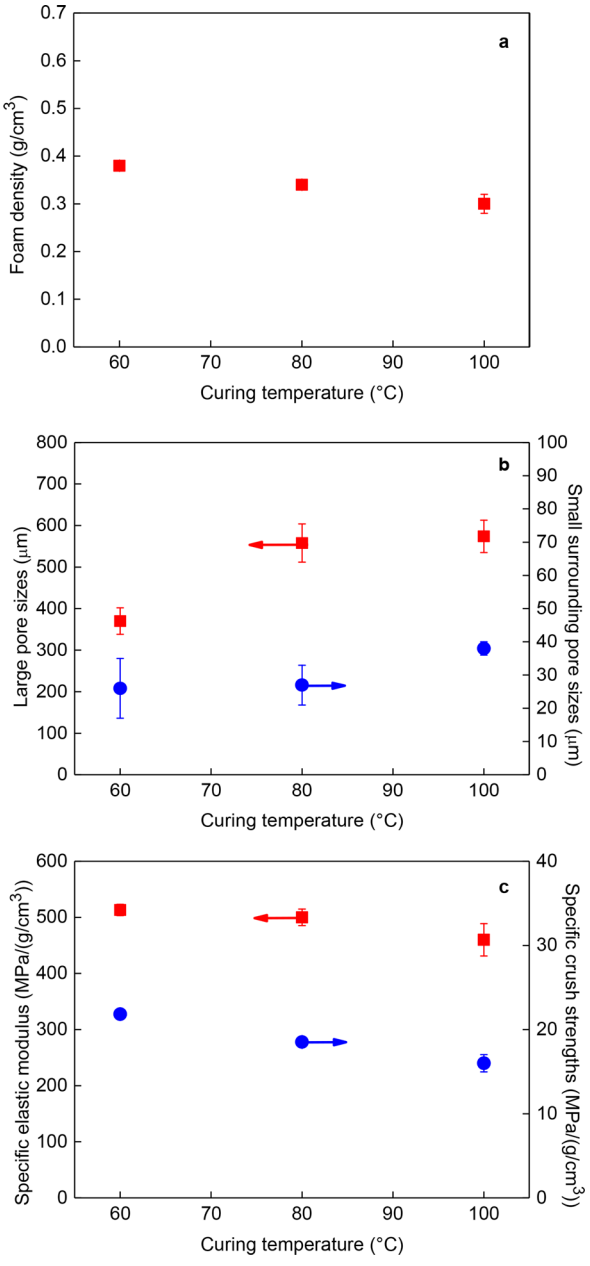

Figure 7. Foam density (a), average pore size (b), and specific elastic moduli and crush strengths (c) of the epoxy foams as a function of curing temperature of the epoxy froths.

To compare the mechanical properties of the epoxy foams produced by us using the air templating method with the reported ones, the elastic moduli and crush strengths of the epoxy foams as a function of their foam density are plotted in Figure 8a. The curves were fitted using the power law:[2]

$$E = a\rho_f^{\ m} \tag{3}$$

$$\sigma = b\rho_f^{\ n} \tag{4}$$

where E is the elastic moduli, σ the crush strengths of the epoxy foams, and a and b material related constants, while m and n are structure related constants. The elastic moduli and crush strengths of the epoxy foams as a function of their density fit well to the power-law equation; a and b had values of 513 and 27, respectively, and m and n had values of 1.03 and 1.30, respectively. Ashby[39] reported that the failure of a porous material is due to stretching (m = 1 and n = 1) or bending (m = 2 and n = 1.5) of the pore struts or walls: in most cases foams exhibit a bending-dominated failure. However, our epoxy foams had lower m and n values, indicating more stretching of the pore walls prior to failure, as compared to previously reported epoxy foams.[2,6,9] In Ashby's model, the force exerted on a strut of a nonrigid porous structure results in bending of strut and causes the deformation of the pore. In our epoxy foams, a majority of the large pore walls indeed underwent bending. Nevertheless, due to the hierarchical pore structure of our epoxy foams, the bending of the large pore wall must cause the deformation of each individual small pore therein. At this secondary scale, the smaller pores are considered as rigid structure and, therefore, the bending of the large pore walls was transferred to stretching of the small pores, resulting in an apparent stretching-dominated failure behavior of our epoxy foams.

The elastic moduli (Figure 8a) and crush strengths (Figure 8b) of our epoxy foams are in line with other epoxy foams reported in the literature;[2,6,9,40] the difference in the absolute values of the stiffness and strengths is due to the different epoxy resin/hardener formulations that have been used to prepare those samples. However, the stiffness and strengths of our epoxy foam composites did not decrease with foam density as steeply as for other reported epoxy foams: this indicates that the hierarchical pore structure is beneficial for the mechanical properties of low density epoxy foams (e.g., <0.25 g/cm^3) (Figures 8b and c).

The specific elastic moduli and crush strengths were not affected by the average pore size of the large pores when the pore sizes increased from 50 to 450 μm. A further increase of the average pore size above 600 μm resulted in a slight decrease of the elastic moduli and crush strengths. At normalized foam density, the presence of larger pores in epoxy foams indicates thinner pore walls, which have lower resistance to buckling during compression, resulting in reduced elastic moduli and crush strengths.

The thermal stability characterized by thermogravimetric analysis of the foamed epoxy composites characterized in air and nitrogen showed that the epoxy foams were stable without any significant weight loss up to at least 200 °C in air. The experimental and results can be found in the Figure S5.

DOI: 10.1021/acsapm.8b00084
ACS Appl. Polym. Mater. 2019, 1, 335−343

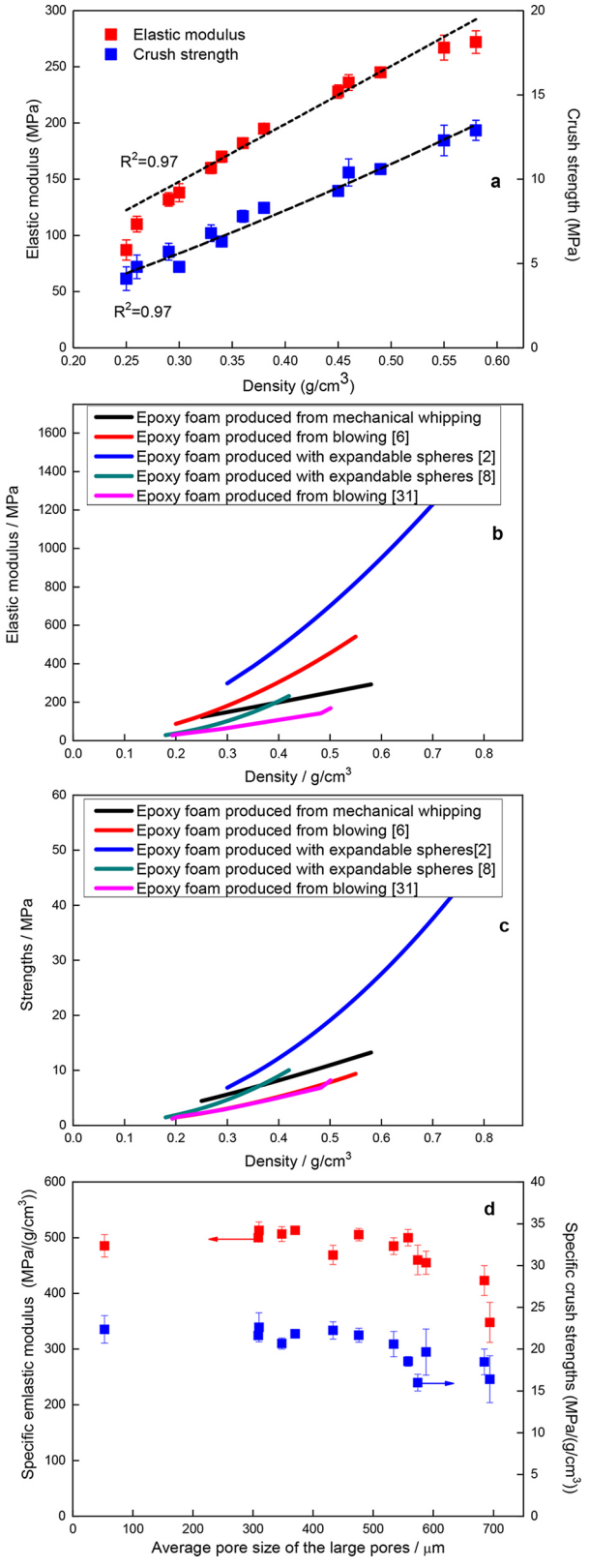

Figure 8. Elastic moduli and crush strengths of epoxy foams as a function of their foam density (a); comparison of the mechanical properties of epoxy foam composites with epoxy foams reported in the literature (b and c);[2,6,9,40] specific elastic moduli and crush strengths as a function of pore sizes of the epoxy foams (d).

4. CONCLUSIONS

Epoxy foams were successfully produced by mechanically whipping air into an epoxy resin, hardener, surfactant, and silica particle mixture, resulting in a stable liquid froths, which could be subsequently cured into solid epoxy foams. Increasing silica particle loadings increased the stability of the froths by increasing the viscosity of the liquid phase of the froths, enabling the curing of the epoxy at elevated temperatures. Epoxy foams containing silica particles had a hierarchical macropore structure where the large pores were surrounded by smaller pores. Increasing the silica particle loading in the epoxy froths resulted in an increasing foam density and a decrease of the average (large and small) pore sizes in the epoxy foams. However, when the silica loading exceeded 5 wt %, air bubbles introduced into the epoxy froths could not assume their equilibrium spherical shape after whipping stopped, leading to epoxy foams with nonspherical pores. The epoxy foams containing silica particles possessed specific elastic moduli and crush strengths higher than those of the epoxy foam with a monomodal pore size distribution.

■ ASSOCIATED CONTENT

Supporting Information

The Supporting Information is available free of charge on the ACS Publications website at DOI: 10.1021/acsapm.8b00084.

Dimensions of the dough kneading head, heat flow of epoxy froths during curing, glass transition temperature of epoxy foams, summary of the properties of the epoxy foams, morphology of epoxy foam produced from froths produced from different whipping time, and thermal degradation behavior of epoxy foams (PDF)

■ AUTHOR INFORMATION

Corresponding Authors

*E-mail: qixiang.jiang@univie.ac.at.
*E-mail: alexander.bismarck@univie.ac.at.

ORCID

Qixiang Jiang: 0000-0002-4315-2229
Alexander Bismarck: 0000-0002-7458-1587

Notes

The authors declare no competing financial interest.

■ ACKNOWLEDGMENTS

The authors acknowledge the financial support of JSP (https://www.jsp.com), which enabled this work. The authors also acknowledge the financial support from the HIPERM project (Grant I 1800 Internationale Projekte) provided by Austrian Science Fund (FWF).

■ REFERENCES

(1) Alonso, M. V.; Auad, M. L.; Nutt, S. R. Modeling the compressive properties of glass fiber reinforced epoxy foam using the analysis of variance approach. *Compos. Sci. Technol.* **2006**, *66*, 2126–2134.

(2) Wang, L.; Yang, X.; Zhang, J.; Zhang, C.; He, L. The compressive properties of expandable microspheres/epoxy foams. *Composites, Part B* **2014**, *56*, 724–732.

(3) Gupta, N.; Maharsia, R. Enhancement of Energy Absorption in Syntactic Foams by Nanoclay Incorporation for Sandwich Core Applications. *Appl. Compos. Mater.* **2005**, *12*, 247–261.

(4) Russick, E. M.; Rand, P. B. Epoxy foams using multiple resins and curing agents. US6110982A, 2000.

DOI: 10.1021/acsapm.8b00084
ACS Appl. Polym. Mater. 2019, 1, 335–343

(5) Alonso, M. V.; Auad, M. L.; Nutt, S. Short-fiber-reinforced epoxy foams. *Composites, Part A* **2006**, *37*, 1952−1960.
(6) Stefani, P. M.; Barchi, A. T.; Sabugal, J.; Vazquez, A. Characterization of epoxy foams. *J. Appl. Polym. Sci.* **2003**, *90*, 2992−2996.
(7) Foaming epoxy systems. http://www.sicomin.com/products/epoxy-systems/foaming (accessed January 30, 2018).
(8) Allameh-Haery, H.; Kisi, E.; Fiedler, T. Novel cellular perlite−epoxy foams: Effect of density on mechanical properties. *J. Cell. Plast.* **2017**, *53*, 425−442.
(9) Xu, Y.; Li, Y.; Bao, J.; Zhou, T.; Zhang, A. Rigid thermosetting epoxy/multi-walled carbon nanotube foams with enhanced conductivity originated from a flow-induced concentration effect. *RSC Adv.* **2016**, *6*, 37710−37720.
(10) Chen, K.; Tian, C.; Lu, A.; Zhou, Q.; Jia, X.; Wang, J. Effect of SiO2 on rheology, morphology, thermal, and mechanical properties of high thermal stable epoxy foam. *J. Appl. Polym. Sci.* **2014**, *131*, 40068.
(11) Wang, J.; Zhang, C.; Du, Z.; Xiang, A.; Li, H. Formation of porous epoxy monolith via concentrated emulsion polymerization. *J. Colloid Interface Sci.* **2008**, *325*, 453−458.
(12) Wang, J.; Du, Z.; Li, H.; Xiang, A.; Zhang, C. Interconnected porous epoxy monoliths prepared by concentrated emulsion templating. *J. Colloid Interface Sci.* **2009**, *338*, 145−150.
(13) Barron, B.; Dunlap, J. Air frothed polyurethane foams. US3821130A, 1974.
(14) Lee, K. Y.; Wong, L. L. C.; Blaker, J. J.; Hodgkinson, J. M.; Bismarck, A. Bio-based macroporous polymer nanocomposites made by mechanical frothing of acrylated epoxidised soybean oil. *Green Chem.* **2011**, *13*, 3117−3123.
(15) Szczurek, A.; Fierro, V.; Pizzi, A.; Celzard, A. Mayonnaise, whipped cream and meringue, a new carbon cuisine. *Carbon* **2013**, *58*, 245−248.
(16) Friberg, S. E. Foams from non-aqueous systems. *Curr. Opin. Colloid Interface Sci.* **2010**, *15*, 359−364.
(17) Wong, J. C. H.; Tervoort, E.; Busato, S.; Gonzenbach, U. T.; Studart, A. R.; Ermanni, P.; Gauckler, L. J. Macroporous polymers from particle-stabilized foams. *J. Mater. Chem.* **2009**, *19*, 5129−5133.
(18) Studart, A. R.; Gonzenbach, U. T.; Tervoort, E.; Gauckler, L. J. Processing Routes to Macroporous Ceramics: A Review. *J. Am. Ceram. Soc.* **2006**, *89*, 1771−1789.
(19) Pan, Y.; Wang, W.; Peng, C.; Shi, K.; Luo, Y.; Ji, X. Novel hydrophobic polyvinyl alcohol-formaldehyde foams for organic solvents absorption and effective separation. *RSC Adv.* **2014**, *4*, 660−669.
(20) Jalalian, M.; Jiang, Q.; Birot, M.; Deleuze, H.; Woodward, R. T.; Bismarck, A. Frothed black liquor as a renewable cost effective precursor to low-density lignin and carbon foams. *React. Funct. Polym.* **2018**, *132*, 145−151.
(21) Schüler, F.; Schamel, D.; Salonen, A.; Drenckhan, W.; Gilchrist, M. D.; Stubenrauch, C. Synthesis of Macroporous Polystyrene by the Polymerization of Foamed Emulsions. *Angew. Chem., Int. Ed.* **2012**, *51*, 2213−2217.
(22) Simpson, S. S.; Yeznach, A.; Barton, C. L. Epoxy foam. US4546118, 1985.
(23) Lau, T. H. M.; Wong, L. L. C.; Lee, K. Y.; Bismarck, A. Tailored for simplicity: creating high porosity, high performance bio-based macroporous polymers from foam templates. *Green Chem.* **2014**, *16*, 1931−1940.
(24) Song, W.; Barber, K.; Lee, K. Y. Heat-induced bubble expansion as a route to increase the porosity of foam-templated bio-based macroporous polymers. *Polymer* **2017**, *118*, 97−106.
(25) Stefani, P. M.; Cyras, V.; Tejeira Barchi, A.; Vazquez, A. Mechanical properties and thermal stability of rice husk ash filled epoxy foams. *J. Appl. Polym. Sci.* **2006**, *99*, 2957−2965.
(26) Mahrholz, T.; Stängle, J.; Sinapius, M. Quantitation of the reinforcement effect of silica nanoparticles in epoxy resins used in liquid composite moulding processes. *Composites, Part A* **2009**, *40*, 235−243.
(27) Wu, R.; Menner, A.; Bismarck, A. Tough interconnected polymerized medium and high internal phase emulsions reinforced by silica particles. *J. Polym. Sci., Part A: Polym. Chem.* **2010**, *48*, 1979−1989.
(28) Ikem, V. O.; Menner, A.; Bismarck, A. Tailoring the mechanical performance of highly permeable macroporous polymers synthesized via Pickering emulsion templating. *Soft Matter* **2011**, *7*, 6571−6577.
(29) Khankrua, R.; Pivsa-Art, S.; Hiroyuki, H.; Suttiruengwong, S. Thermal and Mechanical Properties of Biodegradable Polyester/Silica Nanocomposites. *Energy Procedia* **2013**, *34*, 705−713.
(30) Skelhon, T. S.; Grossiord, N.; Morgan, A. R.; Bon, S. A. Quiescent water-in-oil Pickering emulsions as a route toward healthier fruit juice infused chocolate confectionary. *J. Mater. Chem.* **2012**, *22*, 19289−19295.
(31) Gormley, W. T.; Gillespie, G. J. Thermoset epoxy foam compositions and a method of preparing the same. US4090986, 1978.
(32) Shrestha, L. K.; Aramaki, K.; Kato, H.; Takase, Y.; Kunieda, H. Foaming Properties of Monoglycerol Fatty Acid Esters in Nonpolar Oil Systems. *Langmuir* **2006**, *22*, 8337−8345.
(33) Ameli, A.; Jung, P. U.; Park, C. B. Electrical properties and electromagnetic interference shielding effectiveness of polypropylene/carbon fiber composite foams. *Carbon* **2013**, *60*, 379−391.
(34) Li, J.; Zhang, G.; Ma, Z.; Fan, X.; Fan, X.; Qin, J.; Shi, X. Morphologies and electromagnetic interference shielding performances of microcellular epoxy/multi-wall carbon nanotube nanocomposite foams. *Compos. Sci. Technol.* **2016**, *129*, 70−78.
(35) Rio, E.; Drenckhan, W.; Salonen, A.; Langevin, D. Unusually stable liquid foams. *Adv. Colloid Interface Sci.* **2014**, *205*, 74−86.
(36) Guth, E. On the hydrodynamical theory of the viscosity of suspensions. *Phys. Rev.* **1938**, *53*, 322−325.
(37) Wong, L. L. C.; Ikem, V. O.; Menner, A.; Bismarck, A. Macroporous Polymers with Hierarchical Pore Structure from Emulsion Templates Stabilised by Both Particles and Surfactants. *Macromol. Rapid Commun.* **2011**, *32*, 1563−1568.
(38) Smith, A. K.; Goff, H. D.; Kakuda, Y. Microstructure and rheological properties of whipped cream as affected by heat treatment and addition of stabilizer. *Int. Dairy J.* **2000**, *10*, 295−301.
(39) Ashby, M. F. The properties of foams and lattices. *Philos. Trans. R. Soc., A* **2006**, *364*, 15−30.
(40) Altuna, F. I.; Ruseckaite, R. A.; Stefani, P. M. Biobased Thermosetting Epoxy Foams: Mechanical and Thermal Characterization. *ACS Sustainable Chem. Eng.* **2015**, *3*, 1406−1411.

DOI: 10.1021/acsapm.8b00084
ACS Appl. Polym. Mater. 2019, 1, 335−343

Supporting Information

Air Templated Macroporous Epoxy Foams with Silica Particles as Property-Defining Additive

Mohammad Jalalian, Qixiang Jiang*, and Alexander Bismarck*

Institute of Material Chemistry and Research, Polymer & Composite Engineering (PaCE) Group, Faculty of Chemistry, University of Vienna, Währinger Strasse 42, Vienna, 1090, Austria.

Corresponding authors

*Email: qixiang.jiang@univie.ac.at, alexander.bismarck@univie.ac.at

S1: Hand mixer and dough kneading head

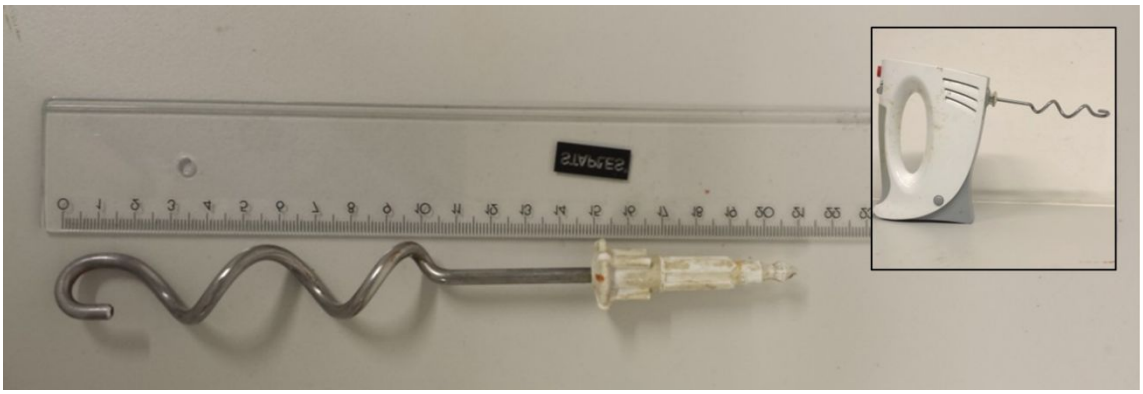

Figure S1. Dimensions of the dough kneading head

S2: Curing of the epoxy resin with and without silica particles.

Epoxy froths without silica particles were cured at room temperature for 24 h following the suggested curing protocol. Silica particles were introduced in the epoxy froths to increase the

resin viscosity to enable curing of the froths at elevated temperature, specifically at 60°C, 80°C and 100°C, without the froths collapsing. The epoxy froths were cured at the elevated temperatures also for 24 h. The curing kinetic was investigated by differential scanning calorimetry (DSC, Discovery DSC, TA Instrument, Germany). The mixtures of epoxy resin, hardener, surfactant and with or without silica particles were heated at 20°C/min to 60°C and held at this temperature for 3 h. The heat flow curves were plotted as a function of time (Figure S3).

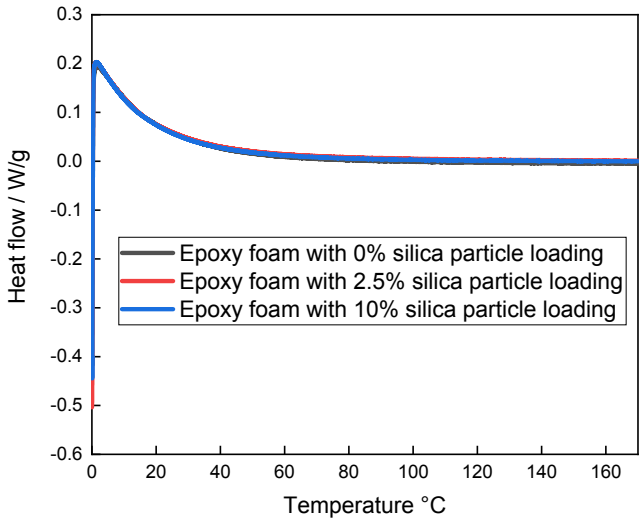

Figure S2. Heat flow of epoxy froths with 0%, 2.5% and 10% silica particles during curing at 60°C.

The heat of reaction ΔH_r was 250±10 J/g irrespectively of silica particle content. The curing was completed after 90 min for all the formulations used.

The glass transition temperature (T_g) of the cured epoxy foams was also investigated using DSC by heating / cooling / heating / cooling the epoxy resin between 20°C to 150°C at a rate of 10°C / min. In the first heating curves of all the samples (Figure S4) either two endothermic heat flow processes, which could be due to impurities or relaxation of the polymer network after curing or one small exothermal heat flow process (upward peak) with an average enthalpy of 1.1±0.4 J/g (0.44% of ΔH_R) centred around 60°C were observed. Should it be post curing, which is unlikely considering that the samples were cured at 60°C for 24 h, it is only a very small effect as

compared to the overall enthalpy of curing. This indicated full curing of the epoxy resin. The T_g, as determined by DSC, of the cured epoxy foams were all about 60°C, regardless the silica particle loadings. The findings were consistent with the T_g determined using DMTA. It is also worth noticing that the T_g from the DMTA and DSC had a difference of 28°C for all the samples due to the different measuring methods. The constant Tg indicated that the silica particles only functioned to stabilise the epoxy froths but did not interact with the epoxy polymer network. Furthermore, all the static mechanical properties of the epoxy foams were measured at room temperature, which is way below T_g.

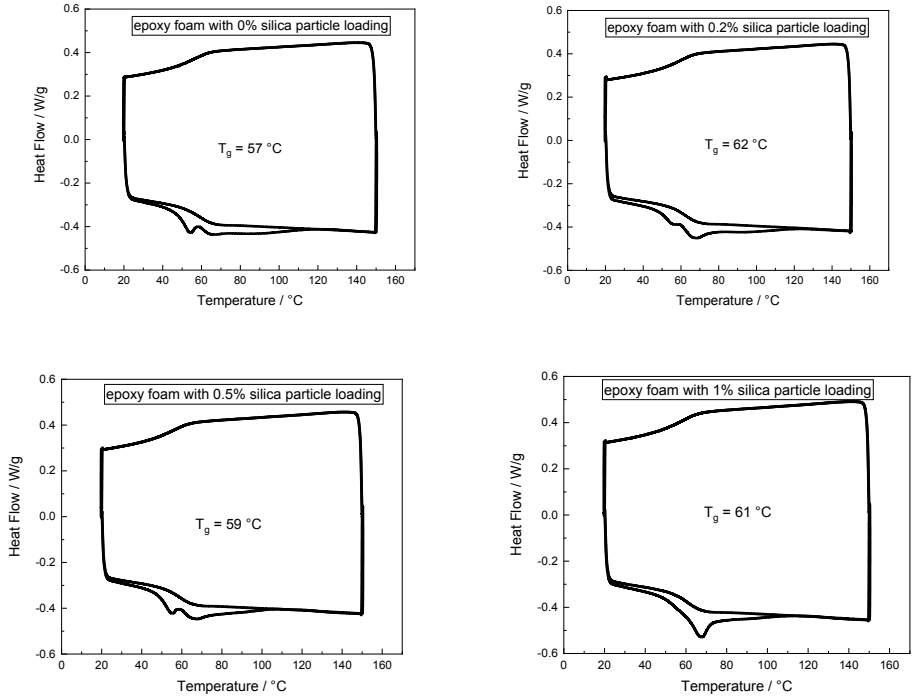

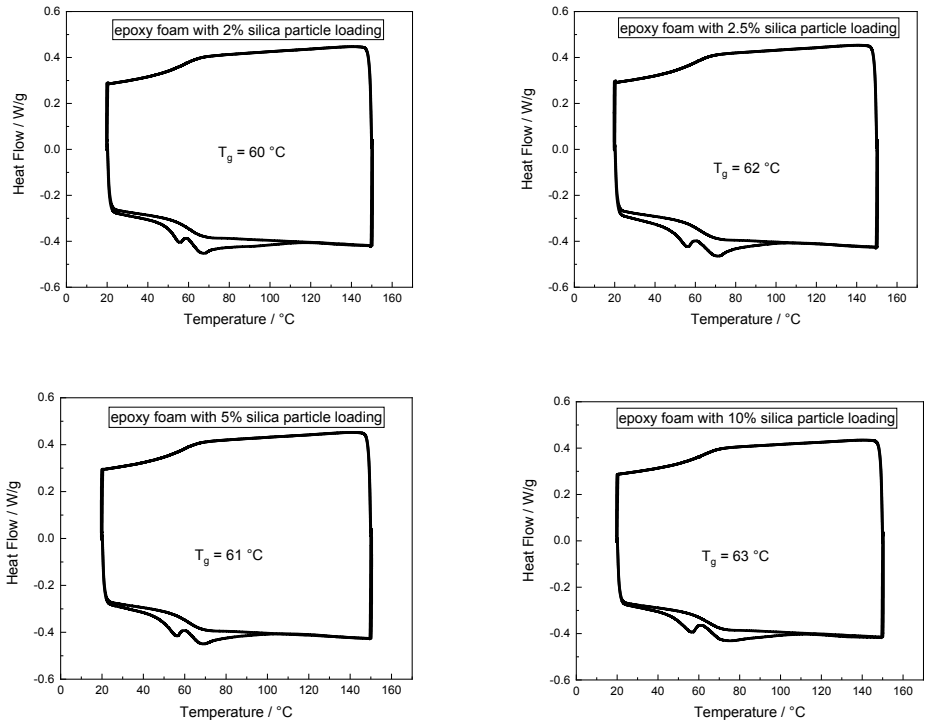

Figure S3. Heat flow curves and T_g of the epoxy foams with silica particles (Exothermal up).

S3: Summary of the physical, morphological and mechanical properties of the air templated epoxy foams with and without silica particles.

Table S1. Summary of foam (ρ_f) and skeletal density (ρ_s), porosity (P), glass transition temperature from DMTA (T_g), average pore sizes of large (x_1) and small pores (x_2), elastic modulus (E) and crush strength (σ) of the epoxy foams

Sample	ρ_f (g/cm³)	ρ_s (g/cm³)	P (%)	T_g (°C)	x_1 (μm)	x_2 (μm)	E (MPa)	σ (MPa)
1A	0.25±0.02	1.18±0.01	79±1	88±0.3	694±57	-	87±9	4.1± 0.7
2A	0.26±0.02	1.18±0.01	78±1	88.7±0.2	685±96	56±18	110±7	4.8±0.4
2B	0.29±0.02	1.17±0.01	75±1	88.8±0.4	588±80	34±15	132±6	5.7±0.8
2C	0.33±0.01	1.16±0.02	71±1	89.0±0.2	534±65	31±16	160±5	6.8±0.5
2D	0.36±0.01	1.17±0.02	69±1	89.0±0.3	476±50	27±11	182±4	7.8±0.3

2E	0.38±0.01	1.18±0.01	68±1	89.2±0.1	370±32	26±9	195±2	8.3±0.2
2F	0.46±0.02	1.19±0.02	61±1	89.2±0.2	310±39	17±4	236±7	10.4±0.8
2G	0.55±0.02	1.20±0.02	54±1	88.6±0.4	53±9	15±3	267±11	12.3±0.9
3A	0.58±0.01	1.17±0.01	50±1	86.7±0.6	433±19	30±12	272±10	12.9±0.6
3B	0.45±0.02	1.17±0.01	62±1	86.0±0.3	348±37	29±15	228±6	9.3± 0.3
3C	0.49±0.01	1.19±0.02	59±1	87.0±0.2	309±10	17±7	245±1	10.6±0.1
4A	0.34±0.01	1.18±0.01	71±1	85.0±0.2	558±46	27±6	170±5	6.3±0.2
4B	0.30±0.02	1.19±0.01	75±1	85.0±0.3	574±39	38±2	138±8	4.8±0.3

S4: Morphology of epoxy foam produced with 2.5% silica particles but different frothing time

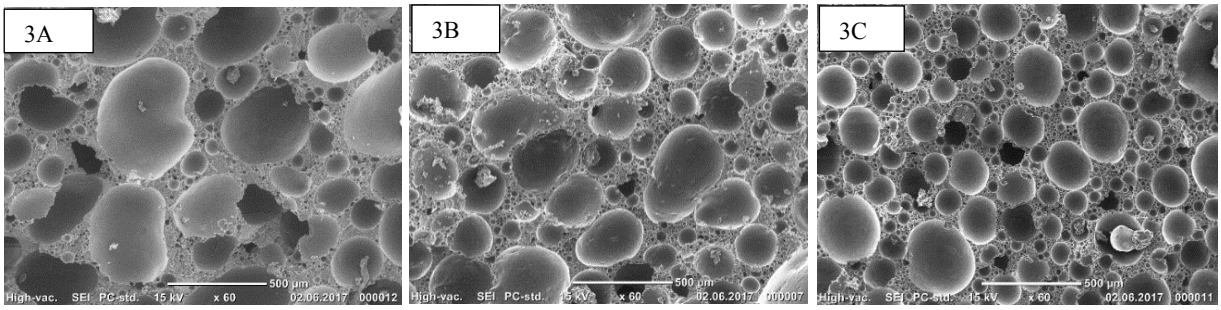

Figure S4. Epoxy foams produced with 2.5% silica particles and a frothing time from 2 min to 24 min exhibited hierarchical porous structure.

S5: Thermogravimetric analysis of epoxy foams

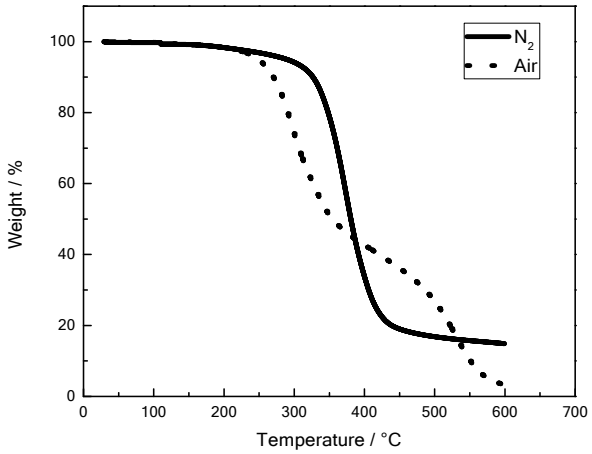

Figure S5. Thermal degradation behaviour of epoxy foams as a function of temperature in nitrogen and air.

The thermal degradation behaviour of the produced epoxy foams in air and N2 was determined using TGA. A representative weight loss curve in air (for sample 2E) showed that the degradation of epoxy foam occurred in three stages. The weight loss occurring in the range from 50°C to 250°C was attributed to dehydration of the epoxy foams with mass loss between 5 to 9%. The second weight loss stage occurring in the temperature range from 250°C to 420°C is caused by degradation of crosslinks, [1] which resulted in a mass loss of around 50%. The third degradation stage between 420°C to 550°C represented the further oxidation of the fragments. The thermal degradation of epoxy foam in nitrogen occurs in a single stage, starting at about 370°C, which is consistent with previous findings. [1, 2]

[1] K. Chen, C. Tian, A. Lu, Q. Zhou, X. Jia, J. Wang, *J. Appl. Polym. Sci.* **2014**, *131*, 40068.

[2] P. M. Stefani, V. Cyras, A. Tejeira Barchi, A. Vazquez, *J. Appl. Polym. Sci.* **2006**, *99*, 2957.

7. CONCLUSIONS

Using templating methods to produce macroporous polymer foams have been widely investigated because of the advantage of creating well-defined porous structures. However, templating methods do require the removal or reuse of the templating phase, which costs energy and materials and thus hinders scale up and practical applications of templating methods. In this work the process of making dairy cream in kitchen was mimicked: air was mechanically whipped into resins to produce stable liquid froths, which were cured to produce air templated macroporous polymers. Here, by frothing and curing different resin systems and investigating the properties of the resulting polymer foams, it was demonstrated that air templated macroporous polymers have a well-defined porous structure. Furthermore, it was shown that the air templating method as a potential industrial foaming procedure, is scalable. Potential applications of different air templated macroporous polymers and the versatility of air templating method for aqueous and non-aqueous resin systems were investigated.

Due to the different polarity of aqueous systems and air, air-in-aqueous froths can be easily produced and stabilised. Therefore, the work started by whipping air into aqueous phenolic formulations. Stable phenolic froths were successfully cured to produce open-porous phenolic foams with a density as low as 180 kg m^{-3}. By adjusting the whipping energy, the density and pore sizes of the resulting phenolic foams can be controlled. Importantly, the liquid nature of the phenolic froths allowed casting of the froths, thus net-shaped phenolic foams were produced. Furthermore, the scale up from 50 ml to about 4L of the phenolic froths and foams was carried out in lab; a further scale up to produce 9L liquid froths and 400 mm x 400 mm x 50 mm phenolic foam panels was also realised using a small industrial mixer. The pyrolysis of large phenolic foams allowed for the production of carbon foam panels with a high carbon yield of 48%.

Possessing a similar chemical structure and aqueous nature as phenolic resoles, as well as large availability and low cost, black liquor was frothed and crosslinked to produce non-hygroscopic lignin foams with a well-controlled structure and good mechanical properties. The porosity and pore sizes of the lignin foams decreased with increasing the solute content (resulting in an increased viscosity) of the black liquor. Furthermore, the lignin foams were also pyrolysed to produce carbon foams. This provided a potential high-value added application for the black liquor.

To demonstrate the versatility of air templating for non-aqueous systems, epoxy formulations were frothed. Beside surfactants, which had been always used in aqueous froths, silica particles were required for stabilising the non-aqueous epoxy froths. Silica

particles increased the viscosity of the epoxy formulations, thus enhancing the kinetic stability of the froths. Furthermore, the surfactant was anticipated to phase separate from the liquid phase due to the slight difference between the surface tension of the surfactant and the epoxy formulation. As a result, it was possible to optimise the rheology of the liquid epoxy. Furthermore, the surfactant did stabilise the epoxy froths, which could then be cured at elevated temperatures providing a means to control the porosity and pore size of the produced epoxy foams by thermal bubble expansion. The density of the resulting epoxy foams increased with increasing silica particle loading. Although the silica particles did not reinforce the epoxy foams, they led to a hierarchical porous structure, enhancing the stiffness of the epoxy foams.